Investigating *Leishmania donovani* PEX14 interactions with glycosomal membrane mimicking liposomes

By

Anwer Hasil Kottarampatel

Institute of Parasitology, McGill University, Montreal

A thesis submitted in partial fulfillment of the degree of Doctor of Philosophy.

Nothing in life is to be feared, it is only to be understood. Now is the time to understand more, so that we may fear less.

-Marie Curie

Science knows no country, because knowledge belongs to humanity, and is the torch which illuminates the world.

- Louis Pasteur

Most people say that it is the intellect which makes a great scientist. They are wrong: it is character.

-Albert Einstein

Table of Contents

Abstract

Glycosomes are unique organelles that compartmentalize several vital metabolic pathways in kinetoplastid parasites, including *Leishmania spp*. Protein transport across the glycosomal membrane occurs with the help of receptor proteins called peroxins (PEX). Cargo proteins bearing a PTS1 (Peroxisome Targeting Signal) and PTS2 motif can bind to the cytosolic PEX5 and PEX7 receptors, and subsequently dock to PEX14 which is anchored to the glycosomal membrane. The binding of cargo-loaded receptors to PEX14 is considered to be a pivotal step in glycosomal function and parasite survival. *Leishmania donovani* PEX14 (LdPEX14) is a peripheral membrane protein with a hydrophobic region, spanning residues 149-179, thought to mediate anchoring and insertion into the glycosomal membrane. Sucrose density flotation centrifugation and dye leakage assays have previously demonstrated that a hydrophobic region spanning residues 120-200 was able to bind glycosome mimetic membranes.

To further examine the interaction of LdPEX14 with glycosomal mimicking membranes, various tryptophan and cysteine mutants were generated for the hydrophobic region spanning 149-179. Dual fluorescence quenching analysis (DQA) carried out with the ldpex14 mutants in the presence of quenching agents revealed that the hydrophobic domain in ldpex14 (120-200) has a deeper penetration into the membrane bilayer, in comparison to the shallow penetration observed with for full length LdPEX14. Dye leakage assays revealed that the fragment ldpex14 (120-200) formed pore structures in membrane. Experiments combining different techniques such as Forster Resonance Energy Transfer (FRET), tryptic peptide analysis, and biotinylated peptides revealed that the N- and C-termini of the inserted hydrophobic region were exposed to the extra luminal space of liposomes. The hydrophobic domain also had potential to oligomerize and form α-helical

structures in the presence of unilamellar vesicles. Our studies suggest that the LdPEX14 hydrophobic region has a propensity to form an amphipathic helix within the lipid bilayer to mediate anchoring and insertion into the glycosomal membrane. ldpex5 (203-391), a region of LdPEX5 that can bind to LdPEX14, was able to induce conformational changes in LdPEX14, triggering its hydrophobic region to migrate deeper into the lipid bilayer. An *in-silico* model was constructed revealing the topology of the hydrophobic domain inserted into the membrane.

Previous experiments suggested that the dynamic rearrangement of the hydrophobic domain of LdPEX14 could result in membrane perturbation and formation of a structural pore. In the absence of LdPEX14-interacting partners such as LdPEX13, LdPEX5, LdPEX7, and RING finger proteins, we utilized altering pH as a surrogate method to induce conformational changes in LdPEX14. We found that LdPEX14 was able to induce membrane pore formation in low pH conditions. Rearrangement of hydrophobic domains was confirmed by experiments utilizing the fluorescence of intrinsic tryptophan located in the hydrophobic domain and an extrinsic probe 1-anilino-8 naphthalene sulfonate (ANS). SEC-HPLC and CD analysis confirmed that the low pH used did not alter the quaternary or the secondary structure of LdPEX14.

To better understand the functions of PEX14 in *L. donovani* we decided to knock out the gene encoding LdPEX14 using the CRISPR/Cas9 genome editing tool. Our aim was to develop a regulatable system for expression of Cas9 in *L. donovani* by fusing the N- and C-termini of Cas9 to the ddFKBP domain (destabilizing domain of FKBP12). The N-terminus ddFKBP fusion provides conditional Cas9 destabilization in *L. donovani* promastigotes, and an increased level of protein expression was detected in the presence of the rapamycin

ligand. This technology was used to knock out LdPEX14 and LdXPRT genes in *L. donovani* and can be exploited to characterize other genes in *Leishmania*.

Abrégé

Le glycosome est une organelle unique qui compartimente plusieurs voies métaboliques chez les parasites kinétoplastides comme *Leishmania*. Le transport des protéines à travers la membrane glycosomale se fait à l'aide de protéines réceptrices nommées peroxines (PEX). Les protéines de cargaisons qui ont un PTS1 (Peroxisome Targeting Signal) peuvent lier avec le récepteur PEX5, et les protéines ayant un signal PTS2 lient avec le récepteur PEX7, pour afin ammarer chez PEX14. La liaison des récepteurs de cargaison avec PEX14 attaché sur la membrane glycosomale est considérée une étape pivotale pour la function du glycosome et la survie du parasite. LdPEX14 est une protéine polytopique comprenant une région hydrophobique entre les acides aminés 149-179 qui est suspect de médier l'ancrage et l'insertion de cette protéine dans la membranes glycosomale. La centrifugation en gradient de densité avec le saccharose, ainsi que des essais de fuite de colorants traceurs, ont démontré que la région hydrophobique comprenant les résidues 120-200 peut lier avec les membranes mimétiques du glycosome.

Pour mieux examiner l'intéraction de PEX14 avec les membranes imitant celles du glycosome, divers mutations chez les tryptophanes et les cystéines ont été introduits dans la région hydrophpbique couvrant les résidues 149-179. L'analyse de l'éxtinction d'une double fluorescence (DQA) a été faite avec les mutants avec la présence d'agents d'étanchement; ceci a révélé que le domaine hydrophobique de ldpex14 (120-200) a une pénétration plus prononcée comparée au WT LdPEX14. Les essais de fuites de colorants traceurs encapsulés avec de la carboxyfluoresceine ont révélé que le morceau de ldpex14 (120-200) peut former des pores dans la membrane. La combinaison des techniques comme le transfert d'énergie de fluorescence par resonance (Fluorescence Resonance Energy Transfer -FRET), l'analyse par digestion tryptyque, et l'utilisation des peptides marqués avec la biotine a révélé que les extrémités N- et C-terminale

de la région hydrophobique insérée sont exposés au niveau luminal des liposomes. Dans la presence de vésicules unilamellaires, ce domaine hydrophobique possède aussi le potentiel de former des oligomères de protéines, ainsi que des structures hélices alpha. Nos études suggèrent que la region hydrophobique de PEX14 a la capacité de former une hélice amphipathique dans la bicouche lipidique membranaire pour médier l'ancrage et l'insértion dans la membrane glycosomale. ldpex5 (203-391), une région qui peut lier avec LdPEX14, a causé un changement conformationnel dans LdPEX14, et a déclanché un movement de la region hydrophobique vers la bicouche lipidique membranaire. Un modèle topologique a été construit, révélant la topologie du domaine hydrophobique inséré dans la membrane.

Des expériences faites auparavant ont suggéré que la réorganisation dynamique du domaine hydrophobique de LdPEX14 peut résulter en une perturbation membranaire et la formation d'un pore. Dans l'absence de partenaires qui interagissent avec LdPEX14, comme par example LdPEX13, LdPEX5, LdPEX7 et les protéines domaine un domaine RING (Really Interesting New Gene)-finger, le changements de pH a été utilisé comme méthode de substitution pour emmener des changement conformationelles chez LdPEX14. Par un changement de pH (plus bas), nous avons trouvé que LdPEX14 fut capable d'introduir une pore dans la membrane. Le réarrangement du pH du domaine hydrophobique fut confirmé avec des expériences utilisant la fluorescence du tryptophane dans ce domaine, ainsi que la sonde 1-anilino-8naphthalene sulfonate (ANS). Des analyses SEC-HPLC et CD ont confirmé que le pH abaissé n'a pas eut d'effet sur les structures secondaires ou quternaires de LdPEX14.

Afin de mieux comprendre les fonctions de PEX14 chez *L. donovani*, nous avons décidé de supprimer le gène LdPEX14 en utilisant le système CRISPR/cas9. Notre but était de développer un système réglable pour l'expression de Cas9 chez *L. donovani*; nous avons fusionné

les extrémités N- et C-terminale avec le domaine ddFKBP (un domaine déstabilisant de FKBP12). L'extrémité N-terminale fournit une déstabilisation conditionelle de Cas9 chez les promastigotes de *L. donovani*, ainsi qu'un niveau élevé d'expression de protéine dans la présence d'un ligand de rapamycine. Cette technologie fut utilisée pour supprimer les gènes LdPEX14 et LdXPRT chez *L. donovani* et pourrait être exploitée pour characterriser d'autres gènes chez *Leishmania*.

Acknowledgments

Primarily, I would like to express my gratitude to my supervisor, Dr. Armando Jardim for the support and guidance he provided throughout all these Ph. D. years. He provided me with an opportunity to learn and explore the basics of scientific research in an interesting and versatile manner. I will always be grateful for his mentorship and I think it would be amazing to collaborate with him once I set up my own laboratory.

I would like to thank my thesis committee members Dr. Elias Georges, late Dr. Paula Ribeiro and Dr. Albert Berghuis for the valuable time they spent to guide my work.

A huge thanks to all our faculty members including Dr. Tim Geary, Dr. Mary Stevenson, Dr. Reza Salavati, Dr. Robin Beach, Dr. Petra Rohrbach, and Dr. Jeff Xia for their valuable time and advise. A special thanks to Shirley and Christiane.

I would like to thank all my previous and current lab mates for bearing with me and I will always cherish those wonderful moments we had together. I would like to thank all the members of the Institute of Parasitology including the students, faculty and staff members for providing many fantastic years filled with fun and encouragement.

I would like to thank my friends Mark, Georgia, Mifong, Norma, Anand, Haque, and Jiby for investing their valuable time to read my thesis and provide constructive feedback. A special thanks to Georgia for helping me with translating the abstract to French.

A huge thanks to our parents and brothers whose support and encouragement throughout these years helped me to stay solid and composed.

Finally, I owe my greatest thanks to my wife Mehar who always stood by me in the adversities throughout these years. It was a great deal of dedication that you showed in in the upbringing of our lovely kids, Raed and Raha. I am so thankful for your unconditional love, and all the support you have given me.

List of Figures

Chapter 2

Chapter 3

Chapter 4

Chapter 5

List of Tables

Chapter 2

Chapter 3

Abbreviations

10-DN	10-Doxylnonadecane
ANS	8-Anilinonaphthalene-1 Sulfonic Acid
ATP	Adenosine Triphosphate
BSA	Bovine Serum Albumin
Cas9	CRISPR Associated Protein 9
CRISPR	Clustered Regularly Interspaced Short Palindromic Repeats
ddFKBP	Destabilization Domain of FKBP12 Protein
DME-L	Dulbecco's Modified Eagle *Leishmania* Medium
DNA	Deoxyribonucleic Acid
DQA	Dual Fluorescence Quenching Assay
DTT	Dithiothreitol
EDTA	Ethylene Diamine Tetraacetic Acid
ELISA	Enzyme Linked Immunosorbent Assay
FBS	Fetal Bovine Serum
HD	Hydrophobic Domain
HIV	Human Immunodeficiency Virus
HRP	Horse-Radish Peroxidase
HT	Hypotonic Lysis Buffer
IgG	Immunoglobulin G
IPTG	Isopropylthiogalactoside
I-TASSER	Iterative Threading Assembly Refinement
K_D	Dissociation Constant
Ld	*Leishmania donovani*
LdPEX	*Leishmania donovani* Peroxin
Lm	*Leishmania major*
LUV	Large Unilamellar Vesicle
mRNA	Messenger Ribonucleic Acid
NAD+/NADH	Nicotinamide Adenine Dinucleotide
Ni^{2+}-NTA	Nickel Nitrilotriacetic Acid

NTD	Neglected Tropical Disease
PAM	Protospacer Adjacent Motif
PBS	Phosphate Buffered Saline
PBST	Phosphate Buffered Saline + Triton X-100
PEX	Peroxin
PMP	Peroxisomal Membrane Protein
PTS	Peroxisomal Targeting Signal
PVDF	Polyvinylidene Difluoride
RING	Really Interesting New Gene
RNA	Ribonucleic Acid
RNAi	Ribonucleic Acid Interference
SDS-PAGE	Sodium Dodecyl Sulfate Polyacrylamide Gel Electrophoresis
SEC	Size Exclusion Chromatography
SUV	Small Unilamellar Vesicle
TBS	Tris Buffered Saline
TBST	Tris Buffered Saline + Tween-20
TCA	Trichloroacetic Acid
TPR	Tetratricopeptide Motif
VL	Visceral leishmaniasis
WHO	World Health Organization
WD40	40 Amino Acid Tryptophan-Aspartic Domain
WT	Wild type
XPRT	Xanthine Phosphoribosyl Transferase

Statement of Originality

1. This is the first study to investigate the topology of LdPEX14 hydrophobic domain inserted into the membrane bilayer.
2. This is the first study to show that the hydrophobic domain of ldpex14 (120-200) orients in a helix-turn-helix configuration in the membrane with the N- and C-termini exposed to the extra luminal space of liposome.
3. This is the first study to show that the binding of ldpex5 (203-391) to LdPEX14 can trigger deeper insertion of the hydrophobic domain into the membrane bilayer.
4. This is the first study to show that the hydrophobic region of ldpex14 (120-200) forms a discreet pore.
5. This is the first study to show that full length LdPEX14 can form pore structures in the membrane bilayer by pH induced conformational changes.
6. This is the first study to show that the fusion of ddFKBP domain to the N-terminus of Cas9 endonuclease conditionally destabilizes the expression of Cas9 in *L. donovani* promastigotes.
7. This is the first study to show that knocking out *L. donovani* PEX14 is lethal for the *L. donovani* promastigotes.

Contribution of Authors

Chapter 3. Analysis of the *Leishmania donovani* Peroxin 14-membrane interaction

Anwer Hasil Kottarampatel, Normand Cyr and Armando Jardim

AHK performed bioinformatic analysis, protein modelling, mutagenesis, protein purification, and LUV-protein interactions studies. NC performed the CD experiments. AHK and AJ designed the experiments. AJ supervised the work and wrote the initial manuscript. AHK and AJ edited the manuscript and completed the discussion with proposed pore models.

Chapter 4. Study of conformational changes in the hydrophobic region of LdPEX14 induced by low pH

Anwer Hasil Kottarampatel, Normand Cyr and Armando Jardim

AHK designed the experiments, performed the study, analyzed the data, and wrote the manuscript. NC performed the acrylamide quenching experiments. AJ supervised the work and edited the manuscript.

Chapter 5. Destabilization domain mediated regulatable expression of Cas9 in *Leishmania donovani* and CRISPR/ Cas9 based knocking out of LdPEX14

Anwer Hasil Kottarampatel, Phil Yates, Anand Vardhan and Armando Jardim

AHK designed the experiments, performed the study, analyzed the data, and wrote the manuscript. PY was available for constructive discussions and provided pRP plasmids for the studies. AV participated in screening and isolating positive knock out clones. AJ supervised the work and edited the manuscript.

Chapter 1

General Introduction and Thesis Objectives

General introduction

Leishmania spp. infection causes a spectrum of clinical manifestations known as leishmaniasis which is considered as a neglected tropical disease by the WHO [1, 2]. The disease is widely distributed across the globe and is spread in over 88 countries, mostly developing and underdeveloped nations. Around 350 million people are at risk of infection by this devastating disease [3, 4]. There are various clinical signs of leishmaniasis ranging from cutaneous, muco-cutaneous to the visceral form, the latter of which if left untreated is fatal for the host [5-7]. The visceral form of the disease is caused by *L. donovani* and 90 % of its disease burden is distributed across five developing countries including Bangladesh, India, Nepal, Sudan, and Brazil [8, 9]. The disease is spread through the bite of sandflies and the parasites have a digenetic life cycle; a promastigote stage residing in the sand fly vector and an amastigote stage in the human host [10-12]. The treatment for this disease mainly relies on chemotherapeutic agents, but most of the available drugs are facing problems of severe toxicity or drug resistance [13-15]. Consequently, there is an urgent need to find new therapeutic targets which can selectively kill the parasite.

Kinetoplastids have a unique organelle called the glycosome, that compartmentalizes many vital metabolic pathways including glycolysis [16, 17], pyrimidine biosynthesis [18], ether-lipid biosynthesis [19], β-oxidation of fatty acids [20] pentose-phosphate pathway [21] and purine salvage [18]. Glycosomes are essential for parasite viability and evolutionarily related to the peroxisomes of higher eukaryotes. Disruption of glycosome biogenesis and mistargeting of glycosomal enzymes to the cytosol have been found to be lethal for the parasite [22-24]. It has been observed that folded proteins are transported across the peroxisomes or glycosomes [25, 26]. Glycosomes lack genetic material and protein translational machinery; all proteins destined

to the glycosome must be synthesized in the cytosol and post translationally translocated into the glycosome. The proteins destined to glycosomes bear a signal sequence known as peroxisomal targeting signal (PTS). Those proteins with a PTS1 (C-terminal tripeptide) or PTS2 (N-terminal nonapeptide) signal are bound by cytosolic peroxin receptors peroxin 5 (PEX5) and peroxin 7 (PEX7), respectively, and bind to the glycosomal membrane associated protein peroxin 14 (PEX14) which translocate and unload the protein cargo into the glycosome [27-30].

PEX14 has been suggested to be essential for the survival of the *Leishmania* parasite, as RNAi mediated silencing of PEX14 in the related kinetoplastid, *T. brucei,* produced a lethal phenotype [23, 31]. It has been demonstrated that the hydrophobic region of LdPEX14 spanning residues 149-179 is critical for binding to unilamellar vesicles that mimics the glycosomal membrane [32, 33]. A transient pore model that contains PEX14 and PEX5 has been suggested to mediate the trafficking of folded proteins across the peroxisomal membrane [34-36]. Even though there have been advances made in resolving various components of the glycosome/peroxisome translocon, little is known about PEX14-membrane interactions or the mechanism behind the formation of the transient pore.

Biophysical and biochemical analysis of LdPEX14 interactions with the membrane bilayer is important for a better understanding of the mechanism of pore formation. On a broader perspective, our studies explore the underlying mechanism through which these fully folded oligomeric proteins are transported across the glycosomal membrane.

Thesis objectives

The major objectives of this dissertation were to dissect the interaction between LdPEX14 and the glycosomal membrane and investigating possible mechanisms for cargo transport across the membrane. For accomplishing these objectives, various studies were formulated including:

- Investigate the topology of the hydrophobic region of LdPEX14 inserted into the membrane bilayer.
- Study of conformational changes in the hydrophobic region of LdPEX14 induced by pH.
- Perform CRISPR/Cas9 mediated knockout of LdPEX14 and characterize its functions in *L. donovani*.

Chapter 2

Literature Review

Introduction

Leishmaniasis is a vector-borne disease caused by an obligate intracellular parasite of the genus *Leishmania*. It is also known by other names such as *Baghdad boil*, *Kala-azar*, *Sandfly disease*, *Leishmaniosis*, *Leishmaniose*, *Chiclero ulcer*, and *espundia* [1, 37-39]. Twenty species of *Leishmania* parasites are transmitted to human through two species of vectors, namely, the species and subspecies of *Phlebotomus* in the Old World and *Lutzomyia* in the New World [40, 41]. There are various clinical manifestations of this disease, ranging from non-fatal disfiguring forms of mucocutaneous leishmaniasis to fatal visceral leishmaniasis [5]. Approximately 300,000 cases of visceral leishmaniasis (VL) distributed in 70 countries were reported in 2006 with the highest density of VL occurring in Southeast Asian countries and East Africa. Due to the frequent misdiagnosis of VL, as is the case in malaria, the true incidence of VL is often underestimated [42]. In 2007, the World Health Organization (WHO) deemed leishmaniasis as a neglected tropical disease and emphasized the importance of controlling leishmaniasis which affects mainly the poorest of the populations exposed [2, 43].

2.1 Clinical manifestations of leishmaniasis

Cutaneous leishmaniasis is the most common form of the disease and is mainly manifested as skin lesions on face and limbs of the infected host. This form of the disease is caused by the species *L. major* in the Old World, and *L. mexicana* complex in the New World [7]. When an infected sand fly takes a human blood meal, it injects the parasite, causing a skin lesion to develop at the bite site; this ulcerates and subsequently become infected with bacteria. Lesions

typically heal themselves without treatment, but healing rates are found to be slower in immune-compromised people [44, 45].

Mucocutaneous leishmaniasis is characterized by extensive destruction of the mucosal lining of the upper alimentary and respiratory tracts, ranging from the mouth to the pharynx and the nose to the larynx, respectively. Those infected suffer greatly in their social life due to the disfiguring lesions and mutilation of their faces that accompanies infection. These lesions are not self-healing, as macrophages colonize the nasopharyngeal mucosa, leading to a decreased healing capacity of the tissue [46-48]. This type of disease is known to be predominantly caused by *L. braziliensis* and mostly affects Latin American populations [49].

Among the various clinical manifestation of the disease, visceral leishmaniasis (VL), also known as Kala-azar or Black fever, is the most fatal, especially when left untreated. VL garnishes its names due to parasite migration and survival inside internal organs of the host such as the spleen, liver, and bone marrow [5, 6]. A recent report from Brazil indicates that due to human migration from rural to urban areas, the disease now affects more people in urban regions than previously reported [50].

Post-Kala-azar Dermal Leishmaniasis (PKDL) is a cutaneous manifestation of VL characterized by skin lesions, or macular, maculo-papular, or nodular rashes. It is a dermatologic disorder often observed after treatment of VL in Sudan, East Africa, and in the Indian subcontinent [46, 51]. The time interval for detecting PKDL after treatment of VL varies from 0-6 months in Sudan to 3-6 years in India [52, 53].

2.2 Epidemiology of leishmaniasis

Leishmaniasis is considered a major tropical affliction. It is present in over 88 countries, most of them are in developing and underdeveloped nations. Around 350 million people are at risk, and 10 million people are currently affected by this devastating disease. Annually, ~2 million new cases and 20,000 to 30,000 deaths are reported. There is a continual increase in cases of leishmaniasis emerging from newer areas [3, 4, 54].

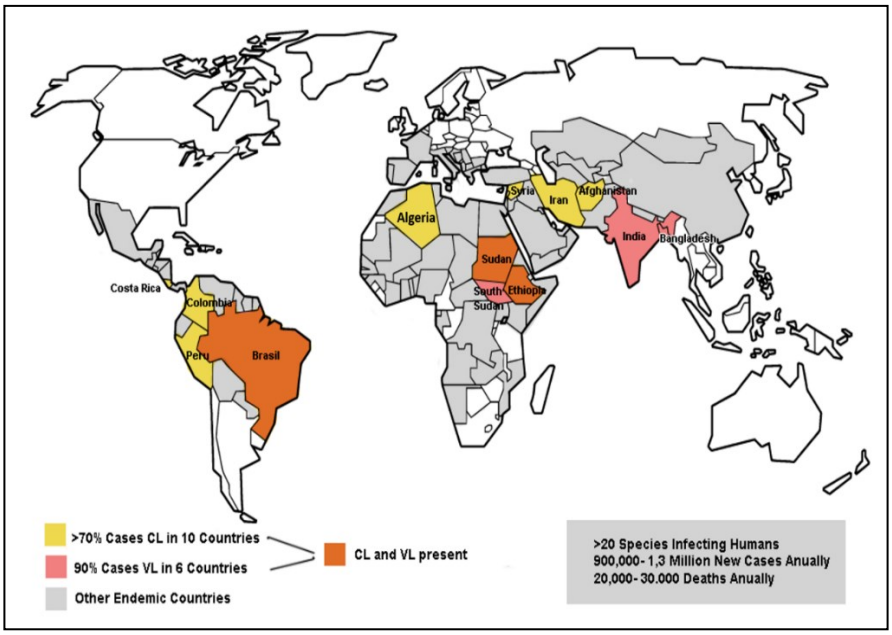

Figure 1: Geographic distribution of leishmaniasis

About 90% of visceral leishmaniasis is distributed in 6 countries and 70% of cutaneous leishmaniasis in 10 countries [8, 9, 55-57].

Bangladesh, India, Nepal, Sudan, Ethiopia and Brazil harbor most of the cases of visceral leishmaniasis (more than 90%) and the State of Bolivia, Brazil and Peru harbor about 90% of mucocutaneous leishmaniasis cases. In India, VL is mainly concentrated in the Eastern portion of

the country, and is especially common within the provinces of Bihar, Eastern Uttar Pradesh, and West Bengal. India, Nepal, and Bangladesh are estimated to account for 67% of the active VL cases [8, 9, 46, 55-57]. In the WHO European region, countries affected by cutaneous leishmaniasis are Israel, Turkey, Turkmenistan, Uzbekistan (accounts for 80% of total cases) and countries affected by visceral leishmaniasis are Albania, Georgia, Italy and Spain (accounts for 75% of total cases) (**Figure 1**) [58].

2.3 Life-cycle of the parasite

Female sandflies are the primary transmission vector of the promastigote stage of the *Leishmania* parasite (~10-12 μm in length); when the sandflies take a blood meal, they inject the parasite into a human host. *Leishmania* has a digenetic life cycle: a promastigote form residing in the sandfly vector and an amastigote form that survive in the phagolysosomal vesicles of macrophages. The amastigote form of the parasite present in the infected host exists as a rounded, non-motile form that is ~3-7 μm in diameter. Following a blood meal, the amastigotes get differentiated into promastigotes in the sandfly midgut. The promastigotes reproduce asexually and then migrates to the proximal end of the gut where they are ready for retransmission during a subsequent blood meal [10-12, 59, 60].

The promastigote injected into the human host undergoes rapid phagocytosis by neutrophils and macrophages, which facilitates the transformation to the amastigote form. Mouse studies have shown that neutrophils are the first cells recruited to the site of infection accompanied by marshaling of macrophages to the sandfly bite site [61]. As neutrophils have a short life span, they act as intermediate host cell. The parasite tends to survive and proliferate inside the macrophages which are considered as the primary resident cell for *Leishmania* [60,

62]. The parasite residing inside the macrophages multiply and eventually rupture the macrophages and infect nearby cells. Released amastigotes taken up by the surrounding macrophages facilitate shuttling of the infection primarily to the liver, spleen liver and bone marrow (**Figure 2**) [12, 63, 64].

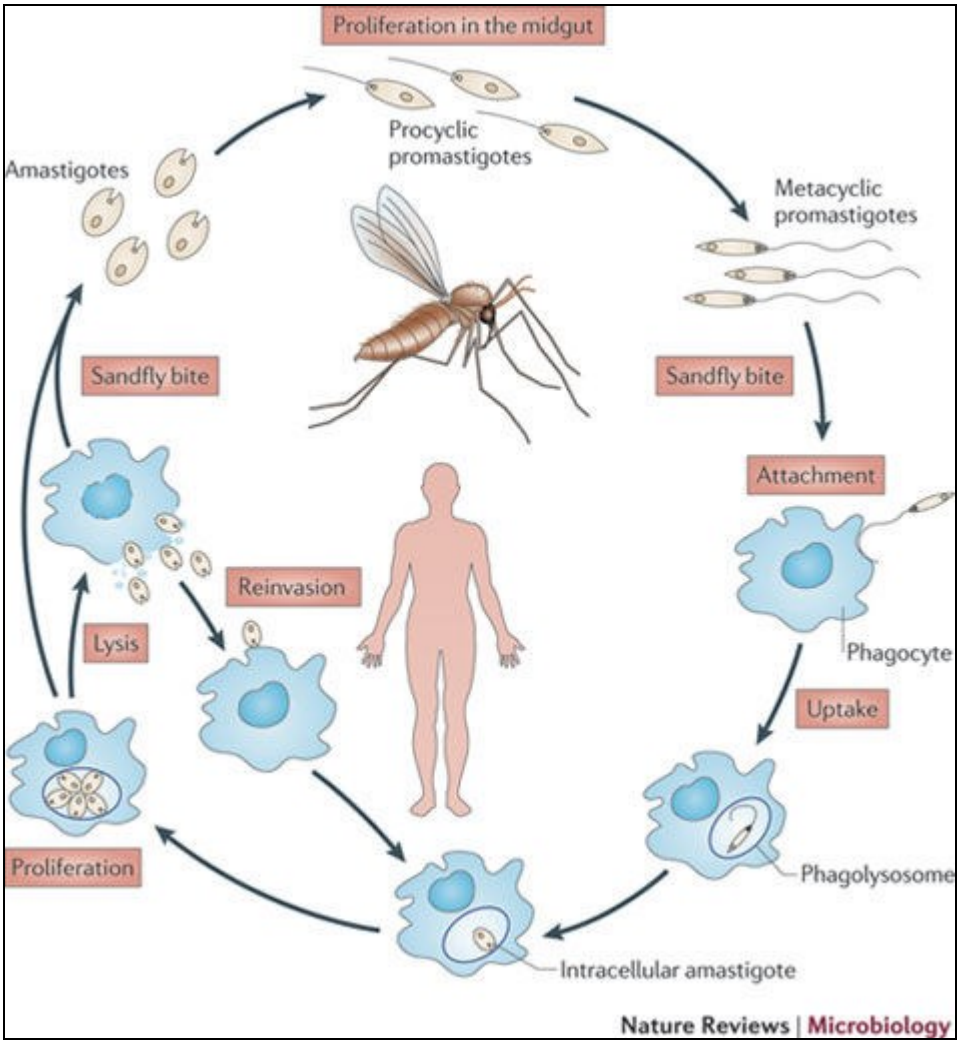

Figure 2: Life cycle of *Leishmania*

The digenetic life cycle of *Leishmania* spp. When a sandfly takes a blood meal it injects the promastigote into the mammalian host where it gets transformed into amastigote. At the next blood meal, the sandfly ingests the amastigote wherein it gets retransformed to promastigote form [65].

2.4 Diagnosis of visceral leishmaniasis

The diagnostic tests used for VL should be highly sensitive and specific because VL is a fatal disease and the clinical symptoms displayed by VL are devoid of specificity. Furthermore, the drugs available for treatment are either highly toxic or susceptible to resistance problems, reiterating the necessity for sensitive tests to discriminate between asymptomatic infections and acute disease. Testing for the presence of amastigotes in the splenic aspirates, bone marrow, and lymph nodes by microscopy is highly specific and confirmatory, but as they are invasive and may cause severe haemorrhages, these methods demand high technical expertise and can be done only in a hospital or clinical setting. Detection of parasites by PCR is more sensitive than microscopy, but this technique is not readily accessible in many field clinics. Several antibody-based detection methods such as Direct Agglutination Test (DAT) and rK39-based immunochromatographic test (ICT) are employed to detect VL in the field. However, the major limitation of an antibody-based detection method is that even after successful treatment of the disease, the antibody level remains detectable for many years and even healthy individuals living in endemic areas test positive with these tests. DAT works on the principle that when stained, killed *L. donovani* promastigotes are mixed with increasing dilution of patient serum, and agglutination can be observed after 18 hours, indicating the presence of antibodies. The ICT exploits the principle of ELISA; rK39 is a 39- amino acid repeat, a part of the kinesin-related protein in *L. chagasi* and *L. donovani* complex. Some novel antigen-based detection testing has been developed, such as latex agglutination testing that detects a heat-stable, low molecular weight carbohydrate antigen in urine samples of VL patients. Limitations of this test include low sensitivity, difficulty in distinguishing weakly positive from negative results, and a need to boil the urine to avoid false positive results [66-70]. Elimination of this neglected tropical disease is

certainly hampered by the unavailability of accurate, sensitive, and readily accessible diagnostics.

2.5 Strategies for control and treatment of visceral leishmaniasis

Control of VL can be carried out either at the reservoir or vector level. For zoonotic VL caused by *L. infantum,* dogs are considered as a major reservoir for parasites that can potentially infect humans, although treating infected dogs is not practical as they are prone to relapses, and prolonged use of these drugs may give rise to resistant strains [46, 71].

Vector control can be an effective strategy, as the sandfly vector is susceptible to insecticides such as Dichloro-Diphenyl-Trichloroethane (DDT). In fact, in India, VL is mainly spread through a single species of sandfly, the *Phlebotomus argentipes* and mass spraying of DDT was found to be effective for vector control, although cases of resistance have been reported from Bihar, India. Factors such as inadequate quality assurance (QA) of Indoor Residual Spraying IRS and arising drug resistance rates are impeding current VL elimination efforts. Furthermore, in some countries such as Sudan and East Africa, people are infected while working outside the household area, therefore indoor spraying is not an effective strategy [72-76]. Also, there are contrasting reports on the efficiency of insecticidal nets for protection against visceral leishmaniasis; it was found to be an effective method for controlling VL in Sudan and Bangladesh [77, 78] while no additional protection was observed in the Indian subcontinent [79].

In most parts of the world, treatment of VL relies on conventional antimonial therapy. Pentavalent antimonials such as sodium stibogluconate and meglumine antimoniate are first line

drugs for treating VL. Use of these drugs is, however, limited due to their severe toxicity, adverse drug reactions (ADR), and the emergence of resistance [46, 80-82].

Miltefosine was the first drug available for oral administration for treatment of leishmaniasis. Unfortunately, apart from side effects such as severe gastric toxicity, the drug also has teratogenic potential and a long half-life (~150 hours), increasing the risk of toxicity when compared to other anti-leishmanial drugs [13-15, 46, 83, 84].

Amphotericin B is currently used as an alternative therapy to antimonials when the latter face resistance complications and treatment failures. This drug causes severe adverse effects such as nephrotoxicity, and hypokalemia, and requires a complex therapeutic regimen that includes fifteen slow infusions of the drug on alternate days. Modified dosage preparations of amphotericin, such as liposomal amphotericin B (AmBisome from Gilead Pharma), has significantly less nephrotoxicity; however, it still has dose-limiting renal toxicity. Also, formulation of amphotericin encapsulated within liposomes is a highly expensive option and often the treatment course is unaffordable by infected patients in the impoverished countries where the disease is endemic [46, 75, 85-89]. In Bihar, India, the outcome of trials involving patients suggests that a single dose of liposomal amphotericin B (AmBisome from Gilead Pharma) or indigenously manufactured liposomal amphotericin B (Fungisome from Lifecare Innovations) was equally effective and less expensive than 15 alternate-day infusions of amphotericin B deoxycholate [14, 90].

Although all the above control strategies and treatment options were adapted to control VL (**Table 1**), none have been successful in eliminating the disease from endemic areas. As such, there is an urgent need for more detailed research and development to find new drug targets, specifically those necessary for the viability of the parasite.

Table 1: Available options for combating visceral leishmaniasis

Drug	Advantages	Disadvantages	Mode of action
Dichloro-Diphenyl-Trichloroethane (DDT)	Effective for sand fly vector and control of disease from the root cause by preventing transmission through sand flies	Emergence of resistance, Inadequate quality assurance (QA) of IRS (Indoor residual spraying)	Opens voltage gated sodium channels found in the insect nerve cell membrane leading to paralysis and death [74, 76].
Amphotericin B deoxycholate	Efficient and more effective for treatment of patients non-responsive to Sodium stibogluconate	Renal toxicity, Need of lengthy treatments, infusion reactions.	Bind with ergosterol of membrane causing pores and eventually leakage of cell contents [87-89].
Liposomal amphotericin B	Less nephrotoxicity than amphotericin B and can be given as short courses of therapy.	Expensive, hence cost-prohibitive in poor countries	Same as amphotericin B but liposomal formulation passively targets amphotericin B to macrophage-rich organs [13, 14, 86].
Miltefosine	Oral formulation available, affordable, well tolerated	Gastro-intestinal side effects vomiting and diarrhoea, low efficacy, not used in pregnant and breast-feeding women.	Interacts with membrane synthesis, causing programmed cell death [13, 15].
Paromomycin	Low cost, broad spectrum activity.	Adverse reactions like ototoxicity, injection site reactions, elevated hepatic transaminases.	Inhibit protein synthesis by interfering with the ribosomes [82].
Pentavalent antimonials (SbV) (Sodium stibogluconate (SSG) and meglumine antimoniate (MA))	Well established for treatment of leishmaniasis, still a first line drug for treatment of VL in east Africa	Emergence of resistance, efficacy low in HIV-VL co-infected patients, like cardiac arrhythmias, prolonged QT interval, ventricular tachycardia, torsade's de pointes, elevation of cardiac and liver enzymes.	A decline in the synthesis of ATP and GTP from ADP and GDP results in reduced cell viability [13, 81].
Pentamidine	Used as secondary prophylaxis in HIV-leishmaniasis coinfection	Reported cases of insulin dependent diabetes mellitus and high rates recurrence of disease	Known to bind with the DNA, also inhibit the topoisomerase II [89, 91].

This table summarizes options for controlling VL, from vector control to the use of various chemotherapeutic agents.

2.6 Biology of the Parasite and distinctive features of an organelle called a "Glycosome"

Leishmania belong to the order kinetoplastida which includes mostly flagellated, obligate parasites residing in their animal or human hosts and they are divided into two subgroups Bodonina and Trypanosomatina. Bodonina is comprised of two families Bodonidae and Cryptobiidae, and include organisms bearing two flagella and a large kinetoplast. Bodonina is composed of free living species including; *Bodo*, *Cruzella*, *Dimastigella*, *Rhynchobodo*, *Parabodo*, as well as parasites residing, as ectoparasites in fish skin and gills (*Ichtyobodo*), and endoparasites of snails and fish (some *Cryptobia* species). The second group of Trypanosomatina comprise of a single family, Trypanosomatidae, where organisms are obligate parasites, bearing one flagellum and a small kinetoplast. These groups comprise of monogenetic parasites such as *Blastocrithidia*, *Crithidia*, *Herpetomonas*, and *Leptomonas* that exploit the invertebrates as hosts, or digenetic parasites such as *Trypanosoma* and *Leishmania* [92-94]. The trypanosomatids have numerous communal biological traits, such as the presence of a kinetoplast organelle, compartmentalization of metabolic pathways, unusual RNA editing, and transcription of long multicistronic mRNA molecules [95-98].

One of the unique characteristics of the kinetoplastid is the compartmentalization of several metabolic pathways in an organelle called the glycosome. These organelles are evolutionarily related to peroxisomes of fungal and mammalian cells, and glyoxysomes of plants. Glycosome lack genetic machinery and are circumscribed by a single membrane and a proteinaceous dense matrix [99-101]. Examples of metabolic functions which take place in glycosome are glycolysis [16, 17, 102], pyrimidine biosynthesis [18], ether-lipid biosynthesis [19], β-oxidation of fatty acids [20, 103], pentose-phosphate pathway [21] and purine salvage pathway [18].

Features making glycosomes distinct from peroxisomes are the presence of purine salvage and glycolytic pathways, and absence of catalase in *Trypanosoma and Leishmania* (while *Phytomonas* and *Crithidia* have catalase in their glycosome) which is a characteristic peroxisomal enzyme present in higher eukaryotes [18-21, 95, 99, 103, 104]. Peroxisomes are found to be non-essential for the survival of yeast, as yeast cells lacking peroxisomes could survive on most carbon sources [105]. Even though disorders of peroxisomal biogenesis cause death in early infancy, mammalian cells devoid of peroxisomes have sustained in cell culture [106, 107]. In contrast, glycosome function was found to be vital for parasite viability as the disruption of glycosome biogenesis and mistargeting of glycosomal enzymes to the cytosol resulted in a lethal phenotype, making glycosomes and their biogenesis machinery an attractive chemotherapeutic target [22-24].

The glycosomal membrane is poorly permeable to most glycolytic metabolites, and consequently a mechanism to balance the ADP/ATP and NAD^+/NADH is required [108]. In the bloodstream form of *T. brucei* enzymes required to catalyze the first seven steps of glycolysis are located in the glycosomal matrix, whereas the downstream enzymes that convert 3-phosphoglycerate to pyruvate are cytosolic (**Figure 3**) [16, 108-110].

Glycolysis is the primary ATP-providing process in these parasites during their multiplication in the mammalian host, the two ATP consumed during the first part of the glycolytic process are returned or reproduced by the action of downstream kinases [110]. Also, the NADH produced by the actions of glyceraldehyde-3-phosphate dehydrogenase (GAPDH) is subsequently re-oxidized to NAD^+ by the actions of glycerol-3-phosphate dehydrogenase (G3PDH). The electrons from NADH are transferred to the mitochondrion through a shuttle pathway that includes the transport of glycerol 3-phosphate to the outer face of the inner

mitochondrial membrane where it is converted into dihydroxyacetone phosphate by the glycerol-phosphate oxidase system. The dihydroxyacetone phosphate (DHAP) produced is exchanged with another glycerol-3-phosphate (G3P) through a putative G3P/DHAP antiporter system. Subsequently NADH is again oxidized to NAD^+ resulting in no net gain of NADH after glycolysis (**Figure 3**) [16, 109-113].

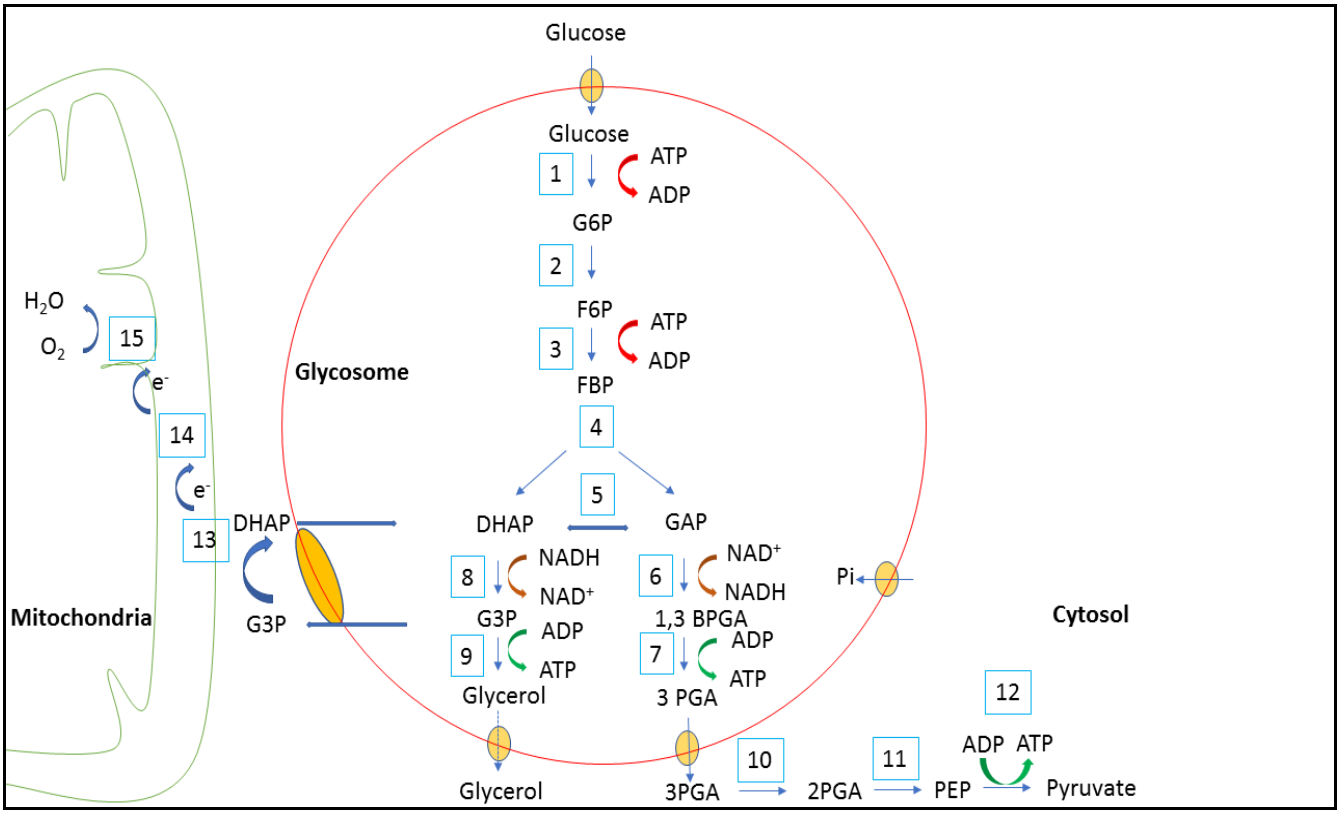

Figure 3: Schematic diagram of glycolytic pathway in blood stream form of *T. brucei*

In the above figure the enzymes catalyzing reactions are numbered from 1 to 15, glucose is used as substrate and glycerol and pyruvate (boxed) are end products. (1) hexokinase, (2) glucose-6-phosphate isomerase, (3) phosphofructokinase, (4) aldolase, (5) triosephosphate isomerase, (6) glyceraldehyde-3- phosphate dehydrogenase, (7) phosphoglycerate kinase, (8) NAD-dependent glycerol-3-phosphate dehydrogenase, (9) glycerol kinase, (10) phosphoglycerate mutase, (11) enolase, (12) pyruvate kinase, (13) FAD-dependent glycerol-3- phosphate dehydrogenase, (14) ubiquinone, (15) SHAM-sensitive alternative oxidase, adapted from [110].

It has also been demonstrated that partial reduction of various glycolytic enzymes leads to reduction of glycolytic flux, of which a 50 % reduction has been shown to be enough to kill the parasite [114, 115]. The compartmentalization of glycolysis was initially hypothesized to be responsible for the maintenance of a high glycolytic flux [116]. However, other studies show that high glycolytic flux is only associated with trypanosomatids that live on high glucose media [117, 118], that the catalytic activity of individual enzymes determines the rate limiting step of glycolytic flux in *T. brucei* [95], and the presence of high glycolytic flux (two fold) in yeast cells that are devoid of compartmentalization [119]. These data all provide evidence against the hypothesized relationship between glycolytic flux and compartmentalization of glycolysis. Mistargeting of phosphoglycerate kinase, hexokinase and phosphofructokinase in to the cytosol was found to be toxic to the blood stream form of *T. brucei,* indicating the importance of compartmentalization to overcome the metabolic interference. It is proposed that compartmentalization helps with recovering from starvation as the closed system prevents loss of ATP and restarts glycolysis when the substrates are again available [103, 120]. Another interesting feature involving the enzymes hexokinase and phosphofructokinase which catalyze the rate limiting steps of glycolysis is that they are not regulated by the feedback inhibition of products as seen in human and yeast cells. (**Figure 4**) [121, 122].

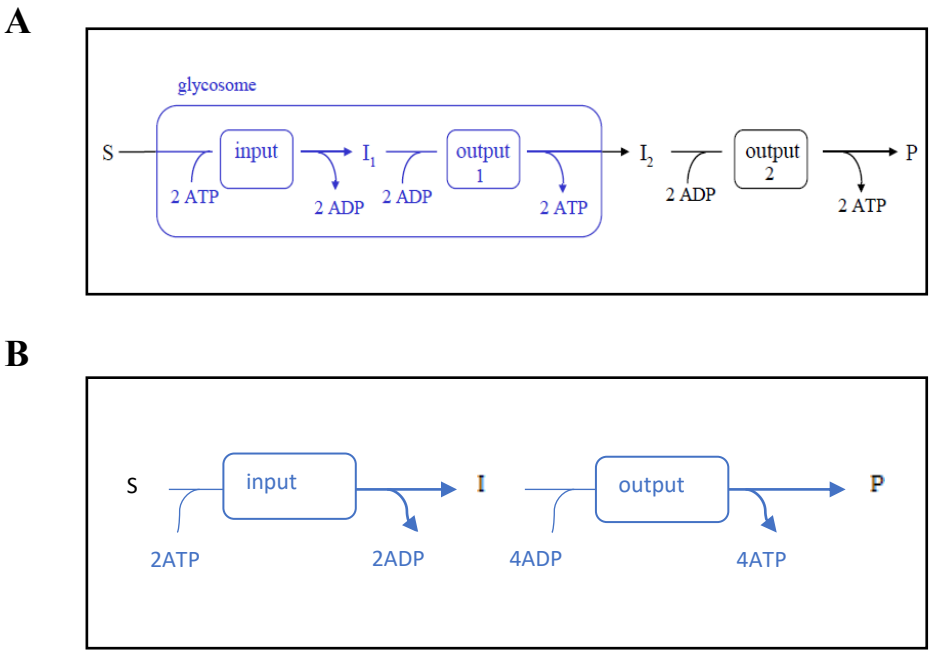

Figure 4: Compartmentalization keeps the enzymes under control without product or feedback inhibition

(**A**) The first steps of the glycolytic pathway involving hexokinase and phosphofructokinase resulting in constant investment of ATP and accumulation of intermediates which is not under control of negative feedback mechanism (P: product, I: metabolic intermediate, S: substrate) [95]. (**B**) The compartmentalization of the first few steps of glycolysis enables the maintenance of a low ATP/ADP ratio (no net ATP production in the glycosome) reducing the turnover rate of the enzymes and avoiding accumulation of intermediates (P: product, I: metabolic intermediate, S: substrate) [95].

The lower ATP/ADP ratio in the glycosome than to the higher cytosolic ATP/ADP ratio would also control the activity of phosphofructokinase and hexokinase. The decreased level of ATP reduces the turnover rate of phosphofructokinase and hexokinase which can maintain hexose phosphate levels below toxic range [95, 116, 122, 123]. Hence, compartmentalization of glycolysis has been shown to be crucial for regulation of the glycolytic pathway.

2.7 Compartmentalization of the purine salvage pathway in the glycosome

Trypanosomatid parasites lack the capacity for *de novo* synthesis of purines and therefore, completely depend upon the salvage of purines from the host [97, 124, 125]. Most of these enzymes have either a PTS1 or PTS2 signal sequence, and these parasites highly depend on purine salvage. In case of mammalian cells, they can synthesize the purines *de novo* but parasites like *Leishmania* are auxotrophic for purines and have to scavenge the purines from the host organism. Some of the enzymes participating in this purine salvage pathway, such as hypoxanthine guanine phosphoribosyl transferase (HGPRT), adenine phosphoribosyl transferase (APRT) (present in cytosol of *Leishmania*) and xanthine phosphoribosyl transferase (XPRT) are very well characterized [125-128]. In human and yeast cells, these enzymes are found in the cytosol but are localized to the glycosome of trypanosomatids [97]. It was demonstrated that glycosomal targeting was not essential for the function of these enzymes, as HGPRT and XPRT devoid of PTS signals were able to complement Δhgprt and Δxprt in *Leishmania* cells. Reasons postulated for this dual compartmentalization of the enzymes were compartmentalization may serve to increase metabolic flux or it may be providing higher metabolic flexibility to adapt to the changing host environment [129-131].

2.8 Protein transport across glycosomal membrane

Peroxisomal or glycosomal matrix proteins can be imported into peroxisomes or glycosomes as folded or oligomeric complexes without undergoing any processing (such as unfolding of proteins prior to transport) [25, 26]. Glycosomal matrix proteins are synthesized in the cytosol and are targeted for post-translational translocation across the glycosomal membrane by the

presence of peroxisomal targeting signals (PTS), namely the C-terminal PTS1 or N-terminal PTS2 topogenic signal sequence respectively [27, 28]. Proteins with a PTS1 (C-terminal tripeptide) or PTS2 (N-terminal nonapeptide) signal are bound by cytosolic peroxin receptors peroxin5 (PEX5) and peroxin7 (PEX7), respectively and bind to the glycosomal membrane associated protein peroxin14 (PEX14) which translocate and unload the protein cargo inside the glycosome [29, 30]. A third type of protein targeting involving a polypeptide internal sequence (iPTS) has been established. Additionally, some glycosomal proteins have no recognized import sequence; it is assumed that the transport of such proteins occurs by a piggy-back transport mechanism in complex with a PTS1 or PTS2 signal bearing protein [132-134]. More details about the PTS-1 and PTS-2 mediated transport across the membrane will be discussed in the following sections.

2.8.1 PTS-1 pathway

The peroxisomal targeting sequence type 1 (PTS1) signal sequence is characterized by a C-terminal degenerative tripeptide peptide S/A/C-K/R/H-L/M [123] and is present on the majority of peroxisomal matrix proteins. Around 75% of glycosomal matrix proteins bear a PTS1 signal, which is recognized by six to seven tetratricopeptide repeats (TPRs) located at the C-terminus of Peroxisomal Biogenesis Factor 5 (PEX5). TPRs are composed of 34 degenerate amino acids and comprise of a helix-turn-helix motif with interacting anti-parallel alpha helices [33, 135]. Interaction of PEX5 with PEX14 is mediated through a canonical pentapeptide motif of WXXXF/Y, or a recently identified pentapeptide motif with a LVXEF sequence located at the N-terminus of PEX5. There are eight pentapeptide motifs in human PEX5 and three in *T. brucei*

and L. donovani, of which six human and two *T. brucei* are known to interact with PEX14 (**Figure 5**) [135-138].

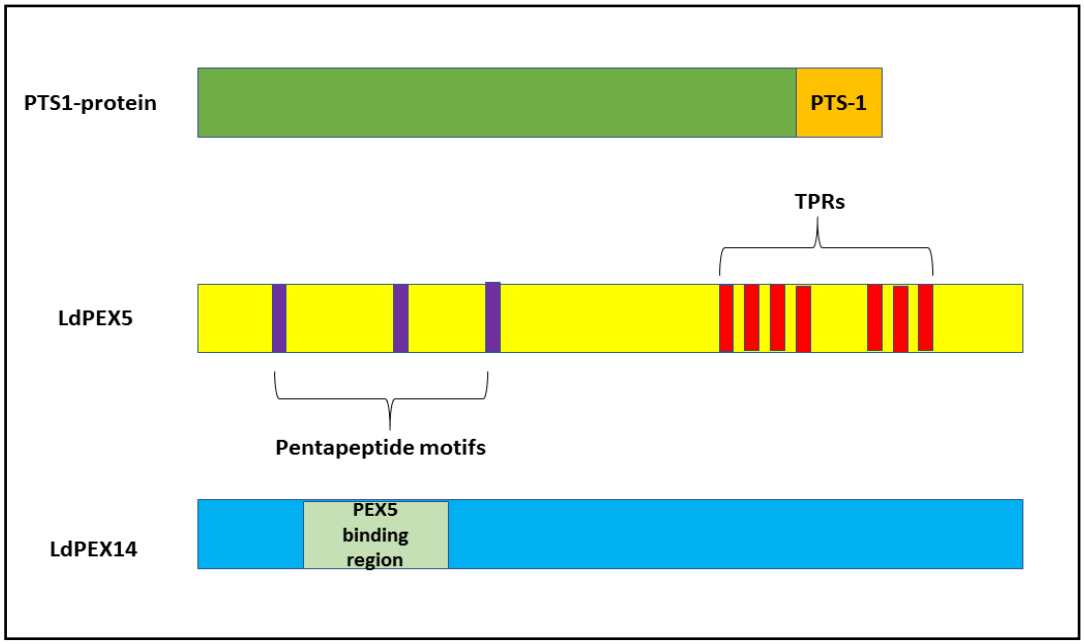

Figure 5: Schematic representation of major elements of LdPEX5 interacting with LdPEX14 and PTS-1 signal bearing protein

There are 3 canonical pentapeptide motifs at the N-terminus of LdPEX5 that can interact with the LdPEX14-NTD (N-terminal domain) and this interacting region in LdPEX14 is mapped to residues spanning 41-72 amino acids of LdPEX14. TPRs located at the C-terminus of LdPEX5 can interact with the PTS-1 signal located at the C-terminus of the cargo proteins [135, 138].

A closer look at the interaction of PEX5-PEX14, the PEX14 N-terminal domain (pex14-NTD) adopts a three-helical bundle (α_1, α_2 and α_3) where the α_1 and α_2 are the main binding interfaces for pex14-NTD and pex5 (57-71). The orientation of LVXEF motif binding to pex14-NTD was found to be in the same orientation as the pex5 W*XXX*(F/Y) peptide (mainly through electrostatic interactions). The difference lies at the interaction between the first residues of the motif (LV in LVAEF and W in WAQEF) in which Leu_{62} interacts with K_{56} of PEX14 and is not deeply buried in the hydrophobic pocket, in contrast to W_{118}. Thus, these residues (LV in

LVAEF) do not completely occupy the hydrophobic pockets, but rather establish alternative contacts with the neighbouring residues around the hydrophobic pocket (**Figure 6**).

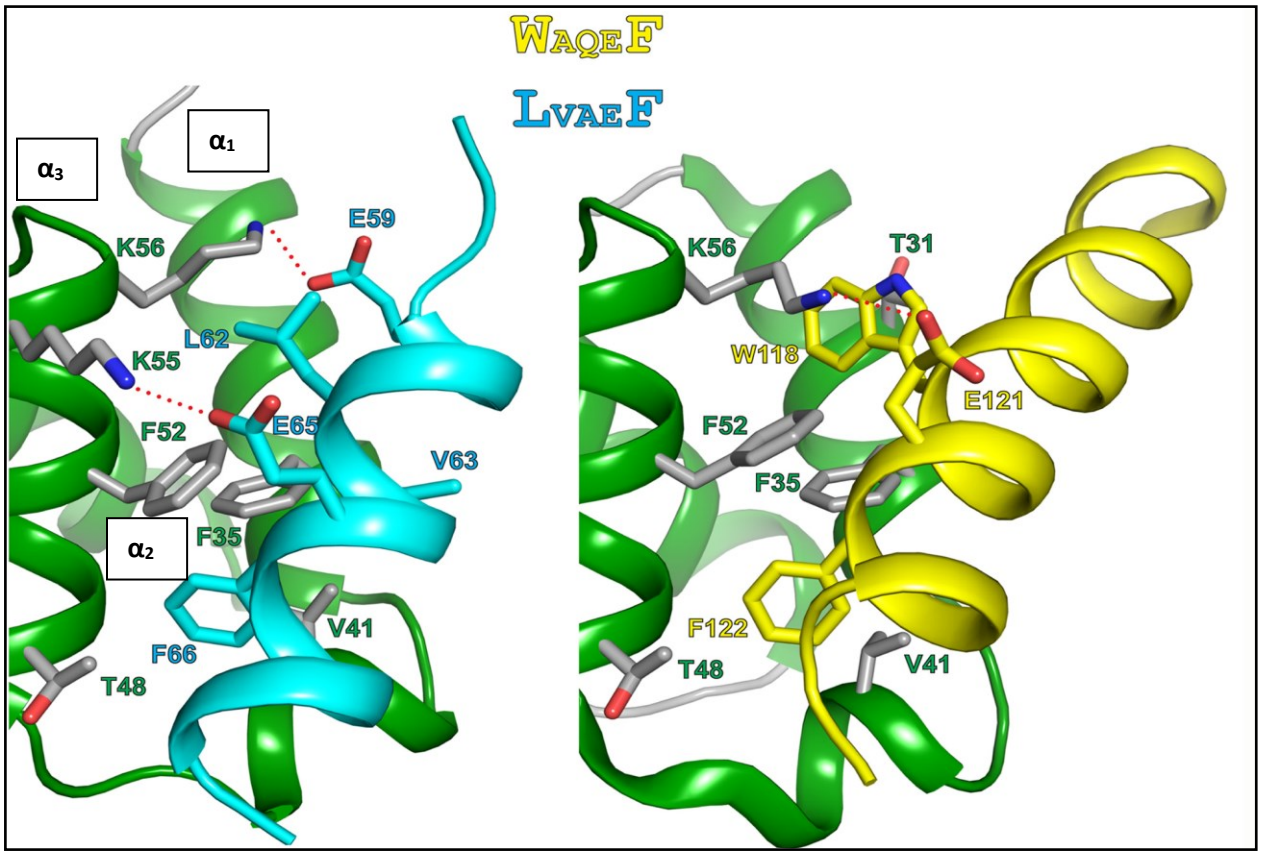

Figure 6: NMR structure of pex14-NTD -Pex5-(57–71) complex

A structural comparison of pex14-NTD (green helices) interactions with peptides LVAEF in teal (*left*) and WAQEF in yellow (*right*). The Phenyl-alanine (F_{66} in LVAEF and F_{122} in WAQEF) is depicted interacting with the hydrophobic pocket of pex14-NTD. Differences in peptide binding lies at the interaction between the first residues of the motif (LV in LVAEF and W in WAQEF) in which Leu_{62} interacts with K_{56} of pex14, and is not as deeply buried in the hydrophobic pocket compared to the W_{118} peptide [139].

The association rate of LV*X*EF with PEX14 is 3 times faster and the dissociation rate is 33 times slower, implicating its role in establishing initial contact with PEX14. PEX14 is then transferred to subsequent W*XXX*(F/Y) motifs for cargo release in the peroxisomal lumen. *In vivo* studies replacing LVAEF with a high-affinity W*XXX*(F/Y) motif showed impairment of transport across

peroxisomes. All these data confirm that the N-terminal LVAEF motif of PEX5 is crucial for peroxisomal protein import machinery (**Figure 6**) [139]. Furthermore, the N-terminus of PEX5 containing many W*XXX*F-like motifs can act as a fly-casting (similar to fishing by casting artificial flies using a lightweight rod) for binding PEX14 at the peroxisomal membrane and this may be helpful for formation of higher ordered oligomers at the surface of the membrane [140].

2.8.2 PTS-2 pathway

The peroxisomal targeting sequence type 2 (PTS2) signal sequence is characterized by an N-terminal nonapeptide with a consensus R/K-L/V/I-X_5-H/Q-L/A where X is any residue [141]. Approximately 25% of glycosomal matrix proteins bear the PTS2 signal sequence, which is believed to interact with tryptophan-aspartate repeats (WD motifs) present on receptor proteins [103, 142]. WD motifs are composed of 40-60 amino acids and form a β-propeller fold. In yeast there are six WD40 motifs on PEX7 receptor than can interact with PTS2 proteins and PEX21. PEX7 assumes a β-propeller structure and interacts with both the amphipathic PTS2 helix and PEX21 (**Figure 7**) [143]. In *L. donovani*, six WD40 repeats were predicted to form the circularized β-propeller structure [142, 144].

PEX7 contains a proline-rich region located near the C-terminal region which can form a helix that has been found to interact with the SH3 class 11 domain in Src and Grb2 proteins [145-147]. Several PEX7 co-receptors such as PEX18, PEX20, and PEX21 along with PTS2-PEX7 are required to form the import-competent complex in yeast [30, 148]. Whereas, in plants, mammals, and most probably in trypanosomes, PEX5 performs the role of a PEX7 co-receptor [30, 149, 150].

Leishmania major PEX7 (LPEX7) was found to interact with LdPEX14 and LdPEX5. The first 52 amino acids of LPEX7 mediate binding with LdPEX14. In the absence of interacting partners, LPEX7 forms a homotetrameric quaternary structure with an apparent molecular mass of ~160 kDa. The presence of a surface-exposed hydrophobic domain and interactions with the liposome also suggest the possibility of an extended shuttle for transport of PTS-2 proteins across the glycosomal membrane [144].

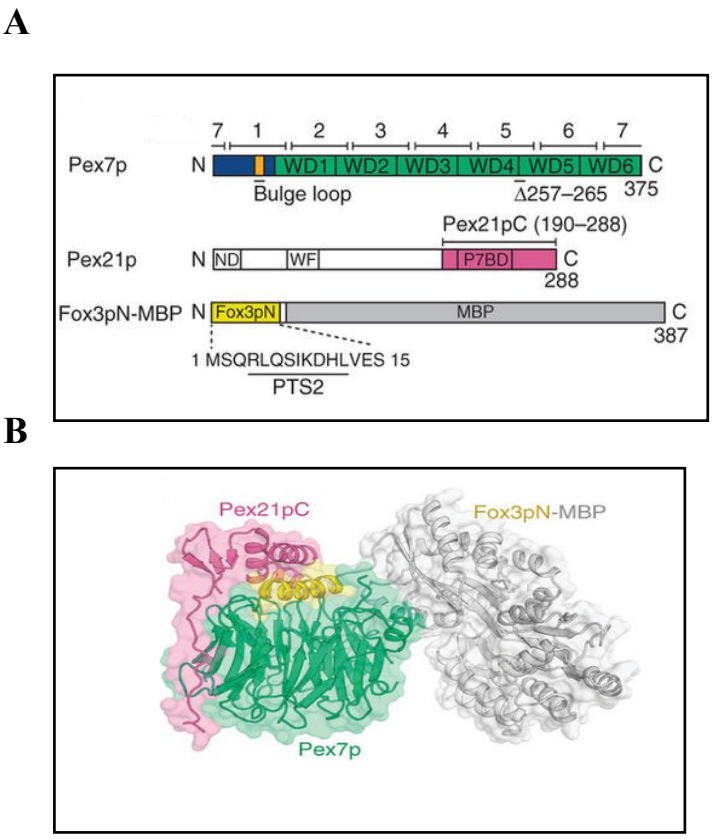

Figure 7: Crystal structure of PEX7 bound to peptides PEX21, PTS2 and Fox3pN-MBP

(A) Diagram showing various structural elements (relative secondary structure motif locations) of the crystallized protein. WDs indicate the WD40 motifs of PEX7, WF represents W*XXX*[F/Y] motifs that can bind PEX14 PEX7BD represents PEX7 binding domain. **(B)** Skeleton representation of the PEX7–PEX21C–Fox3pN-MBP complex [143].

In the current model of protein transport across the glycosomal membrane in *Leishmania*, the PTS2 containing protein is first bound to LdPEX7, then the PTS2-LdPEX7 complex with or

without LdPEX5 (under investigation) moves towards the glycosomal membrane where they bind LdPEX14 to form the docking complex. Proteins bearing PTS-1 signal bind to LdPEX5 and then docks to LdPEX14. After unloading the protein cargo, LdPEX5 and LdPEX7 are recycled back to the cytosol (under investigation). The above findings suggest that there are disparities between the import machinery in *Leishmania* and other eukaryotes, making the glycosomal import machinery a viable drug target (**Figure 8**).

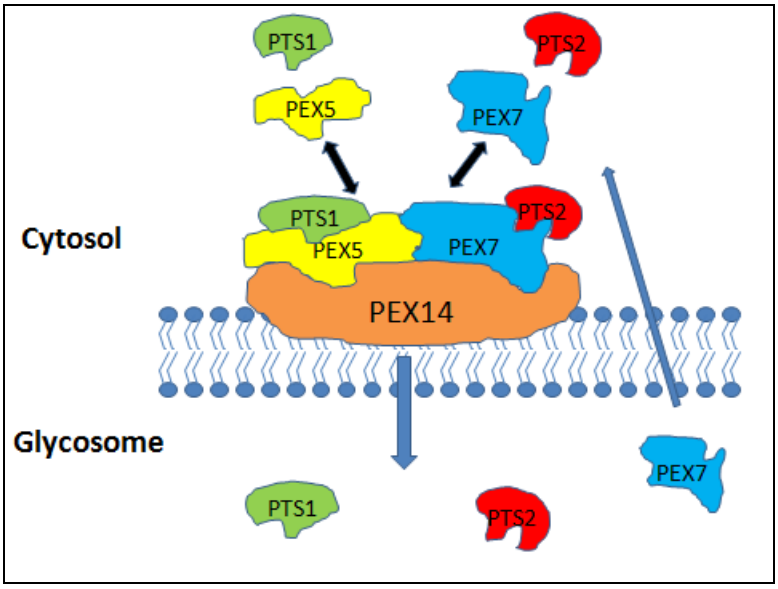

Figure 8: Current working model of glycosomal protein import

Leishmania glycosomal proteins are synthesized in the cytosol and post-translationally imported into the glycosome via a C-terminal PTS1 or N-terminal PTS2 signal sequence. These are bound by the cytosolic receptor proteins LdPEX5 and LdPEX7, respectively, which then dock to the glycosomal membrane-associated protein LdPEX14. The cargo proteins are translocated to the lumen of glycosome followed by possible recycling of receptors back to the cytosol [33, 135, 142].

2.9 Glycosomal receptor interactions as a drug target

The glycosome was found to be essential for the viability of the kinetoplastid parasites [151] and functional glycosomal peroxin proteins were found to be critical for the survival of the parasite

[23, 31, 150]. Inhibitors of protein-protein interactions (PPIs) have emerged as a new class of potential drugs and the drug discovery process depends upon availability of highly defined protein structures [152, 153]. Various PPIs have entered clinical trials, some of which producing excellent drugs that are now are available to patients for treating various diseases. One such example is tirofiban and target integrins used for treating cardiovascular diseases [154]. Recently there have been improvements in elucidating structural components of the protein-protein interactions between glycosomal PEX proteins.

Inhibitors designed to disrupt PEX5-PEX14 interactions are predicted to mislocalize glycosomal enzymes to the cytosol resulting in metabolic toxicity and death of the parasite (cell-based assay) [155, 156]. Even though the hydrophobic pockets in the PEX14-PEX5 binding surface of human and *T. brucei* are conserved, subtle differences in amino acids found at the PEX5 binding pockets of PEX14 drive the specificity of inhibitors. For example, *T. brucei* has a E_{34} compared to K_{34} in human PEX14, and a more soluble and potent inhibitor was designed with an -NH_2 group oriented towards the carboxylate end of E_{34} resulting in electrostatic attraction as compared to repulsion from the positively charged K_{34} (**Figure 9**) [155]. Studies conducted in *T. brucei* infected mice reported reduced parasitemia after 5 days of oral treatment with these PPI lead compounds[156]. These results are promising and indicate a new avenue for development of PPIs that can kill parasites and reduce the mortality and morbidity associated with these infections.

A

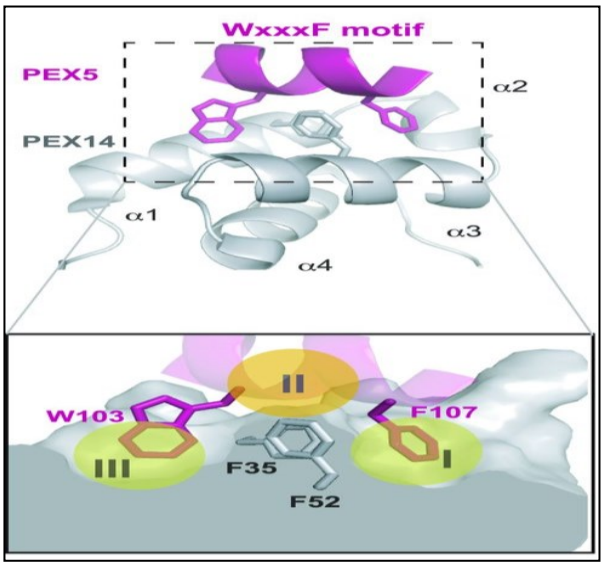

B

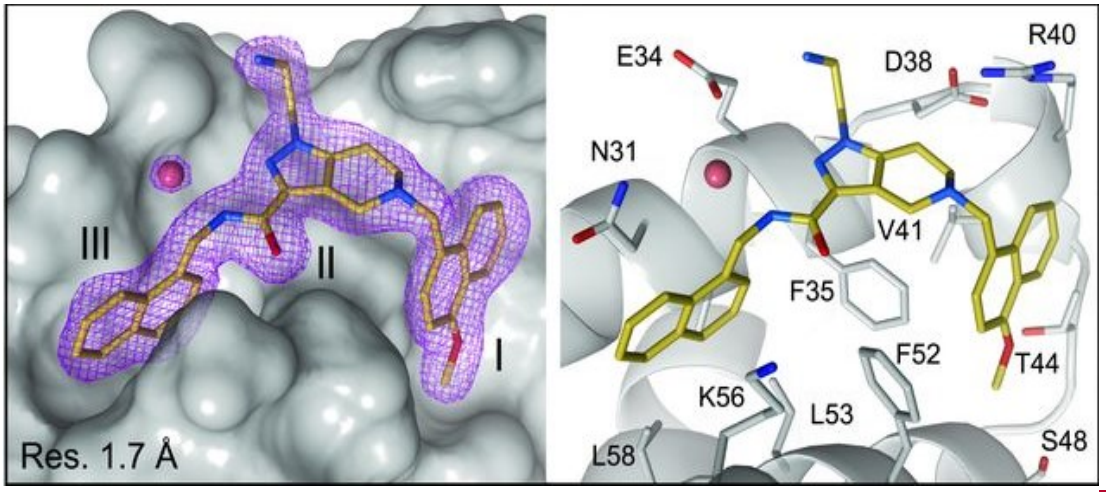

Figure 9: Design of PEX14-PEX5 interaction inhibitors

(**A**) Structure showing PEX14-PEX5 interface. PEX14-PEX5 interaction are mainly mediated through N-terminal PEX14 helical folds and the W*XXX*F motif of PEX5. The F_{35} and F_{52} are partially exposed residues between cavities **I** and **III** and docking of the ligand shields it from solvent exposure. PPIs could disrupt the PEX14-PEX5 interaction. The W_{103} and F_{107} of PEX5 occupies the cavities **I** and **III.** (**B**) Crystal structure of PEX14-PEX5 interaction inhibitor. Structure of PEX14 bound with pyrazolo[4,3-*c*] pyridine scaffold derivative-based inhibitor that target the PEX14-PEX5 interaction [155].

2.10 Transport of folded proteins across glycosomal membrane: A mystery still unresolved

Intense research has been conducted in the field of peroxisome biology for the past 50 years, but it is still obscure how exactly large folded proteins get transported across the peroxisomal membrane. Novel approaches involving structural biology have been used to gain insights to crucial protein-protein interactions but lack a perspective of the actual milieu containing a lipid (peroxisomal) membrane.

Transport across the peroxisome is unique as it involves the transport of folded, co-factor-bound and oligomeric proteins across its membrane [26, 157]. In yeast and higher eukaryotes, PEX5 has been shown to follow two possible pathways to unload cargo into the peroxisomal lumen. The first scenario is a shuttle model where PEX5 dips into the membrane and releases cargo into the peroxisomal lumen. The second pathway is an extended shuttle model where PEX5 gets translocated into the peroxisomal matrix, releases its cargo inside the peroxisomal matrix and a shorter form of modified PEX5 get released into the cytosol [158, 159]. PEX7 was shown to follow an extended shuttle model where it goes in and out of the peroxisomes. From the above experiments it was illustrated that PEX5 and PEX7 are exposed to the lumen of peroxisomes [160, 161].

There are various hypotheses regarding the transport of protein across the peroxisomal membrane but is commonly thought to be mediated through membrane invagination events, vesicle fusion or the presence of large import pores. It was demonstrated that a gated ion-conducting channel (formed by membrane-associated import receptor PEX5 and PEX14) can be opened to a diameter of roughly 9 nm by the cytosolic receptor-cargo complex [35]. Large complexes (~600-800 kDa) of PEX14 and PEX5 have been identified in yeast peroxisomal membranes. Electrophysiological experiments with this complex in the presence of liposome

showed that it can form pores in the liposome with a diameter of around 0.6 nm. When the same complexes were purified from yeast mutants lacking PEX8 and PEX7 co-receptors, they form gated and stable pores with a diameter of 3.8 nm. Subsequent docking with the above-mentioned complexes with the cytosolic receptor–cargo complex resulted in widening of the channel (~9 nm) to a size sufficient to pass large oligomeric proteins. Previous studies suggested the presence of a pore large enough to pass a PTS1-decorated gold particle [35, 36, 162, 163].

The convergence of both PTS-1 and PTS-2 pathways at the level of the PEX14 receptor are still accepted in the field, but recent reports suggest co-convergence. The presence of a functional import pore in the absence of PTS-2 receptors as mentioned above, and identification of a PTS-2 pore having an estimated pore size of ~4.7 nm (completely in open state) facilitated by PEX18 and the PEX14/PEX17 heteromer, support the presence of distinct pores for the PTS-1 and PTS-2 transport system [34, 164]. PEX14 is a critical component of both PTS-1 and PTS-2 pores and is thought to mediate a crucial role in building the translocation pore to transport the cargo across the membrane. Similar electrophysiology experiments with isolated glycosomes from *T. brucei* in planar lipid bilayers revealed the presence of conductance channels, hypothesized to be pore-forming channels connecting the glycosomal lumen and the cytosol [143].

In the case of mammalian PTS-2 mediated peroxisomal transport, PTS-2 cargo-bound receptor protein PEX7 binds to the co-receptor PEX5L. Cargo binding was found to be a prerequisite for PEX7-PEX5 interaction and the interaction strength of the cargo and PEX7 was highly increased in the presence of an alternatively-spliced longer variant of co-receptor PEX5L to form a stable ternary complex (PEX5L/PEX7/PTS2). It was found that formation of this ternary complex was a prerequisite for PTS-2 mediated transport across the peroxisomes [165].

In yeast, it was found that the ternary complex is formed hierarchically; PEX7 binds to the PTS-2 proteins in the cytosol, then the co-receptor binds to this complex to form a ternary complex (PEX20/PEX7/PTS2). Specifically, in *S. cerevisiae* the role of PEX20 is performed by the redundant proteins PEX18 and PEX21. It was also observed that PEX13 and PEX14 provides initial binding sites for the ternary complex at the peroxisomal membrane surface [166, 167].

It is unclear whether PEX7 follows a normal shuttle or an extended shuttle pathway. In yeast it was shown that PEX7 can be completely translocated into the peroxisomal matrix [161]. In mammalian systems, PEX7 was found to be retained at the peroxisomal docking/translocation machinery (DTM) comprised of PEX13, PEX14, and the RING peroxins PEX2, PEX10, and PEX12 (**Figure 10**) [168]. Until now, at least two proteins have been found to be part of the docking complex in all organisms. In *S. cerevisiae* the docking complex consists of membrane proteins PEX13, PEX14 and PEX17 [169, 170]. In *T. brucei*, the docking complex may have PEX13 along with PEX14 as two contrasting isomers of PEX13 (PEX13.1 and PEX13.2) has been identified to be associated with glycosomes [171]. Also, in *L. donovani*, PEX13 and PEX14 may be forming the docking complex, as PEX13 associated with glycosomal fractions have been recently identified [172]. Apart from the docking complex, several other PEX proteins are believed to participate in the import cycle, such as the RING finger proteins PEX2, PEX10 and PEX12 [173-175].

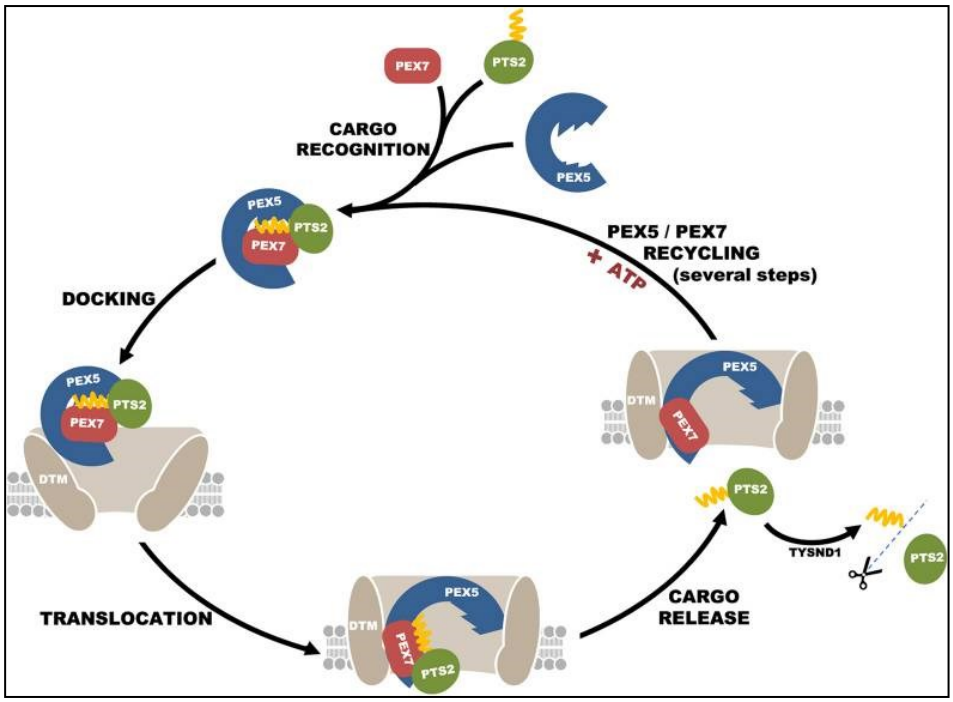

Figure 10: PTS2-mediated protein import into peroxisomes

The PTS-2 signal bearing proteins bind to the PEX7 and then to the PEX5 to form a stable ternary complex. This complex dock to the docking/translocation machinery DTM (comprising of PEX13, PEX14, and the RING peroxins PEX2, PEX10, and PEX12) at the membrane and then get inserted into the DTM. Subsequent conformational changes brought at PEX5 weakens the interaction between PEX7-PTS-2 and results in the release of PTS-2 into the peroxisomal matrix. The peroxisomal matrix peptidase TYSND1 cleaves the PTS-2 signal and the receptors are recycled back into cytosol [168].

2.11 Targeting of membrane proteins to peroxisomes and glycosomes

Peroxisomal membrane proteins (PMPs) are targeted to the peroxisomes by one of two pathways, either directly, or indirectly through the endoplasmic reticulum (ER). The PMPs are translated in the cytosol with the help of free polyribosomes and translocated into the peroxisomal membrane. The targeting signal for the PMPs called membrane PTS (mPTS) is composed of a cluster of positively charged, or a mixture of positively charged and hydrophobic residues flanked by one or two transmembrane segments. There are two types of mPTS, those

can bind and are imported to the peroxisomes with the help of PEX19, called class 1 or mPTS1, and those that not need a PEX19 aid are called class 2 or mPTS2 [176-178].

In the direct targeting pathway of PMPs, PEX19 acts as a soluble recycling chaperone which binds the newly formed PMPs and helps to keep them in soluble and stable conformations. The PEX19 bound to the cargo then docks on PEX3, which acts as the membrane anchor to form a ternary complex, and the PEX3–PEX19 interaction inserts PMPs into the peroxisomal membrane (**Figure 11A**) [179, 180]. In the indirect targeting pathway, the PMPs destined for the peroxisomes are first inserted into the ER membrane and subsequently translocated into the peroxisome (**Figure 11B**).

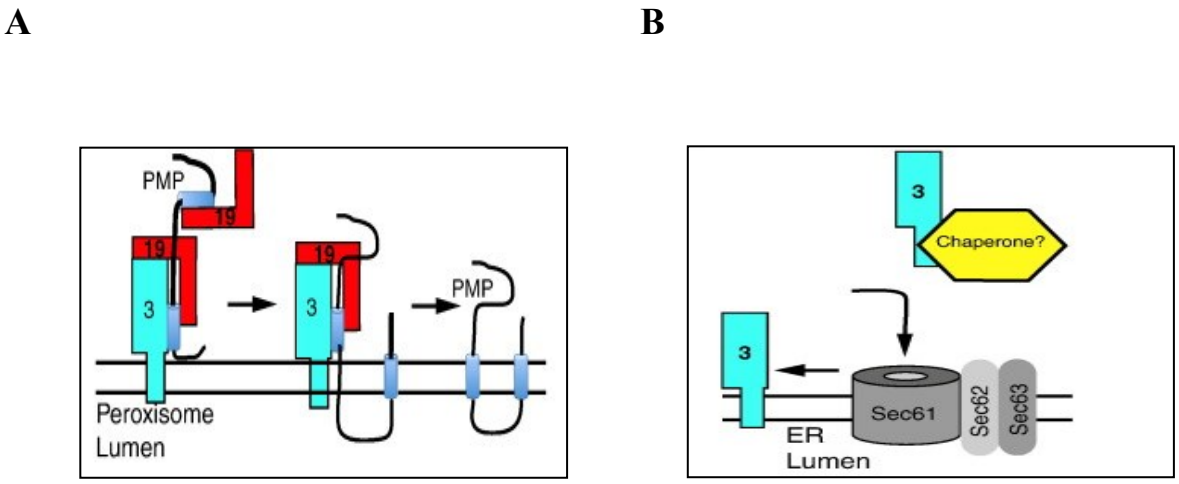

Figure 11: PMPs targeting pathway

(**A**) Direct PMP targeting pathway. Insertion of PMPs to the peroxisomal membrane with the help of cytosolic receptor/chaperone PEX19 and the membrane anchor PEX3 [adapted from [160]]. (**B**) Indirect PMP targeting pathway. In yeast, it was shown that PMPs and PEX3 are inserted into the ER with the help of Sec translocon and subsequently transported to the peroxisomes. The role of a chaperone is not clear in this pathway [adapted from [160]].

The finding of glycosylation of PEX2 and PEX16 gave a clue about the role of ER sorting in targeting of PMPs to peroxisomes. Different proteins including PEX3, PEX16

(mammals), and PEX3, PEX15 and PEX22 (yeast) follow this ER to peroxisome pathway. In yeast, it was shown that depletion of Sec62/Sec63 translocon resulted in mislocalization of GFP labelled PEX13 indicative of the role of the ER to peroxisome pathway [181, 182].

Whether the targeting of PEX14 into the peroxisomal membrane is Pex19-dependent or not is still under investigation. NMR studies have revealed that human PEX14 binds the soluble receptors PEX19 and PEX5. The N-terminus of PEX14 was found to adopt a three-helical fold where PEX5 (WXXXF/Y motif) and PEX19 (F/YFXXXF motif) ligand helices bind competitively at the same surface of PEX14 with opposite directionality. Mutational studies altering residues of PEX14 that interact with PEX5/PEX19 disrupted the binding, and corresponding full length PEX14 forms were unable to localize to the peroxisomal membrane, indicating that the N-terminal domain can modulate the targeting of PEX14 into peroxisomes [183, 184].

Regarding protein targeting in kinetoplastids, the specificity of *T. brucei* PEX19 was found to be very similar to human and yeast PEX19. The requirement of a PEX19 binding site and a transmembrane domain for inserting proteins to *T. brucei* glycosomal membrane are indications of conservation of PMP transport across distant phyla. The *T. brucei* PEX10 and PEX12 were found to traffic to human peroxisome but *T. brucei* PEX14 was unable to get into the human peroxisomes [185]. *T. brucei* PEX14 lacks a significant PEX19 (prediction performed by using algorithm) binding site, and expression of GFP-TbPEX14 in human fibroblasts ended up in the cytosol whereas the same construct (GFP-TbPEX14) targeted to glycosomes in *T. brucei,* indicating that the PEX14 in kinetoplastids is a special candidate of PMPs, which are targeted to the glycosomes through a different targeting pathway as seen in higher eukaryotes [185-187].

Also, in contrast to the large set of peroxins required for matrix protein import in human and yeast, only a limited number of peroxins are identified in kinetoplastid parasites. A

comprehensive list of peroxin proteins present in *Leishmania* species, yeast/fungi and human have been listed in **Table 2**.

Table 2: **Peroxin (PEX) proteins found in various species**

Peroxin	*Leishmania* species	Yeasts/fungi	Human
PEX1	X	X	X
PEX2	X	X	X
PEX3		X	X
PEX4		X	
PEX5	X	X	X
PEX6	X	X	X
PEX7	X	X	X
PEX8		X	
PEX9		X	
PEX10	X	X	X
PEX11	X	X	X
PEX12	X	X	X
PEX13	X	X	X
PEX14	X	X	X
PEX15		X	
PEX16	X	X	X
PEX17		X	
PEX18		X	
PEX19	X	X	X
PEX20		X	
PEX21		X	
PEX22		X	
PEX23		X	
PEX24		X	
PEX25		X	
PEX26		X	X
PEX27		X	
PEX28		X	
PEX29		X	
PEX30		X	
PEX31		X	
PEX32		X	

Table 2 lists Peroxin homologues found in *Leishmania species (including L. major, L. infantum, L. mexicana, L. braziliensis*, and *L. donovani*) Yeast or fungi (*Saccharomyces cerevisiae, Yarrowia lipolytica, Pichia pastoris, Hansenula polymorpha* and *Neurospora crassa*) and human. X denotes potential homologues of this peroxin; however, not all have been confirmed experimentally [16, 30, 148, 172, 188-191].

2.12 Significance of LdPEX14 and the role of the hydrophobic region

In the earlier sections we discussed the general concepts of protein transport across peroxisomal/glycosomal membranes. The cargo loaded PEX5 and PEX7 receptors dock to the membrane associated PEX14 protein and helps to translocate the cargo proteins across the peroxisomal/glycosomal membrane. Little is known about the mechanistic details of the role of PEX14 in the formation of the translocation pore. PEX14 was found to be very important for survival of kinetoplastid parasites as knockout cells of *L. donovani* were not viable and silencing of PEX14 was lethal to *T. brucei*[23, 31]. From analysis of the primary structure of LdPEX14 (464 amino acids), many interacting domains have been mapped: the LdPEX5 binding domain, LdPEX7 binding domain, leucine zipper, and a hydrophobic region (**Figure 12**). It has been demonstrated that the hydrophobic region of ldpex14 (120-200) is essential for binding to liposomes that mimic the glycosomal membrane and that this binding event caused leakage of carboxyfluorescein dye encapsulated liposomes [29, 32, 135, 142, 144].

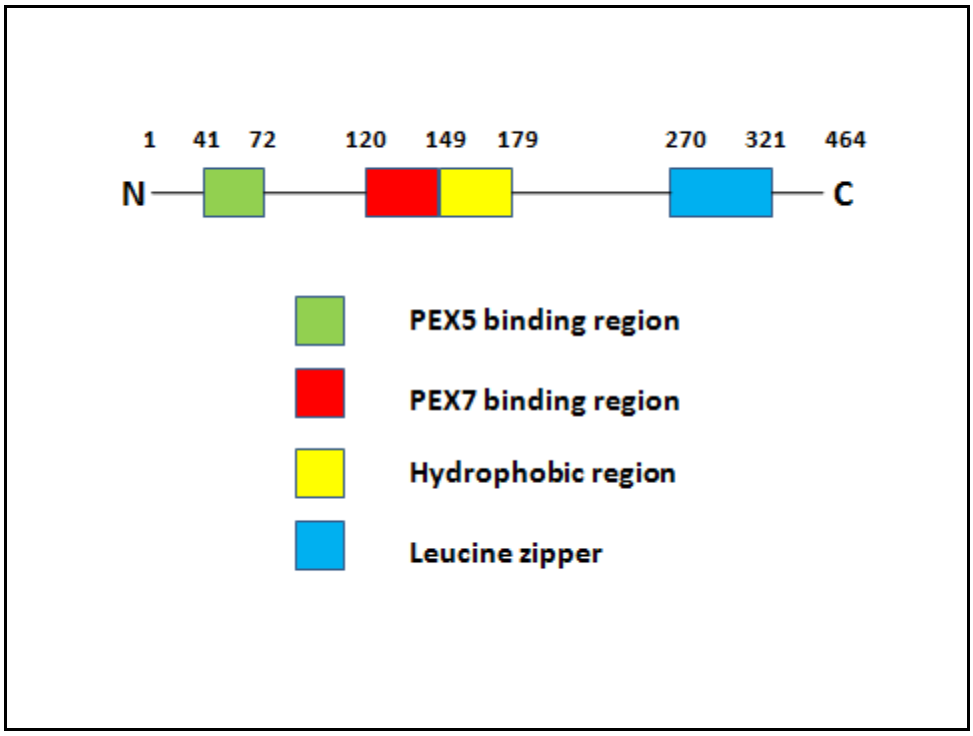

Figure 12: Primary structure of LdPEX14

Several interaction domains are present on LdPEX14 including a LdPEX5 binding site, LdPEX7 binding site, a hydrophobic region, and a leucine zipper [29, 32, 135, 142, 144].

Multiple protein sequence alignments of PEX14 from different species show that only 6 amino acids are conserved. A conserved transmembrane domain however; was observed among all species, indicating the potential importance of this region (**Figure 13**) [29].

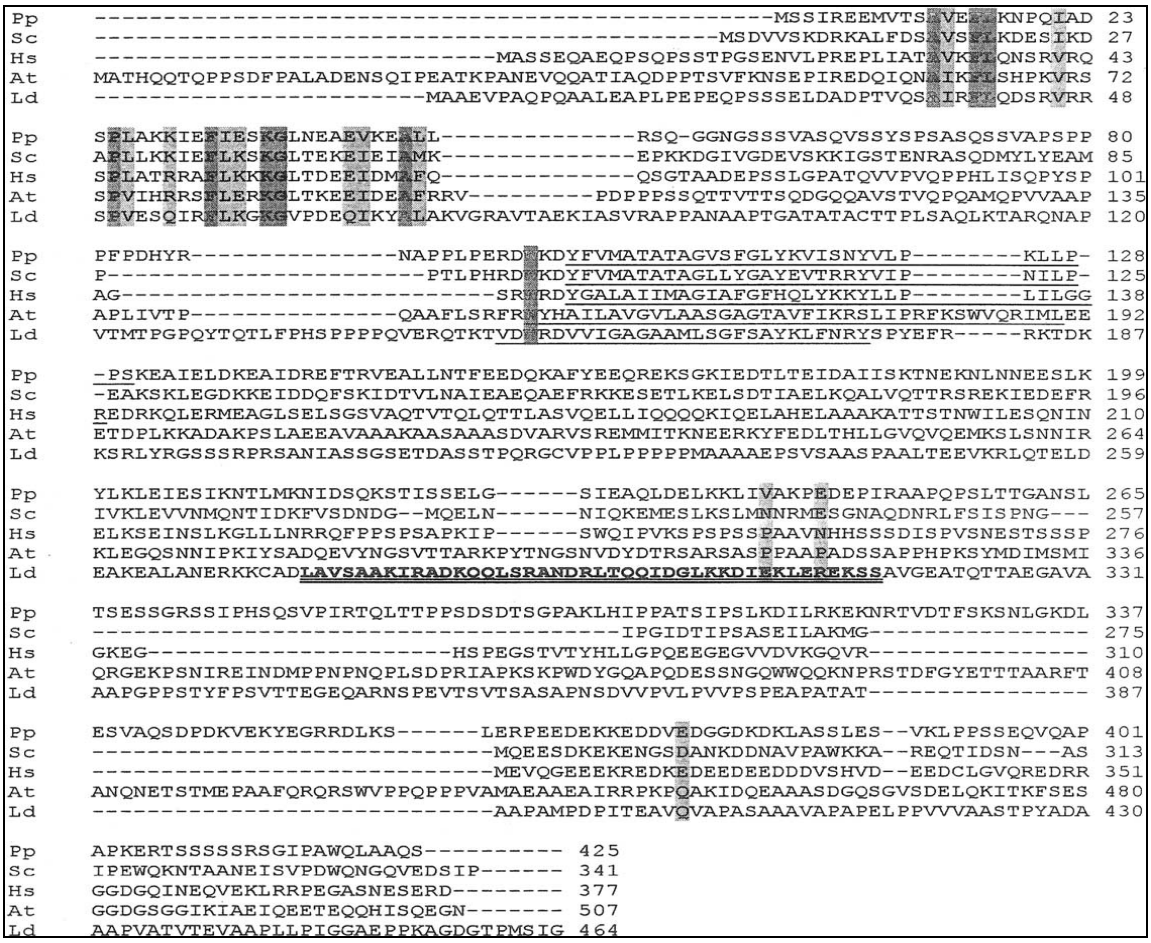

Figure 13: Sequence alignment of PEX14 proteins

A CLUSTALX based multiple sequence alignment of PEX14 proteins indicating putative PEX14 transmembrane regions (underlined) (Pp: *P. pastoris*, Sc: *S. cerevisiae*, Hs: *Homo sapiens*, At: *A. thaliana*, and Ld: *L. donovani*) [29].

Flotation density centrifugation studies (membrane binding assay) using large unilamellar vesicles (LUVs) that mimic the lipid composition of glycosomal membrane, phosphatidylethanolamine (DOPE-55%), phosphatidylcholine (DOPC-25%), phosphatidylglycerol (DOPG-15%), phosphatidylinositol (PI-2.5%), cholesterol (2.5%) (**Figure 14**) demonstrated that the proposed hydrophobic region ldpex14 (120-200) bound to membrane; whereas the internal deletion mutant ldpex14 (Δ149-179) lacking the hydrophobic region failed to bind to membranes (**Figure 15A**). Phospholipids found in the glycosomal membrane were

modified primarily with C18 and C22 unsaturated fatty acid [32]. It was also demonstrated that anionic phospholipids were required for LdPEX14 association with lipid bilayers. Monolayer experiments demonstrated that the presence of anionic phospholipids and phospholipids with unsaturated fatty acids increases the membrane fluidity, that aids in the insertion of LdPEX14 into biological membranes. (**Figure 15B**) [32]. These physiochemical properties of the phospholipids might be crucial for allowing large scale structural rearrangements of the LdPEX14 proteins to induce formation of a transient pore in the glycosomal membrane.

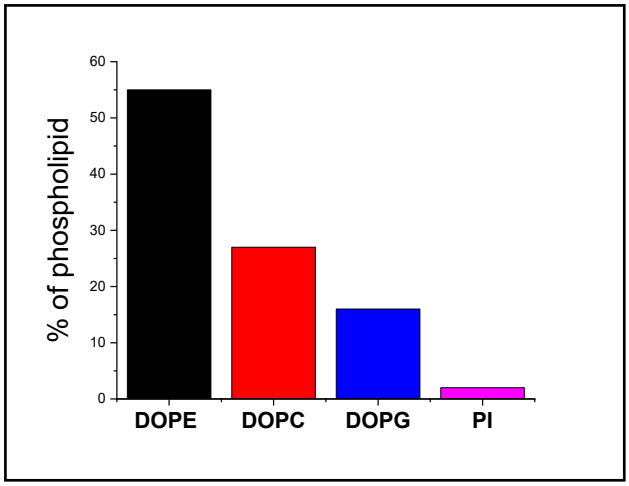

Figure 14: Relative distribution of phospholipids in the *Leishmania* glycosomal membrane

The distribution of phospholipid in the liposome were 1,2-dioleoyl-sn-glycero-3-phosphoethanolamine (DOPE-55%), 1,2-dioleoyl-sn-glycero-3-phosphocholine (DOPC-25%), 1,2-Dioleoyl-sn-glycero-3-phosphoglycerol (DOPG-15%), phosphatidylinositol (PI-2.5%) and cholesterol (2.5%) [32].

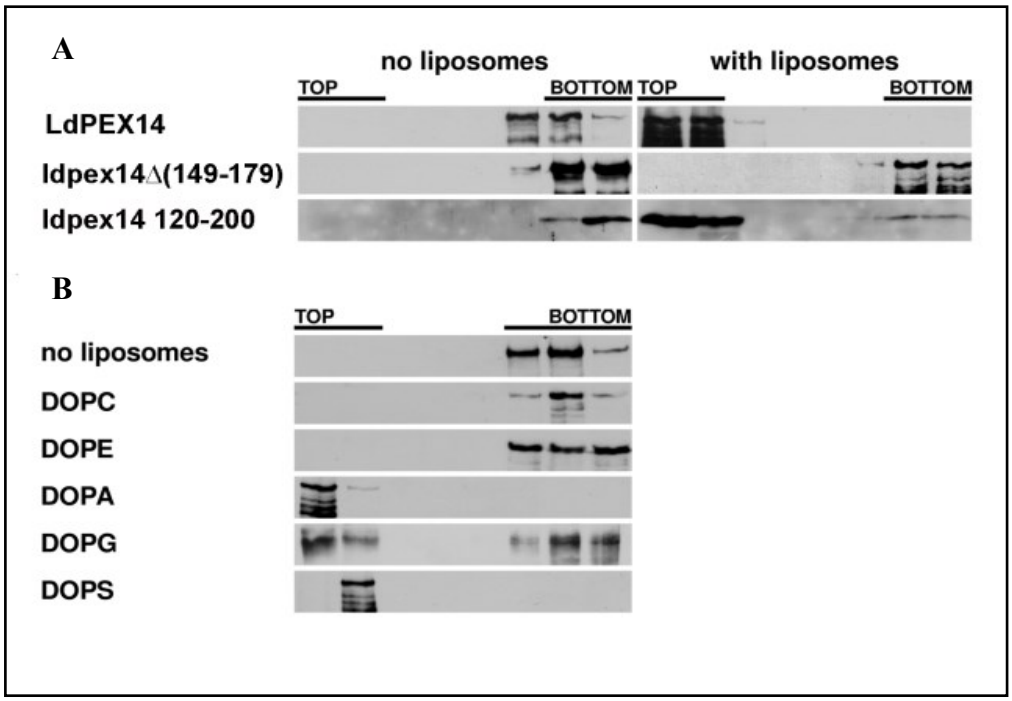

C

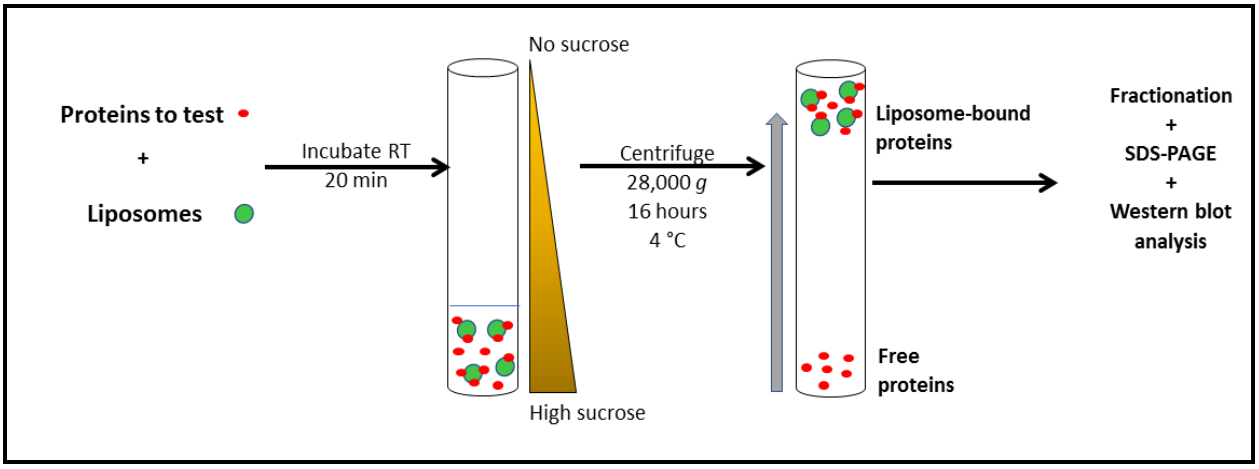

Figure 15: Membrane binding assay (flotation assay)

The sucrose density flotation assay (**A**) with proteins LdPEX14, ldpex14 (Δ149–179) and ldpex14 (120–200)) were performed in the presence and absence of liposomes, showing fragments encompassing the hydrophobic region, ldpex14 120-200 exclusively bound to the liposomes, showing that LdPEX14/membrane interaction is dependent on the hydrophobic domain of ldpex14 (120-200), (**B**) with protein LdPEX14 in presence of single phospholipids DOPC, DOPE, DOPA, DOPG, or DOPS, showing anionic phospholipids were required for LdPEX14 association with lipid bilayer (top means first fraction (Fraction:1) of the sucrose gradient collected from an open tube and bottom is the last fraction (Fraction:8)) [32], (**C**) Schematic representation of basic steps involved in a flotation assay.

FACS analysis conducted using LUVs with fluorescently labelled LdPEX5 (Oregon Green) and LdPEX14 (Bodipy 630/650) demonstrated that the association of LdPEX5 with the LUVs was dependent on the presence of LdPEX14 (**Figure 16**) [32].

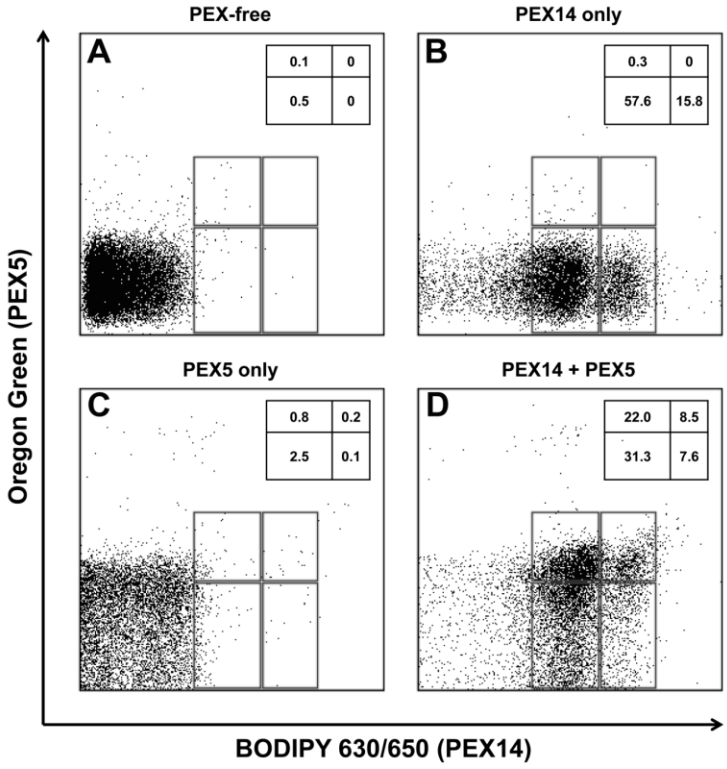

Figure 16: FACS analysis of LdPEX5 and LdPEX14 in presence of LUVs

(**A**) LUVs (**B**) Oregon Green-tagged LdPEX5 (**C**) Bodipy 630/650 tagged LdPEX14 **(D)** LdPEX5 (5 µg)/LdPEX14 mixture. The LUVs showed low auto fluorescence; hence the proteins in (**B**), (**C**), and (**D**) were analyzed in presence of LUVs. It demonstrated that interaction of LdPEX5 in presence of LdPEX14 were able to give rise to subpopulations of LUVs with intermediate (~22%) and high fluorescence intensities (~9%) that contain both LdPEX5 and LdPEX14 indicating association of LdPEX5 with the LUVs was dependent on LdPEX14 [32].

Connecting statement

Sucrose density centrifugation and fluorescence-activated cell sorting techniques have established that LdPEX14 membrane-binding activity is dependent on a predicted transmembrane helix found within residues 149-179 of LdPEX14. A question arises; how does this hydrophobic region integrate into the membrane, and furthermore what are the possible orientations of this hydrophobic domain within a pore forming structure embedded in the glycosomal membrane **Chapter 3** of the thesis will focus on predicting the topology of the hydrophobic region inserted into the membrane and investigating the underlying mechanism of the pore formation for the transport of cargo proteins across the membrane bilayer.

Chapter 3

Analysis of the *Leishmania donovani* Peroxin 14-membrane interaction

Anwer Hasil Kottarampatel[1,2], Normand Cyr[1,2‡], and Armando Jardim[1,2*]

*[1]Institute of Parasitology and [2]Centre for Host-Parasite Interactions, Macdona*ld *Campus of McGill University, Ste-Anne-de-Bellevue QC, Canada.*

Running Title: Topology of the LdPEX14 hydrophobic domain

Keywords: *Leishmania*, glycosome, LdPEX14, peroxin, protein-membrane interaction, fluorescence.

Abbreviations:

LdPEX, *Leishmania donovani* peroxin; PTS, peroxisomal targeting signal; 10-DN, 10-doxylnonadecane; LUV, large unilamellar vesicle; SUV, small unilamellar vesicle; DQA, dual fluorescence quenching assay.

[*]To whom correspondence should be addressed: Institute of Parasitology, Macdonald Campus of McGill University, 21, 111 Lakeshore Road, Ste. Anne-de-Bellevue, Québec, Canada H9X 3V9. Phone: (514) 398-7727; Fax: (514) 398-7857, email: armando.jardim@mcgill.ca; Current address: [‡]Département de biochimie et médecine moléculaire, Faculté de médecine, Pavillon Roger-Gaudry, bureau G-318, Université de Montréal, C. P. 6128, Succ. Centre-ville, Montréal (Québec), H3C 3J7.

Abstract

Leishmania donovani PEX14 (LdPEX14) is a glycosomal membrane associated protein required for binding the cargo receptor LdPEX5 and LdPEX7. Here we show that a hydrophobic region spanning residues (120-200) is essential for the insertion of LdPEX14 into lipid bilayers that mimic the phospholipid composition of the *L. donovani* glycosomal membrane. Investigations of this protein-membrane interaction were facilitated by a panel of tryptophan and cysteine mutants constructed within the hydrophobic region. Fluorescence quenching studies were performed to examine the topology and orientation of the hydrophobic region in the lipid bilayer. Forster Resonance Energy Transfer (FRET) and tryptic analysis utilizing ldpex14(120-200), which formed a functional pore structure, demonstrated that the hydrophobic segment exposes both the N- and C-termini to the extra-luminal space when bound to unilamellar vesicles. The hydrophobic region has a propensity to oligomerize in the presence of unilamellar vesicles. ldpex5(203-391) induce conformational changes in LdPEX14 which triggered the hydrophobic region to insert deeper into the lipid bilayer. These fluorescence properties were utilized to construct a membrane bound topology model for the hydrophobic region of ldpex14.

Introduction

Leishmaniasis is a spectrum of diseases caused by the obligate intracellular parasite *Leishmania spp.* [1, 192]. *Leishmania,* like other kinetoplastid parasites, has a unique microbody organelle called a glycosome that is evolutionarily related to peroxisomes of yeast, fungi, plants, and mammalian cells [22]. Glycosomes are indispensable subcellular structures required for the compartmentalization of a myriad of enzymes vital for a variety of metabolic and biosynthetic pathways that include; glycolysis, pentose phosphate pathway, ether lipid biosynthesis, and purine salvage [18, 104, 123]. A number of genetic and pharmacological studies have demonstrated that correct targeting of metabolic machinery, especially enzymes of the glycolytic pathway, to the glycosome is crucial for parasite viability [23, 155, 156].

Glycosomal proteins synthesized by cytosolic ribosomes are targeted to the glycosome by a C-terminal peroxisomal targeting signal sequence 1 (PTS1) with a typical consensus sequence [A,S]/[K,R,N,H]/[L,M,V,Y] or an N-terminal PTS2 signal that consists of a nona-peptide with the consensus sequence [RK]-[LVI]-[X]5-[HQ]-[LA] [28, 155, 189, 190]. In *Leishmania*, the PTS1 and PTS2 motifs are recognized by the cytosolic receptor proteins, peroxin5 (LdPEX5) or peroxin7 (LdPEX7), respectively; which facilitate the trafficking and import of protein into the glycosomal matrix. The import of newly synthesized matrix proteins is dependent on four major steps that are orchestrated by several heteromeric complexes located in the cytosolic compartment and glycosome/peroxisome membrane surface. These events include, (i) sorting/trafficking of nascent matrix proteins by the receptors PEX5 and PEX7, (ii) binding of the cargo loaded PEX5 and PEX7 to the docking/importomer complex which is situated and exposed to the cytosolic face of the glycosome/peroxisome membrane, (iii)

translocation of the cargo proteins across the organelle membrane, and (iv) recycling of the PEX5 and PEX7 receptors back into the cytosol for another round of protein import.

A key component required for glycosome/peroxisome import of nascent polypeptides is PEX14; a membrane protein that functions as a docking receptor for the cargo loaded PEX5 and PEX7 receptors and in the formation of a translocation pore. In kinetoplastid parasites, PEX14 is a crucial component required for glycosome biogenesis since knocking down the levels of PEX14 blocks glycosomal import of PTS1and PTS2 proteins which results in the mistargeting of the glycolytic enzymes hexokinase and phosphofructokinase in the cytosol which is lethal to these parasites [29, 31, 123, 137]. More recently pharmacological studies have demonstrated that blocking the binding of PEX5 to PEX14 is lethal to *Trypanosoma* parasites and dramatically reduce parasitemia [155].

PEX14 in mammals, *Hansenula polymorpha*, *Pichia pastoris* and *Trypanosoma brucei*, has been reported to exhibit properties that are characteristic of an integral membrane protein [193-197]; whereas in *Leishmania* [29] and *Saccharomyces cerevisiae* [164, 198] this protein exhibited characteristics of a peripheral membrane protein that is anchored to the cytosolic surface of the glycosome/peroxisome. Biophysical studies with recombinant *L. donovani* PEX14 (LdPEX14) confirmed that the hydrophobic region spanning residues 149-179, a domain that is conserved among PEX14 proteins, is required for membrane binding [29]. Several models have been proposed for the transient pore assembly and translocation of PTS1 proteins which involves, i) the binding of cargo loaded PEX5 receptor to PEX14 and membrane insertion of PEX5 to mediate pore opening [35] or ii) the binding of the loaded PEX5 receptor to the docking/translocation module (DTM) which induces pore opening and permits PEX5 to aid in

pushing the cargo protein through the pore [199]. Additionally, in yeast it was suggested that the import of PTS2 proteins into the peroxisome is mediated by an architecturally distinct pore [34].

Despite the advances in dissecting the structure and function of the glycosome/peroxisome translocon, little is known about PEX14-membrane interaction and how the docking of the PEX5 or PEX7 receptors alter the conformation of this protein. In this study we used a panel of cysteine and tryptophan mutants, in conjunction with dual fluorescence quenching assays to examine the topology of the hydrophobic domain in LdPEX14 and ldpex14 (120-200) following insertion into lipid bilayers. These data suggest that the hydrophobic domain adopts a helix-turn-helix motif that is capable of homo-oligomerization and pore formation.

Experimental procedures

Chemicals and reagents – All restriction endonucleases and DNA-modifying enzymes were purchased from Invitrogen or New England Biolabs. Horseradish peroxidase (HRP)-conjugated goat anti-rabbit IgG was purchased from GE Healthcare. HRP-conjugated goat anti-mouse and fluorescence dyes monobromobimane and dansyl chloride were purchased from Sigma-Aldrich. The fluorescent dye pyrene maleimide was purchased from Thermo Fisher Scientific and phospholipids and cholesterol (Chl) were obtained from Avanti Polar Lipids. All other reagents were of the highest commercially available quality.

Protein mutagenesis and purification – A panel of single tryptophan mutations was generated utilizing the full length LdPEX14-His_6 or a fragment encompassing residues 120-200 (ldpex14 (120-200)-His_6) (Table 1) using a PCR based mutagenesis strategy. To construct this panel of

mutant proteins the wild type tryptophan 152, present in LdPEX14-His_6 and ldpex14(120-200)-His_6, was replaced with a phenylalanine (W152F) to produce the pET30b-LdPEX14W152F-*His_6* andpET30b-ldpex*14(120-200) W152F-His_6*, as a template for the PCR mutagenesis reactions. In addition, internal deletion mutants lacking residues 149-179 (ldpex*14Δ149-179)*, 138-165 (ldpex*14Δ138-165),* 160-179 (ldpex*14Δ160-179)* and 179-200 (ldpex*14Δ179-200)* were generated by PCR based mutagenesis using the plasmid pET30-Ld*PEX14-His_6* to construct the pET30-ldpex*14Δ149-179-His_6*, ldpex*14Δ138-165-His_6*, ldpex*14Δ160-179-His_6* and ldpex*14Δ179-200-His_6* expression vectors. Truncated forms of ldpex14; ldpex14(1-120), ldpex14(1-200), ldpex14(1-254) and ldpex14(1-321) were expressed and purified as previously described [33].

Cysteine mutants were generated by PCR based mutagenesis utilizing pET30b-ldpex14(120-200)-*His_6* as template to construct, pET30b-ldpex*14(120-200) T147C-His_6*, pET30b-ldpex*14(120-200) S165C-His_6*, pET30b-ldpex*14(120-200) S168C-His_6*, or pET30b-ldpex*14(120-200) S177C-His_6*. For the full length LdPEX14, the three cysteine residues at positions 104, 221, and 272 were replaced with serine residues by PCR mutagenesis to generate an LdPEX14 devoid of cysteines. This cysteine-less LdPEX14 was used as a template to construct pET30b-LdPEX14 *T147C-His_6*, pET30b-LdPEX14 *S165C-His_6*, pET30b-LdPEX14 *S168C-His_6*, pET30b-LdPEX14 *S177C-His_6.*

E. coli strain ER2566 was transformed with the various LdPEX14/ldpex14 plasmid constructs and grown to an OD_{600} of 0.8 at 37 °C and protein expression was induced for 6 h with vigorous shaking at 20 °C in the presence of 0.7 mM Isopropyl β-D-1-thiogalactopyranoside (IPTG). Cells were harvested by centrifugation (6000 x*g* for 15 min) and the bacterial cell pellets were re-suspended in 20 ml of 40 mM Tris-HCl pH 8.0 and lysed with

French Press at 10,000 psi prior to the addition of NaCl to a final concentration of 500 mM. The lysates were clarified by centrifugation (24,000 xg for 25 min) and supernatants were applied to Ni^{2+}-NTA resin (Qiagen) column equilibrated with 40 mM Tris-HCl pH 8.0 containing 500 mM NaCl (TBS500). The loaded column was sequentially washed with 250 ml of TBS500 containing 10 mM imidazole, 100 ml of TBS500 containing 20 mM imidazole, and 100 ml of TBS500 containing 40 mM imidazole. The LdPEX14/ldpex14 mutant proteins were eluted with 15 ml of TBS500 containing 500 mM imidazole.

For the ldpex14 (120-200) purification, bacterial lysates were clarified by centrifugation at 24,000 x*g* for 25 min at 4 °C and the inclusion body pellet was re-suspended in 20 ml TBS500 containing 8.0 M urea. The suspension was clarified by centrifugation and the supernatant was loaded onto a 1.0 ml Ni^{2+}-NTA resin (Qiagen) column then washed with 100 ml of TBS500 containing 8.0 M urea to remove unbound proteins. The ldpex14 (120-200) fragment protein was eluted with 5 ml of 40 mM Tris-HCl pH 8.0, 100 mM NaCl (TBS) containing 500 mM imidazole, 4.0 M urea, concentrated to 6.0 mg/ml using Amicon Ultra filter 3 kDa (Millipore), dialyzed against TBS containing 4.0 M urea and stored as aliquots at -80 °C. Purified proteins were analyzed by SDS-PAGE, concentrated using an Amicon Ultra filter 3K or 10K MWCO unit (Millipore), quantified spectrophotometrically at 280 nm [200] and stored at -80 °C. The recombinant ldpex5 (203-391) W246,293,361F, ldpex14 (1-120), ldpex14 (1-200), ldpex14 (1-254), and ldpex14 (1-321) fragments were expressed and purified as previously reported [33].

Labeling ldpex*14 (120-200) with fluorophores* – Purified ldpex14 (120-200) T147C, ldpex14 (120-200) S165C, ldpex14 (120-200) S168C, and ldpex14 (120-200) S177C were resuspended in 4 M urea in PBS then reduced with 5-fold molar excess of dithiothreitol at 25 °C for 1 h, and

labeled with 25-fold molar excess of monobromobimane at 25 °C for 1 h with mixing. For 1-pyrene maleimide labeling, proteins were reduced with 5-fold molar excess of Tris-(2-carboxyl)-phosphine for 2 h at 25 °C then labeled with 5-fold molar excess of 1-pyrene maleimide for 4 h at 25 °C. Unreacted monobromobimane and 1-pyrene maleimide were removed by precipitating proteins with 15% trichloroacetic acid (TCA) and then washing the protein pellet with acetone. Precipitated proteins were dissolved in PBS containing 8.0 M urea to a concentration of 5.0 mg/ml.

Purified full length LdPEX14 or ldpex14 (120-200) mutants T147C, S165C, S168C, and S177C in PBS were reduced with 5-fold molar excess of Tris-(2-carboxyl)-phosphine for 4 h at 4 °C, and then labeled with 5-fold molar excess of monobromobimane or 1-pyrene maleimide for 16 h at 4 °C. The labeled proteins were applied to a Ni^{2+}-NTA column (1.0 ml of packed beads) and the bound protein was washed with 50 ml PBS. Labeled proteins were eluted with 400 mM imidazole in PBS and dialyzed overnight against 4.0 L of PBS. Labeling efficiency was determined spectrophotometrically at 380 nm for monobromobimane conjugates (ε value bromobimane group is 5000 $M^{-1}cm^{-1}$) and 338 nm for pyrene conjugates (ε value for pyrene group is 40,000 $M^{-1}cm^{-1}$) [201]. The protein concentration was measured spectrophotometrically at 280 nm by the method of Pace *et al.* [200].

Preparation of unilamellar vesicles – Large unilamellar vesicles (LUVs) and small unilamellar vesicles (SUVs) were prepared from dioleoyl phosphatidylethanolamine (DOPE), dioleoyl phosphatidylcholine (DOPC), dioleoyl phosphatidylglycerol) (DOPG), bovine liver phosphatidylinositol (PI) and cholesterol in a 55:25:15:2.5:2.5 molar ratio, as previously described [32]. The lipids were dissolved in chloroform and thin films were prepared by

evaporation of the solvent under a nitrogen stream. Residual chloroform was removed under vacuum for 16 h. Multilamellar vesicles were prepared by re-suspending the lipid film in 40 mM phosphate buffer pH 7.2, 100 mM NaCl (PBS) at a concentration of 5.0 mg/ml with vigorous mixing. The suspension was then extruded 20 times through a 0.2 μm polycarbonate membrane (Millipore) to generate large unilamellar vesicles (LUV) with a diameter of 200 nm, a size comparable to *Leishmania* glycosomes.

Alternatively, lipid films containing 10-doxylnonadecane (10-DN) or 16:0-18:0 (4,5-dibromo) phosphatidylcholine with the following phospholipid compositions DOPE:DOPC:DOPG:PI:Chl:10-DN (45:25:15:2.5:2.5:10) or DOPE:DOPC:DOPG:PI:Chl:4,5 dibromo PC (45:10:15:2.5:2.5:25) were rehydrated with PBS and sonicated with a probe sonicator on ice for 5 min to generate small unilamellar vesicles (SUV) with a diameter of ~30-50 nm for fluorescence and circular dichroism experiments. SUV preparations were centrifuged at 15,000 rpm for 20 min at 4 °C to remove lipid aggregates.

Dye leakage assay – Lipid films made with a composition of DOPE:DOPC:DOPG:PI:Chl (55:25:15:2.5:2.5) were re-suspended in PBS containing 100 mM 5(6)-carboxyfluorescein (CF) and vortexed for 15 minutes to generate multilamellar vesicles which were extruded through a 0.2 μm polycarbonate membrane to generate large unilamellar liposomes (LUVs). Dye loaded LUVs were purified by gel filtration on Sephadex G-50 column (1 x 20 cm) equilibrated in PBS. Dye loaded LUVs were mixed with LdPEX14, ldpex14 (120-200), ldpex14 (1-120), ldpex14 (1-200), ldpex14 (1-254), or ldpex14 (1-321) and dye release was monitored using an excitation and emission wavelengths of 492 nm and 515 nm for CF. The total CF content of LUVs was

determined by addition of Triton X-100 (0.1% v/v). All dye leakage assays were performed at 25 °C. Percent dye leakage was calculated using the following equation:

$$\% \text{ leakage} = F_{LdPEX14}/F_{\text{Triton X-100}} \text{ x } 100.$$

Alternatively, LUVs were loaded with 10 mg/ml solution of fluorescein-isothiocyanate (FITC) conjugated-dextran's with molecular weights, 4, 10, 45 and 70 kDa and extravesicular dextran was removed by gel filtration on SephadexG-200 column. To assess dextran leakage, LUVs (400 μg) were incubated with ldpex14 (120-200) (protein:phospholipid ratio 1:200) and incubated at 25 °C for 15 min. The reaction mixture was centrifuged at 100,000 x*g* for 45 min at 4 °C in a Beckman-Coulter tabletop centrifuge using a TLA100.3 rotor to separate LUV entrapped and free FITC-dextran. The supernatant was carefully removed, and LUV pellet was solubilized in 0.5 % Triton X-100, 50 mM Tris pH 7.5 and the fluorescence intensity in the supernatant and pellet fractions was measured using excitation and emission wavelengths of 495 and 515 nm, respectively. The extent of leakage was calculated using the equation:

$$\% \text{ leakage} = (F_{con}-F_{LdPEX14})/F_{con} \text{ x } 100$$

where, F_{con} is total fluorescence in the control LUVs and $F_{LdPEX14}$is the fluorescence of CF released by LdPEX14 or ldpex14(120-200).

Membrane binding assay – Purified proteins (20 μg) were incubated with LUVs (400μg) in 300 μl of PBS for 15 min at 25 °C then diluted with 1.2 ml of 66% sucrose, 500 mM NaCl in PBS buffer. These preparations were topped with 3.0 ml of PBS, supplemented with 500 mM NaCl and 40% sucrose and then 0.7 ml of PBS. Samples were subjected to centrifugation at 28,000 rpm for 16 h at 4 °C in a Beckman SW55 rotor. Fractions (0.65 ml) were collected from the top

of the gradient and proteins were precipitated with 15% TCA. Protein pellets were resuspended in SDS-PAGE sample buffer and examined by Western blot analysis.

ldpex*14 (120-200) oligomerization* – Purified ldpex14 (120-200) (5 μg) was re-suspended in 20 μl of SDS-PAGE sample buffer and the unboiled sample was resolved on 12% Bis-TrisPAGE using a 50 mM MES – 50 mM Tris (pH 7.3) running buffer containing 0.02% Coomassie Blue G250 dye [202]. Alternatively, DOPE:DOPC:DOPG:PI:Chl LUVs loaded with ldpex14(120-200) were solubilized with 0.5% 3-[(3-cholamidopropyl)dimethylammonio]-1-propanesulfate (CHAPS), n-octyl-β-glucoside (OG), taurodeoxycholate (TDOC), or sodium dodecyl sulfate (SDS) prior to electrophoresis. Protein bands were visualized by silver staining. Alternatively, increasing amounts (5 to 100 ng) of ldpex14 (120-200) were resuspended in 10 μl of SDS-PAGE sample buffer and loaded directly onto a 10% SDS-PAGE with or without boiling and proteins were electro-transferred to polyvinylidene difluoride membrane and ldpex14 (120-200) species were detected by Western blot using anti-hexahistidine monoclonal antibody (Abcam, Cambridge, MA).

Fluorescence spectroscopy – Intrinsic fluorescence measurements were performed on a Varian Cary Eclipse spectrofluorometer at 20 °C using an excitation wavelength of 290 nm. Insertion of LdPEX14 or ldpex14 (120-200) into lipid bilayers was monitored by recording the emission spectra from 305-400 nm at a scan rate of 120 nm/min with slit widths of 5 nm. Final spectra were generated by averaging five spectral traces. Insertion depth of LdPEX14 or ldpex14 (120-200) into the bilayer was assessed by fluorescence quenching using the polar quenching agent potassium iodide (KI) or the nonpolar quenching agent 10-doxylnonadecane (10-DN) [203, 204].

Emission spectra were corrected for background fluorescence and Raman scattering by subtracting signals arising from buffer and SUVs. The initial fluorescence (F_0) was measured following the addition of LdPEX14 or ldpex14 (120-200) to SUVs and quenching due to KI was measured following the addition of 160 mM KI to SUVs. Quenching due to 10-DN was determined using SUVs containing a 10 mole percent of 10-DN. To compensate for the presence of 10-DN an equimolar concentration of DOPE was omitted from the 10-DN containing SUVs. Proteins (1μM) were incubated with SUVs (400 μM total phospholipid) for 5 min at 20 °C before all fluorescence measurements were performed. The quenching (Q) ratio to assess the penetration depth of tryptophan residues was calculated using the following equation:

$$\text{Q-ratio} = ((F_0/F_{KI})-1) / ((F_0/F_{10\text{-}DN})-1)$$

where F_0 is the initial fluorescence, F_{KI} is the fluorescence following addition of KI, and $F_{10\text{-}DN}$ is the fluorescence in the presences of 10-DN.

Dansyl-tryptophan Forster energy resonance transfer (FRET) – 50 μM of dansyl chloride were incubated with 5 mM of SUVs (1:100 ratio) in 350μl total volume for 1 h at 25 °C to label DOPE on the outer leaflet of the lipid bilayer. To separate the dansylated SUVs from free dansyl chloride, the labeled mixture was loaded at the bottom of a sucrose gradient and subjected to centrifugation at 28,000 rpm for 18 h at 4 °C. Dansylated liposomes were recovered from the top of the gradient and dansylation was confirmed by emission at 520 nm. Dansylated liposomes were incubated with ldpex14 (120-200) tryptophan mutants (protein:lipid ratio of 1:400) and emission spectra were recorded from 300-550 nm (excitation 290 nm) with slit widths of 5 nm. The proximity of the tryptophan residues to the dansyl fluorophore was assessed as a ratio of

fluorescence intensity at 520 nm to the tryptophan intensity at emission λ_{max} as previously reported [205].

Tryptic analysis of ldpex*14 (120-200) and* ldpex*14 (1-200) topology* – For LUV encapsulation of trypsin, lipid films were gently resuspended in 10 mg/ml trypsin solution in Tris-buffered saline (TBS). The multilamellar vesicle suspension was extruded through a 0.2 μm polycarbonate filter to generate LUVs with a diameter of ~200 nm. To remove free trypsin LUVs were sedimented by centrifugation at 50,000 rpm for 1 h at 4 °C and the pellet was treated with 1 mg/ml soybean trypsin inhibitor for 20 min to inactivate residual extra-luminal trypsin and soybean trypsin inhibitor was removed by LUV sedimentation. The LUV pellet was resuspended in 800 μl of TBS. Control LUVs lacking trypsin were prepared using the above protocol. For topology mapping, ldpex14 (120-200) or ldpex14 (1-200) [33] was added to LUV containing encapsulated trypsin (protein:phospholipid 1:400) and the mixture was incubated at 20 °C. Alternatively, LUVs were mixed with ldpex14 (120-200) or ldpex14 (1-200) and incubated at 20 °C for 20 min prior to the addition of trypsin to a final concentration of 1.0 mg/ml trypsin. Aliquots were removed, resuspended in sample buffer to terminate proteolysis, and the digests were analyzed by Western blot using anti-hexahistidine primary antibodies.

Biotinylated protein-Streptavidin HRP flotation assay – Purified ldpex14(120-200) T147C, ldpex14(120-200) S165C, ldpex14(120-200) T168C and ldpex14(120-200) S177C and ldpex14 (120-200) were reduced with five molar excess of Tris(2-carboxyethyl) phosphine hydrochloride (Sigma C4706) for 4 h at 25 °C. The reduced proteins were labelled with 1.0 mM biotin C2

maleimide (Anaspec AS-60643) for 5 h at 25 °C. The labelled protein was precipitated with 15% TCA, washed with acetone, re-dissolved in 4.0 M urea in PBS and quantified. Biotin labelled proteins were incubated with LUVs (ratio of 1:1000) for 30 min at 25 °C. Streptavidin conjugated horseradish peroxidase (Streptavidin-HRP) (Invitrogen: 19534) was added in a 1:1000 dilution and incubated for 15 min at 20 ^{0}C. The final mixture containing the LUVs-biotinylated protein-streptavidin-HRP were loaded in the bottom fraction of a sucrose gradient and spun for 28,000 rpm for 18 h at 4 °C. The gradient was fractionated from top in 650 µL aliquots and the amount of streptavidin-HRP conjugate in each fraction was measured using the 3,3',5,5'-tetramethylbenzidine substrate assay. Reactions were stopped by the addition of 2.0 M sulfuric acid and color development was quantified by UV/Vis at 450 nm.

Circular dichroism(CD)analysis – A solution of ldpex14(120-200) (50 µM) in 10 mM sodium phosphate,10 mM NaCl pH 7.5 was titrated with SDS (0-16 mM), SUVs (0-400 µM total phospholipids), or diluted into a solution containing 0-75% trifluoroethanol (TFE) and spectra were recorded at 23 °C on a JASCO8100 instrument using a 1 mm cuvette at a scan rate of 100 nm/min and a bandwidth of 1 nm. CD spectra were recorded from 200 nm to 260 nm at 23 °C. Five spectra were collected and averaged.

Results

Analysis of the PEX14 hydrophobic region – Bioinformatic analysis of PEX14 proteins from phylogenetically diverse organisms using programs TMPRED and Phobius (embnet.vital-it.ch/cgi-bin/TMPRED and phobius.sbc.su.se/cgi-bin/) revealed the presence of a putative hydrophobic domain that corresponds to residues 149-179 on LdPEX14 (**Figure 1A**).

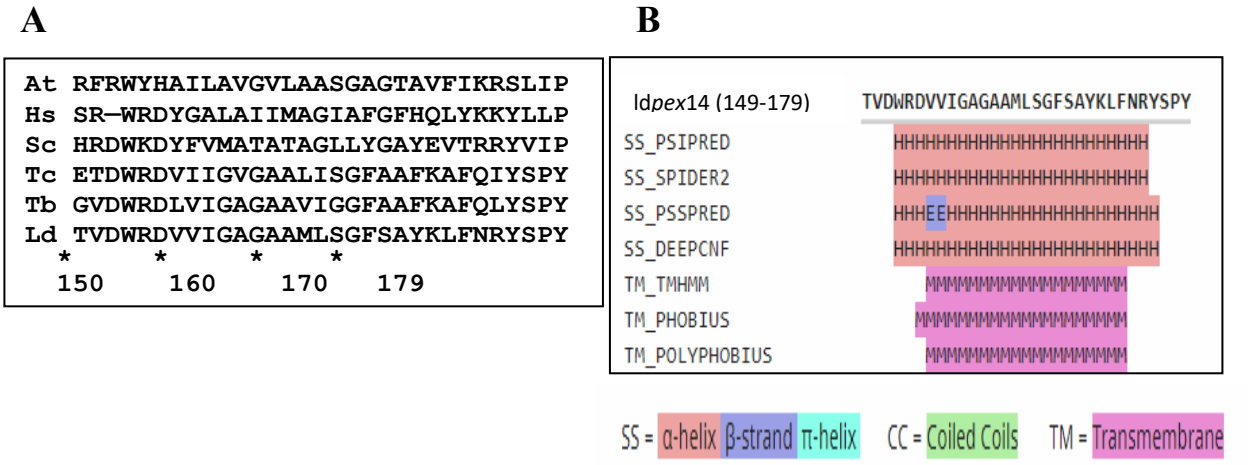

Figure 1: Transmembrane topology

Putative transmembrane domain in the *L. donovani* PEX14. (A) Multiple sequence alignment of the predicted transmembrane region of PEX14 from *Arabidopsis thaliana* (At), *Homo sapiens* (Hs), *Saccharomyces cerevisiae* (Sc), *Trypanosoma cruzi* (Tc), *Trypanosoma brucei* (Tb), and *Leishmania donovani* (Ld). Sequences were aligned with the Clustal X program (B) Predicted transmembrane domain was used as an input for Quick2D [206] that gives an overview of secondary structure features like alpha-helices and transmembrane helices present in the hydrophobic region spanning ldpex14 (149-179).

Further analysis using the Heliquest algorithm [207] suggested that the segment on LdPEX14, in particular residues 155-179, have predicted biophysical characteristics that are highly reminiscent of a transmembrane helix (**Figure 2A**). The residues 147-179 spanning the hydrophobic domain of LdPEX14 were modelled using the QUARK *ab initio* protein prediction online tool [206] and visualized using Jmol [208][352] . There were two different possibilities of folding of the hydrophobic region, an extended alpha helix (Model-1) or a helix turn helix consisting of a helix hairpin (Model-2) (**Figure 2B**).

A

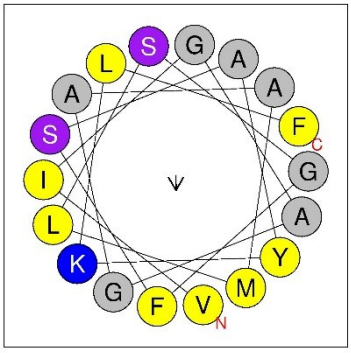

B

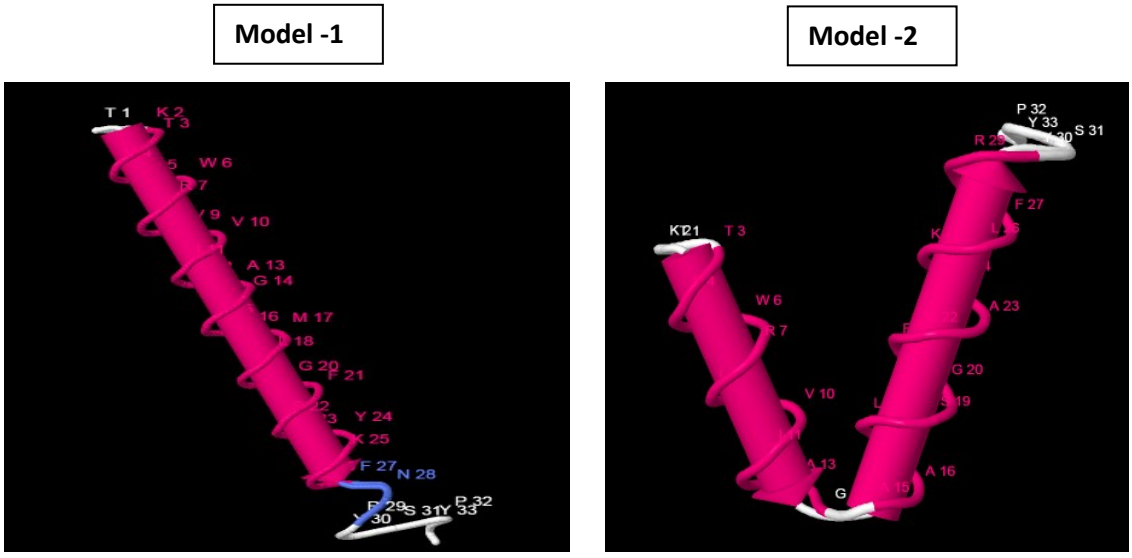

Figure 2: Bioinformatic analysis of the LdPEX14 hydrophobic domains

(**A**) LdPEX14 residues 156-172 analyzed using the Heliquest program showed a helix with amphipathic character with a hydrophobic face represented by AAFGAYMVF amino acids. (**B**) Models (1 and 2) were generated for LdPEX14 hydrophobic domain (149-179) using QUARK algorithm (*ab initio* protein folding) and were visualized using Jmol.

Model-1 comprises a single helix of 27 amino acids (residues 149-175) with a predicted helix length of 41 Å (measured using the UCSF Chimera visualization tool [209]) which was sufficient to span the lipid bilayer. Model-2 contains a helix-turn-helix motif, namely helix-1 comprises of 11 amino acids (residues 149-159) and helix-2 contains 15 amino acids (residues

161-175). The length of the predicted helix-1 and helix-2 were 18 Å and 24 Å, respectively [209].

Previous studies showed that residues 149-179 were critical for LdPEX14 binding to the lipid bilayers. More importantly, these studies indicated that the binding of LdPEX5 to LdPEX14 induced conformational changes in the predicted transmembrane domain [33]. To further define the elements in the transmembrane domain that are essential for membrane binding, a series of internal deletion mutants lacking residues 138-165 (ldpex14 (Δ138-165)), 160-179 (ldpex14 (Δ160-179)) and 179-200 (ldpex14 (Δ179-200) (**Figure 3A**) were constructed and the capacity of mutant ldpex14 proteins to interact with lipid bilayers was assessed using the qualitative sucrose density flotation assay and LUVs with a phospholipid composition that mimic the *L. donovani* glycosomal membrane [32]. As shown in **Figure 3B**, the wildtype LdPEX14 bound to vesicles with a DOPE:DOPC:DOPG:PI:Chl and was recovered at the top of the sucrose density gradient. However, in the absence of LUVs, LdPEX14 was present only at the bottom of the gradient. Similarly, the ldpex14 (Δ149-179) failed to bind LUVs and was only detected at the bottom of the gradient (**Figure 3B**) as previously reported [32]. Surprisingly, deletion of residues 138-166 or 160-179, regions that span much of the hydrophobic domain, did not ablate binding of these ldpex14 deletion mutants to lipid bilayers (**Figure 3B**). Heliquest analysis showed that potential helical structures formed following the above deletion and had a considerable degree of hydrophobicity that would favor the partitioning of the mutant ldpex14 (Δ138-165) and ldpex14 (Δ160-179) into the lipid bilayer (**Figure 3C**). The presence of arginine, serine, and threonine in these hydrophobic regions surprisingly did not influence the propensity for membrane binding as these residues are often detected in transmembrane domains [210]. More importantly, short sequences of 15 to 18 amino acids may be sufficient for the formation of a transmembrane helix

[211]. In contrast, the Δ149-179 completely abolished the hydrophobic domain and membrane binding (**Figure 3B** & **3C**); whereas the Δ179-200 deletion had no impact on the hydrophobic domain (**Figure 3**). As previously demonstrated [32], a fragment spanning residue 120-200 also exhibited robust membrane binding activity and in a sucrose density flotation experiment this fragment was recovered quantitatively at the top of the gradients with the LUVs. Similar floatation experiments with the N-terminal portion of LdPEX14 spanning residues 1-200 (ldpex14 (1-200)) also exhibited near quantitative binding to LUVs (**Figure 3B**).

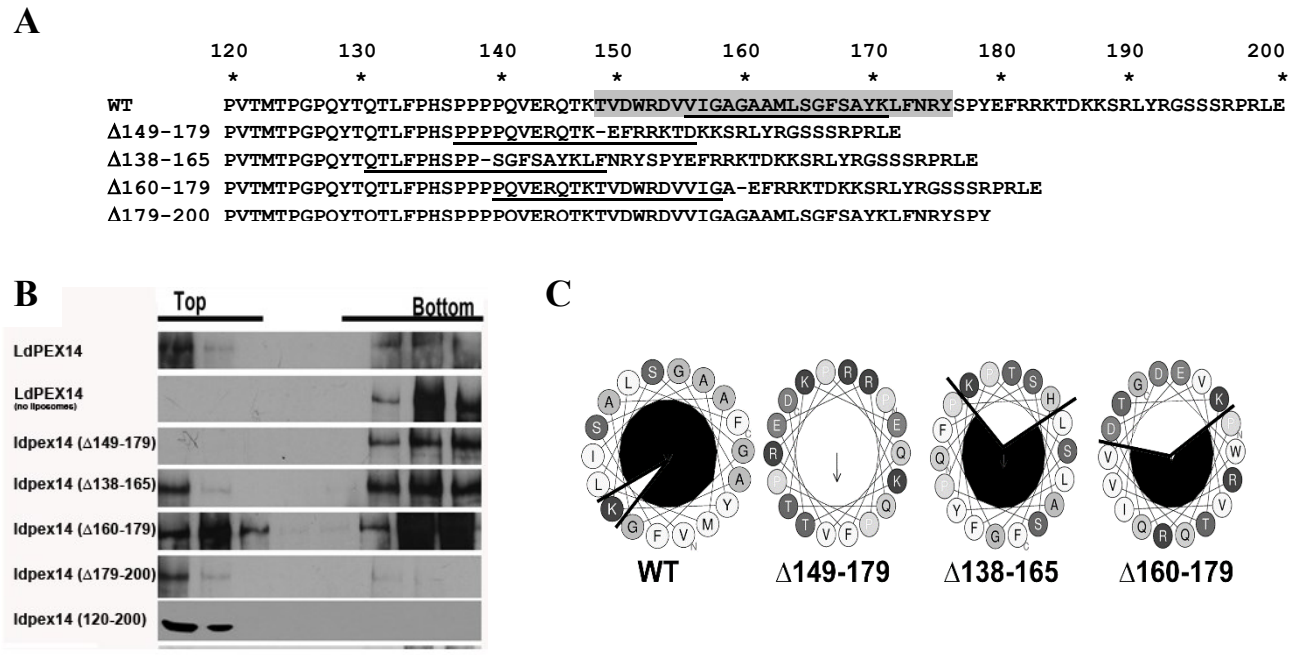

Figure 3: Analysis of the LdPEX14 hydrophobic domain

(**A**) Wildtype sequence of the region spanning residues 120-200 of LdPEX14 and the internal deletion mutants lacking residues 149-179, 138-165, 160-179, or 179-200 that were generated to characterize the hydrophobic domain of LdPEX14. (**B**) LUVs were loaded with LdPEX14 or the ldpex14 deletion mutations and bound protein was separated by sucrose density flotation and proteins were detected by Western blot analysis using anti-LdPEX14. (C) Residues underlined in panel A were examined using the Heliquest software to determine hydrophobicity and hydrophobic moment of these sequences to assess the regions that were involved in membrane binding. The black shading of the inner wheel indicates the section of the helix has a hydrophobic character.

Topology of the Ld*PEX14 hydrophobic region* – To examine the topology of the LdPEX14 hydrophobic region in the lipid bilayer, the single tryptophan (W152) in LdPEX14 or ldpex14 (120-200) was mutated to a phenylalanine and tryptophan residues were inserted at positions 147, 150, 152, 155, 157, 160, 162, 165, 169, 173, and 177. Purified proteins were mixed with SUVs with a lipid composition that mimics the *L. donovani* glycosomal membrane and the emission λ_{max} for each tryptophan residue was determined at an excitation wavelength of 290 nm. Tryptophan residues can be used as an intrinsic probe since λ_{max} emission changes as a function of the environmental polarity [212]. In an aqueous or polar environment, the emission λ_{max} for tryptophan residues ranges from ~340-350 nm; while in a nonpolar environment, as would be encountered in the hydrophobic core of a lipid bilayer, this emission λ_{max} undergoes a hypochromic shift to a wavelength of ~310-335 nm. Analysis of the emission λ_{max} for the panel of ldpex14 (120-200) tryptophan mutants **(Table 1)**, showed that for this fragment, residues W147 and W150 exhibited an emission λ_{max} centered at 350 and 340 nm, respectively. This is consistent with these residues being positioned in an aqueous environment or in association with polar phospholipid head groups (**Figure 4A**). In contrast, the tryptophan residues at positions 152 to 177 exhibited emission λ_{max} ranging from 321 to 332 nm; wavelengths indicative of these residues being situated at various depths in the hydrophobic core of the lipid bilayer (**Figure 4A**).

To evaluate the degree to which the ldpex14 (120-200) hydrophobic domain penetrated into the lipid bilayer, dual fluorescence quenching assays (DQA) were performed using potassium iodide (KI), which quenches the fluorescence of tryptophan residues outside the lipid bilayer or near the phospholipid head group interface [212, 213], and 10-doxyl nonadecane, a hydrophobic nitroso quenching agent that inserts into the hydrophobic core of the lipid bilayer

[203, 204]. KI showed the greatest degree of quenching in ldpex14 (120-200) with tryptophan residues at positions 147, 155, and 157; while tryptophan residues at positions 150, 152, 160, and 167 were protected and exhibited a lower degree of quenching by KI. In contrast, SUVs containing 10-DN caused the most pronounced quenching in tryptophan residues at position 155, 160, 162, and 165, indicative of these residues penetrating deep into the lipid bilayer (**Figure 4B**). Q-ratios exploit the quenching observed with KI and 10-DN to assess the degree to which specific tryptophan residues on ldpex14 (120-200) penetrated the lipid bilayer. Previously reported Q-ratios, ranging from ~0.1-0.5, indicate that a corresponding tryptophan residue is located deep in the membrane near the center of the hydrophobic core; whereas values of ~1.0 or greater indicate that the tryptophan residue has a shallow membrane insertion or is weakly associated with the membrane [204, 213]. As shown in **Figure 4D**, the DQA suggested that residues 150-157 and 162-169 are located deep in the membrane. Surprisingly, residues 158-161 appear to be located within a polar environment. It is possible that these residues could be oriented toward the center of a channel following insertion of ldpex14 (120-200) perpendicular to the lipid bilayer and subsequent assemble to form a pore structure.

A similar analysis of the tryptophan mutations in the full length LdPEX14 showed that association of this protein with the lipid bilayer resulted in modest changes in emissions λ_{max} in the tryptophan residues (**Figure 4A**). Quenching experiments showed that KI and 10-DN had a similar periodicity (**Figure 4C**) and the Q-ratio analysis resulted in values of ~1.0 or greater (**Figure 4D**), which indicated that the hydrophobic region spanning residues 147-177 exhibited a shallow insertion into the membrane.

Table 1: LdPEX14-His$_6$ and ldpex14 (120-200)-His$_6$ mutations

Mutation	**ld**pex**14(120-200)**	**LdPEX14**
W152F, T147W	YES	YES
W152F, V150W	YES	YES
W152 (wild type)	YES	YES
W152F, I157W	YES	YES
W152F, G160W	YES	YES
W152F, A162W	YES	YES
W152F, S165W	YES	YES
W152F, A169W	YES	YES
W152F, F173W	YES	YES
W152F, S177W	YES	YES

Table 1 lists all the tryptophan mutants made in the hydrophobic region of PEX14 that were used for this study.

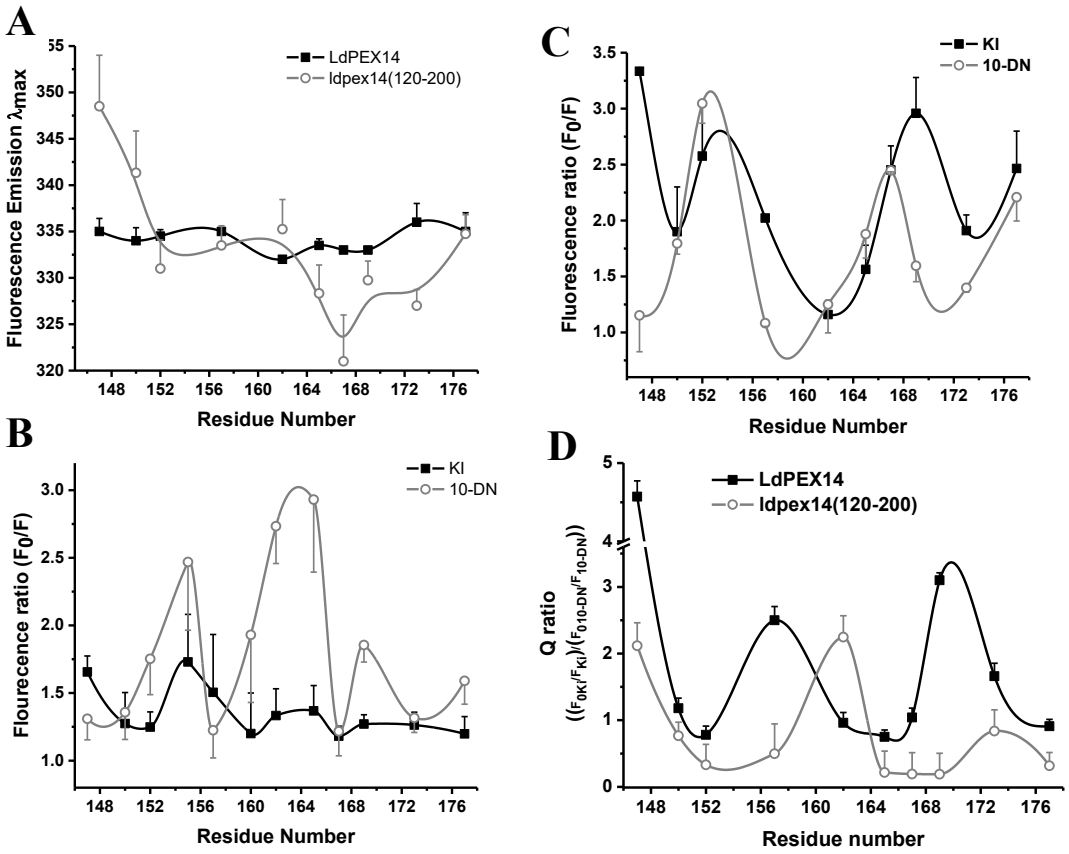

Figure 4: Fluorescence analysis of interaction of the LdPEX14/ldpex14 (120-200) hydrophobic domain with the lipid bilayer

(**A**) The graph shows the emission λ_{max} for the series of tryptophan mutants in LdPEX14 and ldpex14 (120-200) following insertion of these proteins into the SUV lipid bilayer. (**B**) The fluorescence quenching of tryptophan residues in ldpex14 (120-200) inserted into SUV membranes was assessed using the polar quenching agent potassium iodide (KI) and the hydrophobic quenching agent 10-doxyl nonadecane (10-DN). (**C**) The fluorescence quenching of tryptophan residues in LdPEX14 mutants inserted into SUV membranes was assessed using the polar quenching agent potassium iodide (KI) and the hydrophobic quenching agent 10-doxyl nonadecane (10-DN). (**D**) The Q-ratios for LdPEX14 and ldpex14 (120-200) were calculated using the quenching values obtained with KI and 10-DN.

To validate the interaction of ldpex14 (120-200) with glycosome mimetic membranes, cysteine mutations replacing either a serine or threonine were incorporated at positions 147, 165, 168, and 177. Cysteine residues were modified with the environmentally sensitive probe

monobromobimane (MBB) which in a polar environment exhibits an emission λ_{max} at ~470 nm, while in a nonpolar milieu, the emission λ_{max} is blue-shifted to 455-460 nm [213]. Addition of MBB labeled ldpex14 (120-200) T147C to SUVs resulted in emission λ_{max} of ~472 nm which was consistent with this residue being located in an aqueous environment or close to the phosphate head groups of the lipid bilayer. MBB labeled ldpex14 (120-200) S165C and ldpex14 (120-200) S177C, however, exhibited an emission λ_{max} centered at ~465 nm which was indicative of these residues having an intermediate insertion into the membrane [213] (**Figure 5A**). In contrast, the emission λ_{max} for the MBB labeled ldpex14 (120-200) S168C showed a significant blue-shift to 460 nm which was consistent with residue 168 being positioned deep within the hydrophobic region of the lipid bilayer (**Figure 5A**). To verify the insertion depth of MBB-labeled ldpex14 (120-200) cysteine mutants, quenching experiments were performed with potassium iodide and 10-DN. Although previous experiments suggested that residues 147 and 177 were located in an exposed extra-membrane environment, only modest quenching of MBB was observed with KI for the ldpex14 (120-200) T147C and S177C mutants (**Figure 5B**). This was not surprising since previous reports indicated that the fluorescence intensity of MBB can be significantly attenuated by neighboring tryptophan or tyrosine residues [214, 215].

It is likely that residues W152 and Y176 are within range to quench the MBB probe on ldpex14 (120-200) T147C and ldpex14 (120-200) S177C. Alternatively, it is possible that residues 147 and 177 may be located in a polar environment proximal to the phospholipid head groups. Modest quenching of the MBB at position 165 and 168 was noted with KI indicating that the reporter fluorophore partitioned into the lipid bilayer (**Figure 5B**). Quenching with 10-DN was most significant when the MBB probe was at positions 165 and 168 (**Figure 5B**). Q-ratio

analysis suggests that residues 165 and 168 insert deeply into the lipid bilayer; while residue 147 and 177 are predicted to be located near the phospholipid head groups (**Figure 5B**).

To further investigate the topology of ldpex14 (120-200) in membranes and to determine the orientation of residue 147 and 177, Forster Resonance Energy Transfer (FRET) between tryptophan donor and dansyl acceptor fluorophores were utilized [212]. For these FRET experiments ldpex14 (120-200) tryptophan mutants were incubated with asymmetric SUVs containing dansyl chloride labeled phosphatidylethanolamine lipids on the outer leaflet of the lipid bilayer and the emission spectra was recorded from 300-550 nm using an excitation wavelength of 290 nm. The proximity of the tryptophan residue in the hydrophobic region to the dansyl fluorophore was evaluated as a ratio of dansyl fluorescence to tryptophan fluorescence (at the emission λ_{max}). Ratios of fluorescence intensity exhibited a parabolic response with residues 147 and 177 having the largest values which would require the localization of the tryptophan residues at these positions to be close to the phospholipid head group of the outer membrane leaflet (**Figure 5C**). In contrast, residues 155-170 exhibited a lower fluorescence intensity ratio indicating that these residues were buried deeper into the hydrophobic core of the bilayer. These data suggest that following insertion of ldpex14 (120-200) into the membrane, this fragment likely adopts a helix-turn-helix configuration that exposes the N- and C-termini to extra-luminal space of SUVs.

To determine if the C-terminus of ldpex14 (120-200), which contains a C-terminal hexahistidine tag [32], penetrated into the LUV lumen or remained exposed on the outer surface of the LUV, a series of tryptic digests were performed using trypsin encapsulated in LUVs or trypsin added to the LUV extra-lumenal space. Addition of ldpex14 (120-200) to LUVs containing encapsulated trypsin showed no significant degradation of the ldpex14 (120-200) C-

terminus. In contrast, addition of trypsin to ldpex14 (120-200) loaded LUVs resulted in complete cleavage of the hexahistidine tags within 15 min (**Figure 5D**). It should be noted that floatation assays demonstrated that ldpex14 (120-200) binds near quantitative to LUVs (**Figure 3B**).

Previous floatation experiments demonstrated that ldpex14 (1-200) exhibited a robust LUV binding and pore-forming activity (discussed below). The N-terminal portion of ldpex14 (1-200) which contains the LdPEX5 binding domain [138], remained surface-exposed was validated by proteolysis. Addition of ldpex14 (1-200) to LUVs containing encapsulated trypsin showed no significant cleavage of the hexahistidine tag. However, a rapid degradation of the N-terminus was observed following addition of trypsin to ldpex14 (1-200):LUV mixture. Indicating that the N-terminal region was exposed to the outer surface of LUVs. It is unclear why a minor population of ldpex14 (1-200) was resistant to proteolysis (**Figure 5D**). Complete digestion of ldpex14 (1-200) by trypsin was also observed in the absence of LUVs (**Figure S1**). These data confirm that the N-terminus of ldpex14 (1-200) remained at the LUV surface.

We next used the panel of cysteine mutations in the full length LdPEX14 to examine the interaction of the hydrophobic region with membranes. These studies showed that the binding of these proteins to SUVs caused only modest changes in the MBB emission λ_{max} which was centered ~471 nm for residues T147C, S165C, S168C, or S177C (**Figure 5E**). Quenching experiments showed that KI was more effective at quenching MBB fluorescence when compared to 10-DN indicating that the region of LdPEX14 containing these amino acids had a shallow insertion into the lipid bilayer (**Figure 5F**). Q-ratio values of >8.0 further confirmed this orientation in the membrane.

Interaction between biotin and streptavidin are well known for its high affinity binding [216, 217]. We utilized this interaction to assess the topology of ldpex14 (120-200) bound to LUVs. ldpex14 (120-200) cysteine mutants namely, ldpex14 (120-200) T147C, ldpex14 (120-200) S165C, ldpex14 (120-200) S168C and ldpex14 (120-200) S177C were labelled with biotin at positions 147, 165, 168 and 177 respectively. Biotin labelled ldpex14 (120-200) mutants were incubated with LUVs in presence of streptavidin-HRP. Then this mixture consisting of the biotin labelled ldpex14 (120-200) mutants, LUVs and streptavidin-HRP were loaded to bottom of a sucrose gradient and subjected to centrifugation [32]. Once fractionated, tubes containing biotinylated ldpex14 (120-200) T147C and ldpex14 (120-200) S177C had higher absorbances in their top fractions (in fractions: 1-2) indicating these residues (147 and 177) are more exposed and accessible to binding with streptavidin-HRP suggesting its location near the outer membrane leaflet (**Figure S3** inset). In contrast, tubes containing biotinylated ldpex14 (120-200) S165C and ldpex14 (120-200) S168C had lower absorbances in their top fractions (in fractions: 1-2) indicating that these residues (165 and 168) are least accessible to the streptavidin-HRP and are buried deep in the hydrophobic core of the bilayer (**Figure S3** inset). Large absorbance present in the lower fractions of the sucrose gradient including ldpex14 (120-200) devoid of cysteine residues indicate that the unbound streptavidin-HRP remained at the bottom even after centrifugation (fraction 6-8) (**Figure S3**).

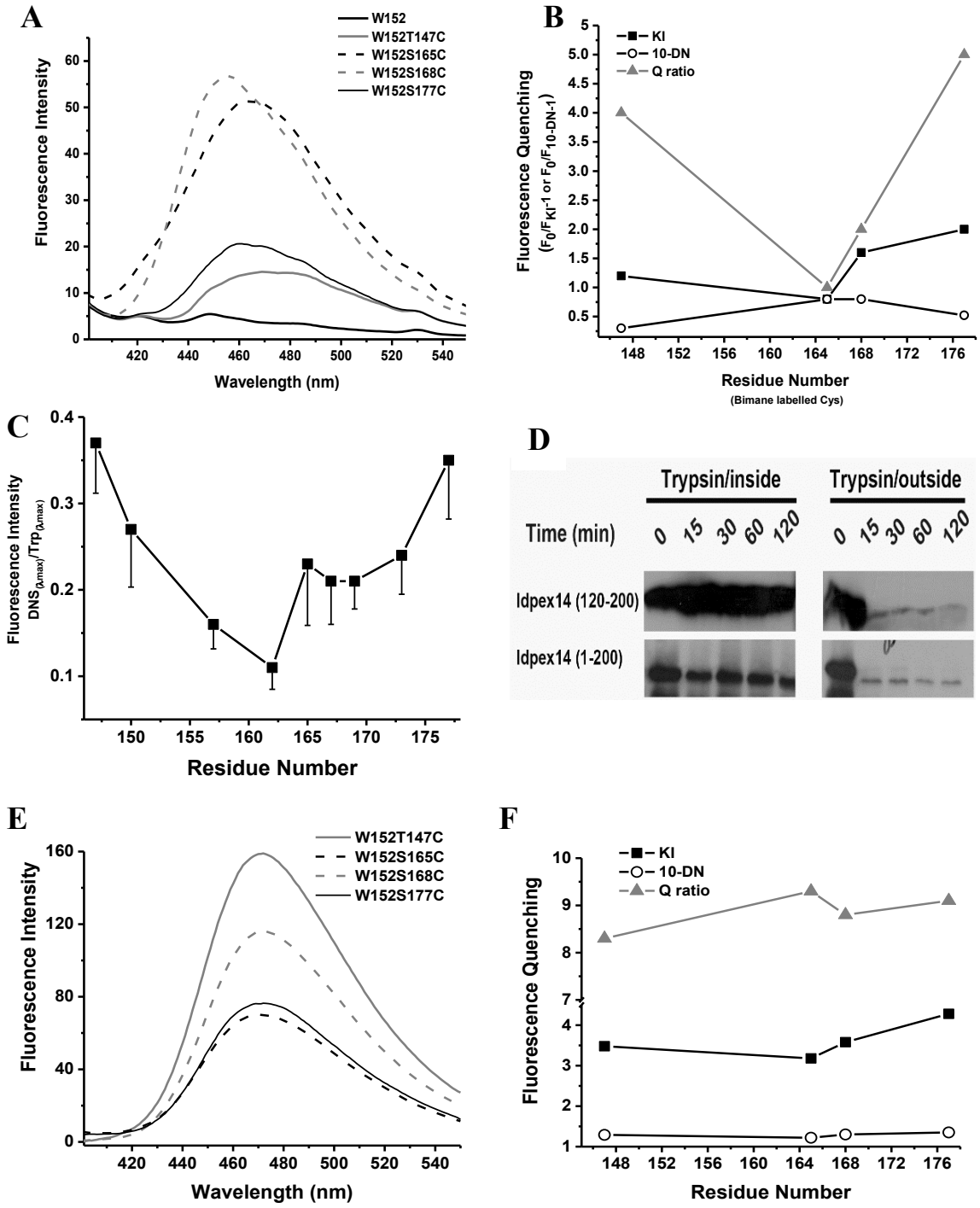

Figure 5 Interaction of monobromobimane (MBB) labeled LdPEX14 or ldpex14 (120-200) mutants with SUVs

(**A**) MBB labeled ldpex14 (120-200) proteins were added to SUVs and emission spectra were recorded at an excitation wavelength of 380 nm. (**B**) The insertion depth of the MBB fluorophore in the lipid bilayer was assessed using the quenching agents KI and 10-DN. These values were used to calculate the Q-ratio. (**C**) The insertion position of the tryptophan residues in the ldpex14 (120-200) mutants was assessed using asymmetric SUVs

containing dansylated phosphatidylethanolamine on the outer membrane leaflet. Distance of tryptophan residues from dansyl (DNS) group was monitored as the ratio of the fluorescence intensity of DNS/Trp. (**D**) The orientation of the ldpex14 (120-200) and ldpex14 (1-200) C-termini following insertion into membranes was assessed in LUVs containing encapsulated trypsin or trypsin added to the exterior of LUVs. Levels of protein were monitored by Western blot analysis. (**E**) MBB labeled LdPEX14 proteins were added to SUVs and emission spectra were recorded at an excitation wavelength of 380 nm. (**F**) The insertion depth of the MBB fluorophore in the lipid bilayer was assessed using the quenching agents KI and 10-DN. These values were used to calculate the Q-ratio.

Ldpex5 (203-391) induces changes in the LdPEX14 hydrophobic region – Previous studies suggested that in solution the binding of LdPEX5 to LdPEX14 induced conformational rearrangements which reoriented Trp152 into a more solvent-exposed environment [33]. The panel of tryptophan mutants in the full length LdPEX14 was next used to assess if the region spanning residues 147-177 shifted following the binding of ldpex5 (203-391), a fragment that exhibits similar binding affinities as the full length LdPEX5 [33]. LdPEX14 tryptophan mutants in solution exhibited an emission λ_{max} ~334 nm indicative of these reporter residues being located in a nonpolar environment (**Figure 6A**). However, upon binding of ldpex5 (203-391), the emission λ_{max} for the LdPEX14 tryptophan residues underwent a red shift to a wavelength ranging from ~338-344 nm consistent with the hydrophobic region relocating into a more solvent exposed environment (**Figure 6A**).

To show that binding of LdPEX5 to membrane bound LdPEX14 induced comparable structural changes in the hydrophobic region, we used a DQA of (4,5-dibromo)-16:0,18:0-PC (4,5-diBr-PC) phospholipid and 10-DN to examine structural changes in LdPEX14. The phospholipid 4,5-diBr-PC, which had the bromine groups ~13 Å from the center of the lipid bilayer [218] was selected since previous experiments suggested that the hydrophobic region in the full length LdPEX14 had a shallow insertion into the membrane. With the exception of LdPEX14 A162W and LdPEX14 S165W mutants no significant quenching was observed using

4,5-diBr-PC SUVs, which indicated that only these two residues penetrated into a region that was proximal to methylene groups 4 and 5 within the outer leaflet of the membrane (**Figure 6B**). This predicted orientation in the lipid bilayer was further supported by the absence of significant quenching of these residues by 10-DN and Q-ratio analysis (**Figure 6C** & **6D**).

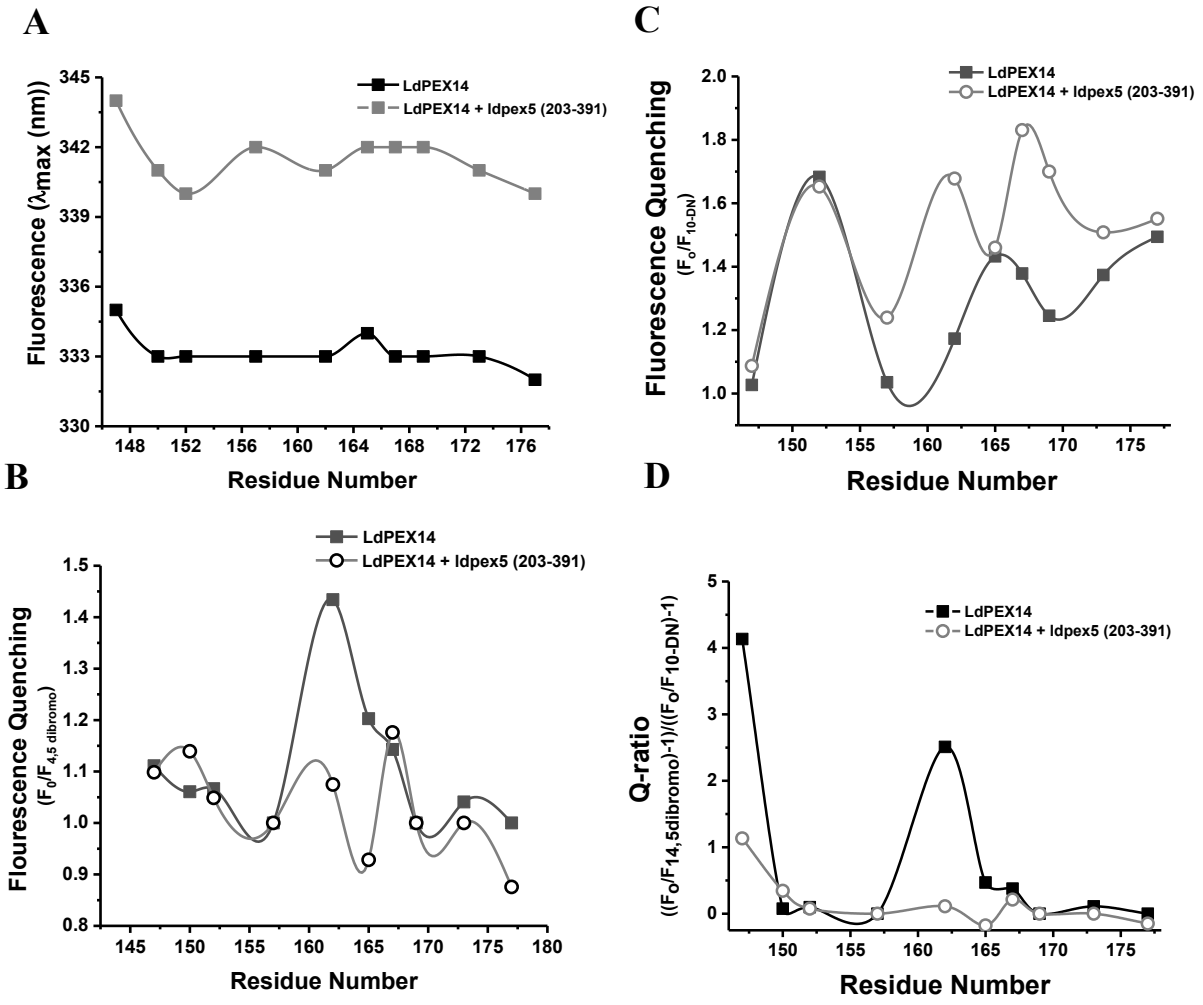

Figure 5: Binding of ldpex5 (203-391) induces conformational changes in the LdPEX14 hydrophobic region

(**A**) The capacity of ldpex5 203-391 (W246,293,361F) [33] to induce conformational changes in the LdPEX14 hydrophobic region was monitored by a shift in the emission λ_{max} of the single tryptophan mutants in the full length LdPEX14 in solution. (**B**) The fluorescence quenching of tryptophan residues in LdPEX14 mutants inserted into SUV membranes was assessed using SUVs with the phospholipid composition of DOPE:DOPC:DOPG:PI:Chl:4,5 diBr-PC(45:10:15:2.5:2.5:25) in the presence or absence of ldpex5 (203-391). (**C**) The fluorescence quenching of tryptophan residues in LdPEX14 mutants inserted into SUV membranes was assessed using SUVs with the phospholipid composition DOPE:DOPC:DOPG:PI:Chl:10-DN (45:25:15:2.5:2.5:10) in the presence or absence of ldpex5 (203-391). (**D**) The Q-ratios for LdPEX14 in the absence and presence were calculated using the quenching values obtained with 4,5 diBr-PC and 10-DN.

Q-ratio analysis showed a significant degree of quenching for LdPEX14 T147W which could arise from the capacity of this residue to partition in and out of the bilayer. The addition of an equimolar amount of ldpex5 (203-391) to SUVs containing LdPEX14 triggered a notable decrease in the quenching of A162W and S165W by 4,5-diBr-PC and the appearance of a periodicity in the quenching pattern (**Figure 6B**) that was indicative of the LdPEX14 hydrophobic region adopting an more helical structure that inserted possibly in a parallel geometry into the membrane [201].

A similar periodicity was also observed with 10-DN and this was accompanied by an increase in quenching, which is indicative of the LdPEX14 hydrophobic region penetrating deeper into the lipid bilayer following the binding of ldpex5 (203-391); this was also supported by Q-ratio analysis (**Figure 6C** & **6D**).

Secondary structure of ldpex*14 (120-200)*–Secondary structure predictions using the Chou and Fasman algorithm [219], suggested that residues 144-174, which are predicted to form a transmembrane domain, exhibit a high propensity to adopt a helical structure; while the region encompassing residues 120-143 and 175-200 favor a strand or random coil conformation, respectively (**Figure 7A**). To experimentally investigate the secondary structure of ldpex14 (120-200) we used circular dichroism (CD) spectroscopy to approximate the helical content of this peptide. These analyses however, were limited to wavelengths ranging from 200 - 260 nm due to the low levels of urea used to solubilize ldpex14 (120-200). CD analysis revealed that ldpex14 (120-200) in an aqueous buffer adopted a largely disordered conformation (**Figure 7B**). However the addition of increasing amount of the helix promoting solvent trifluoroethanol resulted in the emergence of minima at 208 and 222 nm, spectral bands that are indicative of

ldpex14 (120-200) adopting a conformation with increased helical content [220, 221]. Since residues spanning 149-179 seems to adopt conformation similar to a transmembrane domain, we next examined the secondary structure of ldpex14 (120-200) in an SDS micelle hydrophobic environment. A progressive development of helical structure was observed for ldpex14 (120-200) with increasing the concentration of SDS from 1-16 mM (**Figure 7C**). Inorder to determine if the insertion of ldpex14 (120-200) to lipid bilayer was accompanied by an increase in helical structure, CD spectra was recorded in the presence of increasing concentration of SUVs. Again, these results suggested that the ldpex14 (120-200) adopt a structure with increased helical content following membrane insertion or in a nonpolar environment. (**Figure 7D**).

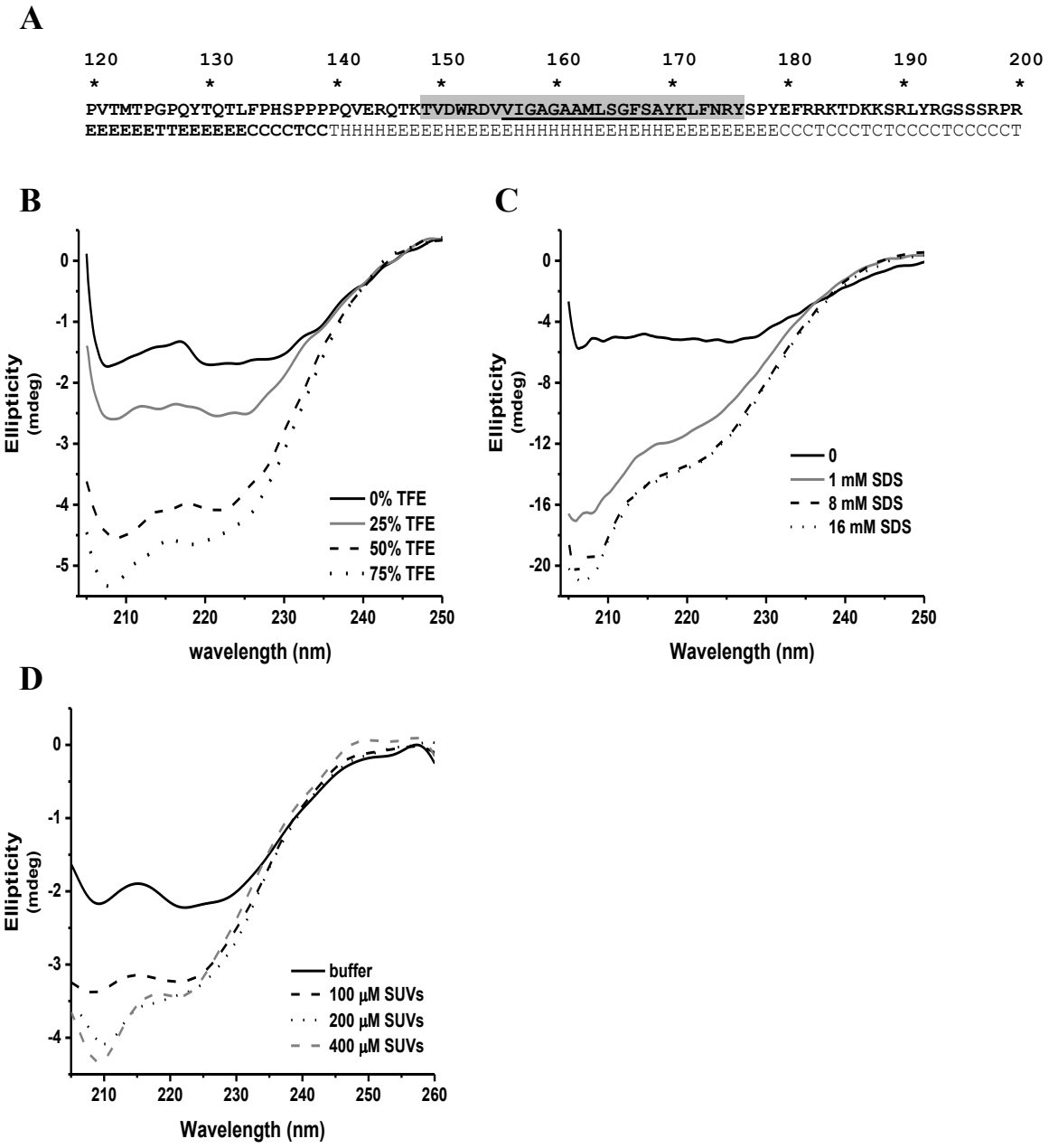

Figure 6: Secondary structure of ldpex14 (120-200)

(**A**) Diagram shows the primary sequence for ldpex14 (120-200) and below each residue is the secondary structure predicted by the Chou-Fasman algorithm [219]; helix (H), sheet (E), and random coil (C). Circular dichroism spectra for ldpex14 (120-200) titrated with increasing concentration of (**B**) trifluoroethanol (TFE), (**C**) SDS, or (**D**) SUVs.

Oligomerization of ldpex*14 (120-200)* – The capacity of ldpex14 (120-200) to induce dye leakage (discussed below) suggested that following membrane insertion the protein undergoes

oligomerization to form a pore structure. The capacity of ldpex14 (120-200) to form oligomers in membranes was assessed by labeling the ldpex14 (120-200) cysteine mutants T147C, S165C, S168C, and S177C with pyrene maleimide. The fluorescence emission spectra of pyrene has five characteristic peaks at 375, 379, 385, 395 and 410 nm; of which bands at 375 and 385 nm are highly sensitive to the microenvironment [222]. A second notable feature of pyrene emission is the emergence of a broad band with emission ranging from ~430-550 nm when two pyrene groups are present within a distance of ~10Å arising from the formation of an excimer [223]. This property can be exploited to examine peptide-peptide association in the lipid bilayer. Addition of pyrene labeled ldpex14 (120-200) T147C and ldpex14 (120-200) S177C to SUVs showed no excimer signal suggesting that packing of helices in the membrane did not position the pyrene groups at position 147 or 177 on adjacent ldpex14 (120-200) within close proximity (**Figure 8A**). In contrast, pyrene labeled ldpex14 (120-200) S165C showed a prominent emission signal at 460 nm which is indicative of both excimer formation and residue 165 of adjacent peptide subunits being in close proximity. A similar excimer signal was detected for pyrene labeled ldpex14 (120-200) S168C, but with a notably weaker emission intensity (**Figure 8A**). When a mixture of pyrene labeled ldpex14 (120-200) cysteine mutants was loaded onto SUVs, a notable decrease in excimer formation by ldpex14 (120-200) S165C and ldpex14 (120-200) S168C mutants (**Figure 8B**) was observed. Plots of the ratio of excimer (emission at 465 nm): monomer (emission at 375 nm) for single mutants or a mixture of ldpex14 (120-200) cysteine mutants support the hypothesis that following oligomerization, residues 165 and 168 are in close proximity (**Figure 8C**).

The capacity of ldpex14 (120-200) to form homo-oligomers was assessed by resolving ldpex14 (120-200) on a 12% Bis-Tris polyacrylamide gel with a MES/0.5% SDS running buffer

[202] without boiling the samples prior to electrophoresis. Results from silver stained gels revealed that ldpex14 (120-200) migrated as a ladder of bands of ~14 to 55 kDa that ranged from monomeric to tetrameric species with ldpex14 (120-200) dimers being the predominant species (**Figure 8D**, *panel i*). Oligomerization of ldpex14(120-200) on DOPE:DOPC:DOPG:PI:Chl LUVs was examined by LUVs with SDS, CHAPS, octylglucoside, or taurodeoxycholate prior to resolving the ldpex14 (120-200) species on a Bis-Tris PAGE modified blue native gel system [224]. ldpex14 (120-200) extracted with these detergents migrated predominantly as monomeric (~15 kDa) and dimeric (~25 kDa) species albeit lower levels of higher order oligomeric species were also observed (**Figure 7D**, *panel ii*). To examine the impact of ldpex14 (120-200) concentration on oligomerization, increasing amounts (5-100 ng/lane) were resolved by SDS-PAGE with and without boiling prior to electrophoresis. At low concentrations (5-20 ng/lane), ldpex14 (120-200) forms predominantly dimers in the presence of SDS, regardless of boiling treatment (**Figure 8E**); while at higher protein concentrations, higher order oligomers (trimers and tetramers) were observed primarily in samples that were not boiled prior to electrophoresis. In contrast, boiling resulted in the formation of ldpex14 (120-200) monomeric and dimeric species (**Figure 8E**). These results indicate that in the presence of SDS, an α-helix potentiating detergent, ldpex14 (120-200) tends to spontaneously form dimers.

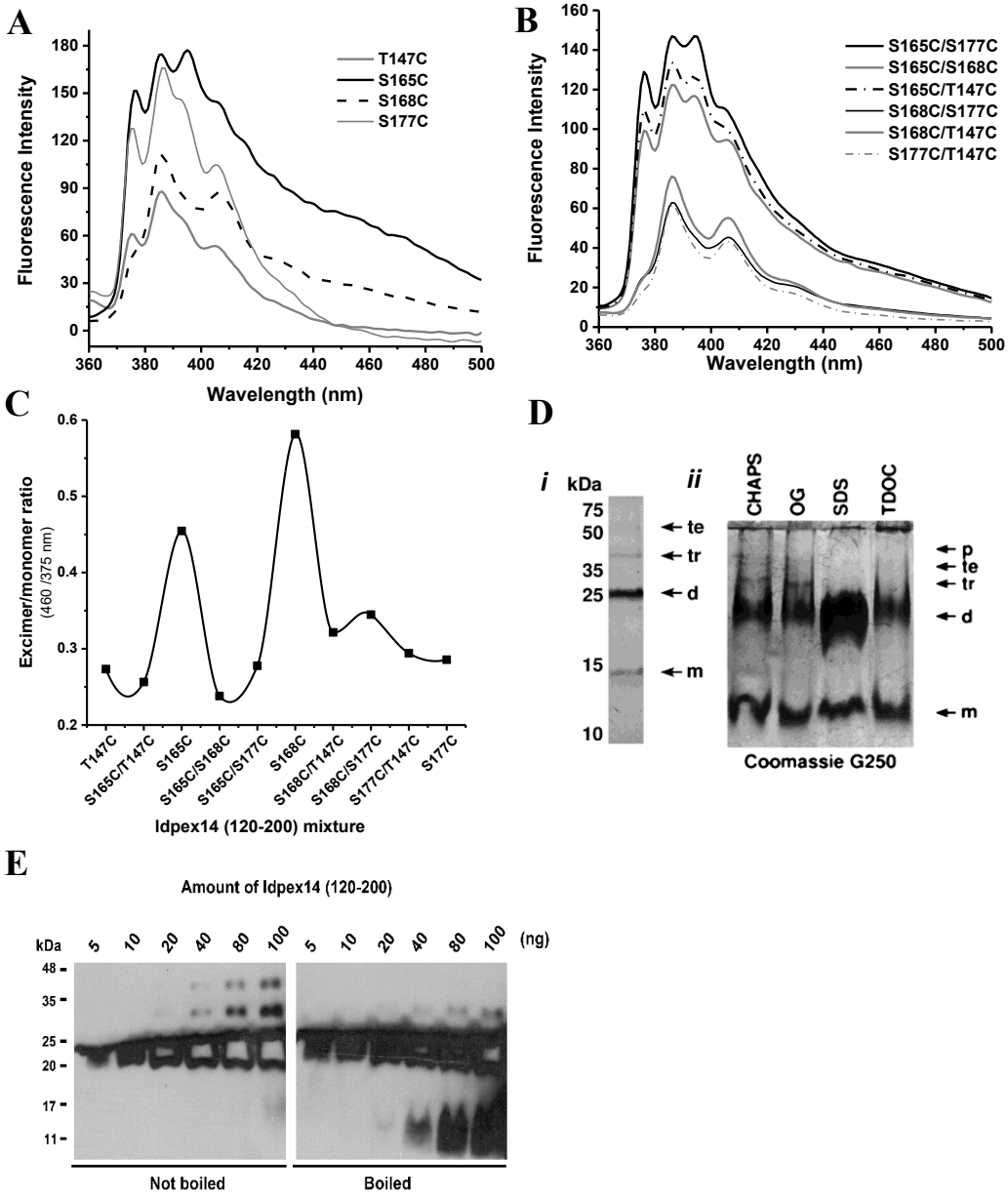

Figure 7: Analysis of ldpex14 (120-200) oligomerization

(**A**) ldpex14 (120-200) cysteine mutants were labeled with pyrene maleimide and then added to SUVs (protein:phospholipid ratio, 1:400) and the emission spectra were recorded using an excitation wavelength of 345 nm. (**B**) Alternatively, the pyrene labeled cysteine mutants were mixed at a 1:1 ratio and the mixture was added to SUVs (protein:phospholipid ratio, 1:400) and the emission spectra recorded using an excitation wavelength of 345 nm. (**C**) The capacity of ldpex14 (120-200) to form dimers in lipid membranes was assessed by calculating the excimer to monomer ratio for the individual cysteine mutant or the 1:1 mixtures of two different cysteine mutants. (**D**) ldpex14 (120-200) oligomerization was assessed by resolving unboiled samples on a 12% Bis-Tris-polyacrylamide gel using MES-Tris buffer containing 0.5% SDS and visualizing protein bands by silver staining (*panel i*). Oligomerization of ldpex14 (120-200) in lipid bilayers was assessed by extracting loaded LUVs with SDS, CHAPS, octylglucoside (OG), or taurodeoxycholate (TDOC) and resolving extracts on a 12 % Bis-Tris polyacrylamide gel using MES-Tris buffer containing 0.02% Coomassie G250 in the electrophoresis buffer.

Ldpex14 (120-200) species were visualized by silver staining (*panel ii*), (m: monomer, d: dimer, tr: trimer, te: tetramer; p: pentamer). (**E**) Concentration dependent oligomerization of ldpex14 (120-200) was examined by resolving increasing amounts (5-100 ng/lane) on an SDS-PAGE gel with and without boiling of the sample. Ldpex14 (120-200) species were detected by Western blot using an anti-hexahistidine monoclonal antibody (1:2000). Areas of clearing (ghosting) for the abundant ~25 kDa species is due to chemiluminescent substrate depletion prior to film exposure.

Ldpex14 (120-200) induces pore formation – It was being proposed that the hydrophobic domain on LdPEX14 is required for transient translocation pore formation. To investigate this function, dye leakage assays were performed using DOPE:DOPC:DOPG:PI:Chl LUVs loaded with the self-quenching carboxyfluorescein dye. In this assay, pore formation on the LUV membrane causes the release and dilution of carboxyfluorescein which resulted in an increase in the fluorescence signal. The capacity for LdPEX14 to form pores was assessed by adding increasing concentrations of LdPEX14 to CF loaded LUVs. Surprisingly, inserting the full length LdPEX14 into the lipid bilayer (**Figure 9C**) failed to trigger dye release which suggests that additional conformational changes may be required for the assembly of a pore structure on the LUV membrane (**Figure 9A**). In contrast, the addition of ldpex14 (120-200) to CF loaded LUVs induced a robust dye leakage that reached a plateau at 38% at a protein concentration of ~0.01 μM or a protein:phospholipid ratio of 1:100 (**Figure 9A**).

To confirm that the tryptophan substitutions introduced into the hydrophobic region did not alter interactions with the lipid bilayer, dye leakage assays were performed with ldpex14 (120-200) tryptophan mutants. As shown in **Figure 9B**, all mutant proteins exhibited significant dye leakage activities of ~35-42%, levels that were comparable to the wildtype ldpex14 (120-200) protein. Dye leakage was not due to non-specific disruption of the membrane since LUVs loaded with a 10 kDa or 45 kDa FITC conjugated-dextran, reporter dyes with a Stokes radii of 2.2 nm and ~3.2 nm respectively [225], were not released by ldpex14 (120-200) (**Figure 9E**).

To further assess the impact of the LdPEX14 regions upstream and downstream of residues 120-200 in pore forming activity, a leakage assay was performed with a number of ldpex14 truncation mutations spanning residues 1-120, 1-200, 1-254, 1-321, and the full-length wild type LdPEX14. As shown in **Figure 9C**, ldpex14 (1-120) at a protein:phospholipid ratio of 1:200 showed no significant pore forming activity. This was not surprising since the flotation assay demonstrated that this N-terminal fragment did not bind to LUVs (**Figure S2**). In contrast, a robust dye leakage activity from 35-42% was observed for truncation mutants ldpex14 (1-200), ldpex14 (1-254), and ldpex14 (1-321) (**Figure 9C**). These results confirmed our previous observations showing that the hydrophobic region spanning residues 120-200 was essential for membrane binding and pore formation [32]. Despite the ability of the full length LdPEX14 to bind to LUVs, it failed to trigger any significant degree of dye leakage, which suggests that the C-terminal segment (residues 322-464) influences the penetration of the hydrophobic domain through the lipid bilayer. It is interesting to note that the rate of dye leakage observed with ldpex14 (120-200) was notably faster when compared to ldpex14 (1-200), ldpex14 (1-254), and ldpex14 (1-321) (**Figure 9D**). Since the latter three proteins have been demonstrated to exist as oligomeric complexes [33], it is likely that the differences in the rate of dye release may be due to the requirement of structural rearrangement prior to insertion of the hydrophobic domain into the lipid bilayer.

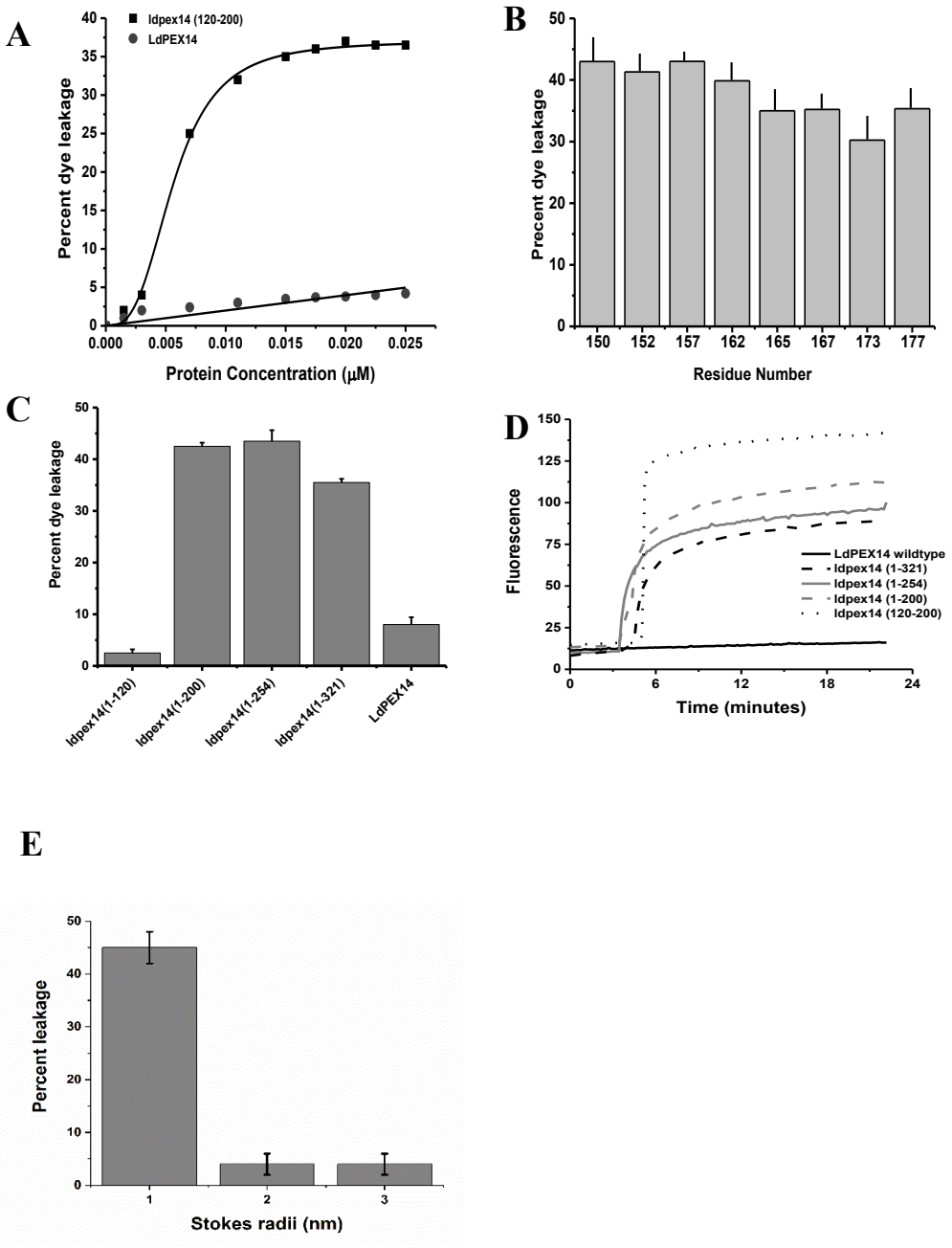

Figure 8: Dye leakage assay

(**A**) Carboxyfluorescein loaded DOPE:DOPC:DOPG:PI:Chl LUVs were titrated with increasing concentrations of ldpex14 (120-200) (squares) or LdPEX14 (circle) and dye release monitored by increased fluorescence using an excitation and emission wavelengths of 492 nm and 515 nm, respectively. (**B**) Similar assays were performed using the panel of tryptophan mutations and the maximum level of dye release was determined spectrophotometrically. These data are the average of triplicated experiments using protein from three separate protein preparations. (**C**) The capacity of various ldpex14 constructs for forming a functional pore was assessed using a dye leakage assay. (**D**) The rate of dye release triggered by the various ldpex14 constructs was monitored as a function of increased fluorescence. (**E**) LUVs loaded with carboxyfluorescein or fluorescein isothiocyanate labelled dextrans with increasing Stokes radii were treated with ldpex14 (120-200) and the percent of dye release determined following sedimentation of LUVs.

Discussion

We investigated the topology of the hydrophobic region of PEX14 inserted into glycosomal membrane mimicking liposomes. Previous studies showed that LdPEX14 can bind liposomes and the region spanning 149-179 is critical for this interaction. This LdPEX14-membrane association was dependent on the presence of anionic lipids in the liposomes [32]. Bioinformatic analysis revealed that the region spanning 149-179 has the propensity to form a transmembrane helix (**Figure 1** and **2**). Deletion of portions of the hydrophobic region was not enough to abolish the binding of the LdPEX14 with the liposome (**Figure 3**). This may be due to an avidity effect that allows weak interaction from the 16-20 subunits of known ~800 kDa homo-oligomeric complex of LdPEX14 stabilizing membrane binding [33, 101]. We have shown that the hydrophobic region of LdPEX14 can undergo conformational changes upon binding with LdPEX5 and can move to a more exposed location [33]. These experiments laid the foundation for our hypothesis that the dynamic rearrangement of the hydrophobic region of the LdPEX14 may be a critical step in the formation of a transient pore for the translocation of cargo proteins across the glycosomal membrane.

A series of tryptophan mutants in region spanning 149-179 of LdPEX14 in combination with Dual quenching analysis (DQA) was utilized to investigate the topology of inserted proteins into the membrane bilayer [203, 204, 226]. DQA revealed that the hydrophobic domain of full length wildtype LdPEX14 showed a shallow penetration and is located near the interface between phosphoglycerol head group and fatty acid chain while ldpex14 (120-200) was found to be inserted more deeply into the membrane bilayer. The region spanning 150-155 and 162-169 of ldpex14 (120-200) exhibited a deeper penetration into the membrane compared to the LdPEX14 hydrophobic domain (**Figure 4D**). These deeper penetrations of the hydrophobic

element in ldpex14 (120-200) was enough for formation of pores in the membrane bilayer (**Figure 9A**).

However, the inability of ldpex14(120-200) to leak higher molecular weight dextran's from encapsulated liposomes indicated that the pore formed was a discrete one with a diameter of ~1.0 nm (**Figure 9E**), and the pore is not formed by a carpet-like mechanism of membrane disruption [227-229]. Similar pores with a diameter of ~1.0 nm were also observed when a yeast PEX5:PEX14 complex was incorporated into planar lipid bilayers [35]. Docking of the cargo loaded PEX5 receptor to PEX14 is postulated to be a primary mechanism that induces the conformational changes which enable the opening of the transient pore [199, 230].

Here we demonstrated that the interaction of LdPEX14 with ldpex5 (203-391) induced structural rearrangements in the membrane bound hydrophobic region, but this fragment alone failed to drive pore formation. Recruitment of interacting proteins such as LdPEX7, LdPEX13, LdPEX2, LdPEX10, LdPEX12, may be required for pore assembly on glycosomes. Dye leakage assays with LdPEX14 C-terminal truncation mutants showed that ldpex14 (1-321), ldpex14 (1-254) and ldpex14 (1-200) triggered robust dye release from LUVs indicating that fragments bearing the hydrophobic region retained pore forming activity. In contrast, wildtype LdPEX14 was unable to form a functional pore, indicating that the C-terminal portion of LdPEX14, which contains a leucine zipper [33], may influence the structural rearrangement of the hydrophobic domain.

Circular dichroism experiments performed with ldpex14 (120-200) in presence of SDS micelles, SUVs [231] or increasing concentrations of trifluoroethanol [221] confirmed that the hydrophobic region can adopt an α-helical structure [232-234]. *Ab initio* modelling of the hydrophobic region spanning residues 149-179 generated two possible models, an extended

alpha helix (**Figure 2B**, **Model-1**) that can transverse the entire lipid bilayer or a helix-turn-helix consisting of a helix hairpin that may extend up to the fatty acyl chain of the inner membrane (**Figure 2B**, **Model-2**). Three independent approaches were employed to examine the orientation of the hydrophobic region in the membrane (**Figure 5C**, **Figure 5D** and **Figure S3).** All those experiments suggested that ldpex14(120-200) preferentially adopted a helix-turn-helix conformation in membranes with N- and C-termini exposed to the exterior space of unilamellar vesicles (**Figure 2B**, **Model-2**).

Another interesting feature of the LdPEX14 hydrophobic domain was its ability to form SDS resistant dimers and potentially oligomers (**Figure 8**). The presence of a GXXX(G/A) motif [233, 235, 236], hydrogen bonding [237, 238] or a combination of both [239] have been demonstrated to assist transmembrane oligomerization. GXXX(G/A) motifs within the hydrophobic domain of LdPEX14 [29] and two serine at positions 165 and 168 that can form hydrogen bonds [240] are likely to contribute to helix packing and oligomerization. The detection of SDS resistant dimers, even at very low protein concentrations is indicative of two ldpex14(120-200) subunits forming a tightly packed transmembrane dimer [233].

Compiling the biochemical and biophysical data has permitted the creation of a comprehensive model (**Figure 10**) showing the orientation of ldpex14(149-200) inserted into the membrane bilayer. We postulate that the pore structure of this protein requires formation of two helices (Helix-1 and Helix-2), from the hydrophobic domain, separated by a turn. Residues 149 and 177 are close to the phospholipid head group and the Helix-1 forms a hairpin turn around residue 160 (**Figure 10E** inset). The length of the inserted helices are too short to transverse the membrane and the pore formed may be due to a combination of factors such as the hydrophobic mismatch between the peptide and the lipid bilayer length that drives the pore formation as

observed by gramicidin A [241] or membrane perturbation resulting in the change of curvature of the membrane as shown by Magainin 2 [242, 243]. The hydrophobic region in the membrane seems to have a hairpin structure and insertion of helix hairpins have been shown to curve the biological membranes. Various proteins have been shown to participate in inducing membrane curvature by inserting their helix hairpins or amphipathic helices into the membrane. For example, hairpins of reticulons (RTNs) have been shown to help in the shaping of ER membrane by insertion of hairpin membrane-binding domain [244], amphipathic helix of structural Nups (Nuclear pore complexes), Nup 133 and Nup 53, generate curvature in the membrane during organization of the nuclear pore [245-247] and hairpins of Mic10 along with a GXXXG oligomerization motif help in membrane tubulation of the mitochondrial cristae [248]. Even though the membrane bilayer is a flat structure, the energy required to curve them can be contributed by membrane associated proteins and alterations of the lipid composition [249-251]. In the actual membrane milieu, the curvature of the membrane may be restricted to a specific area due to lateral compartmentalization of the membrane [252].

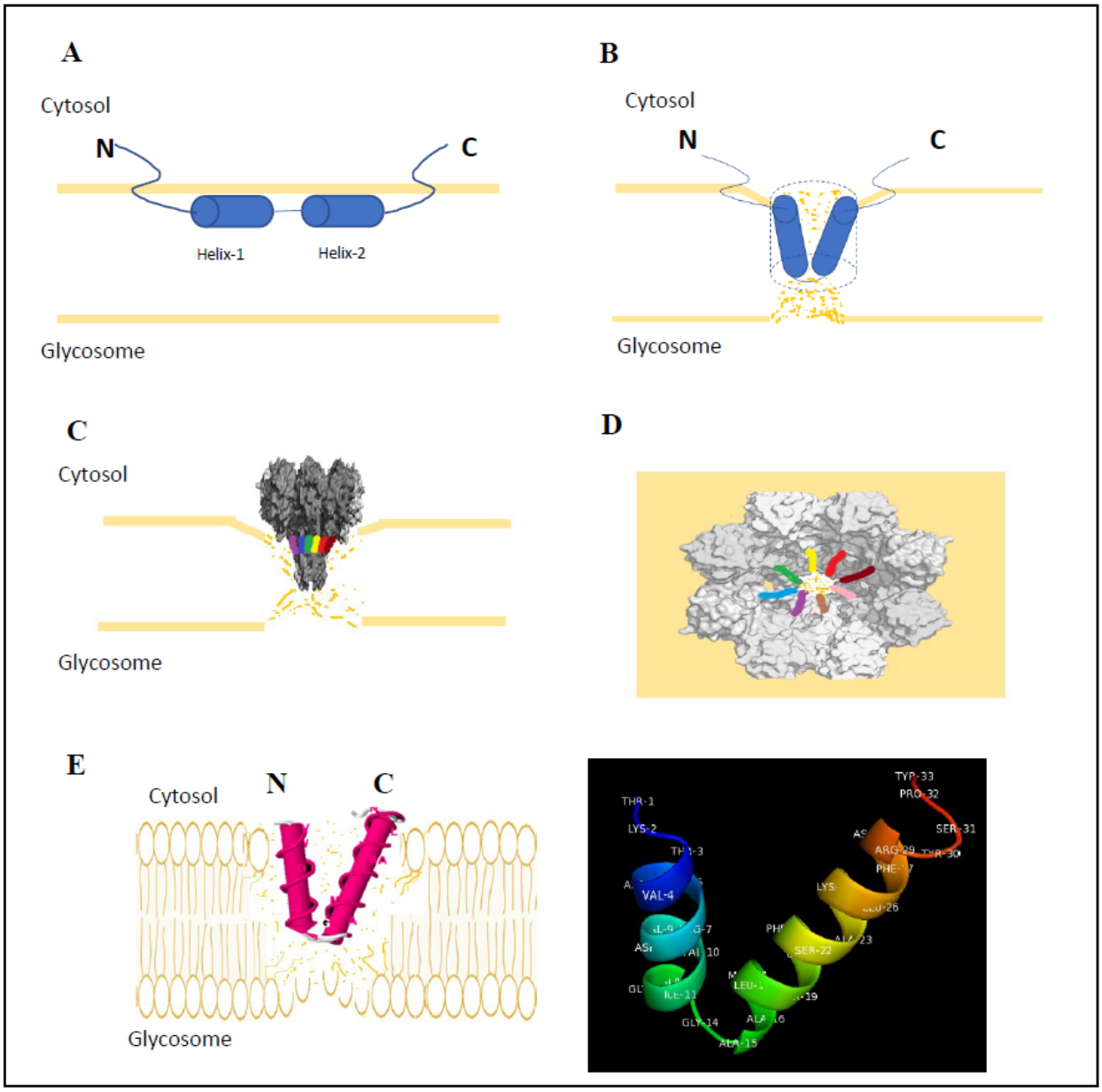

Figure 9: Model of pore formation by hydrophobic domain of LdPEX14

(**A**) Topological analysis of the residues 149-179 (Helix-1 and Helix-2) of wild type LdPEX14 indicated that the hydrophobic domain has a shallow membrane insertion or is weakly associated with the membrane lipids (monomer only shown for simplicity). (**B**) Structural rearrangement of the hydrophobic domain (149-179) results in deeper insertion causing membrane thinning and distortion of nearby lipids (monomer only shown for simplicity). (**C**) Side view (**D**) top view, of the oligomeric pore model of hydrophobic domain in the membrane bilayer. (**E**) Schematic diagram of possible orientation of the Helix-turn-Helix of hydrophobic domain of LdPEX14 inserted in membrane, showing N- and C-termini orienting towards the cytosol, Helix-1 takes a turn around the residues 160 followed by Helix-2.

There are few plausible mechanisms for pore formation by the hydrophobic region of ldpex14. In a normal scenario, the membrane bilayer width is ~30-38 Å and ~17-22 amino acids are required to transverse membrane bilayer [253-256]. However, it has been demonstrated that short hydrophobic helices of < 20 amino acids can form transmembrane structures. Examples include the transmembrane helix (TMH) (14 amino acids) of TatA (Twin arginine translocase A subunit) [257] and helices found in various anti-microbial peptides such as trichogen (11 amino acids) [258] and CM15 (15 amino acids) [259, 260]. The propensity of the hydrophobic domain of ldpex14/LdPEX14 to oligomerize may contribute to pore formation as oligomerization would be a critical step in pore formation by TatA (Twin arginine translocase A subunit) [261] or Cytolysin A (ClyA) (a cytolytic toxin produced by *E. coli*) [261] or actinoporins (pore forming toxin from sea anemone) [262]. The inability of the hydrophobic domain of LdPEX14 to promote leakage of high molecular weight dextran encapsulated LUVs indicate that the pore formed by hydrophobic domain of ldpex14(120-200) is a discrete pore and may be similar to the discrete pore formed by TatA that can accommodate lipids [257].

Twin-Arginine protein translocase (Tat) present on the cytoplasmic membrane of prokaryote and thylakoid membrane of plant chloroplasts share many similar features including the ability to transport folded protein across the membrane, opening of a transient pore and expanding pore diameter to accommodate substrate proteins of various sizes [34, 199, 230, 263-266]. TatA is a central channel forming subunit of the Tat system with a short hydrophobic domain (TMH) followed by an amphipathic helix (APH). The similarities of the LdPEX14 hydrophobic domain to TatA are; (i) the presence of a hydrophobic domain (149-179) that can form a helix-turn helix motif with the potential to penetrate the membrane bilayer and adopt different conformations, (ii) the TMH of TatA is a short helix (~14 amino acids) similar to the short helices found in

hydrophobic domain of PEX14 (Helix-1 (~11 amino acids) and Helix-2 (~15 amino acids), (iii) TMH of TatA can distort and rupture the membrane to form a short pore like that formed by the hydrophobic domain of LdPEX14. The differences include: (i) TatA exists as a monomer and oligomerizes to form the pore while ldpex14(120-200) (this study) or wild type LdPEX14 exist as oligomeric structures g [33] and (ii) TatA is found as a transmembrane protein while LdPEX14 is a peripheral membrane protein. In the TatA mediated transport, the hydrophobic region of TatA inserts into the membrane and the increase in angle between TMH and APH results in deep insertion of the APH into the membrane. Interaction of the TatA with the TatB/substrate complex results in the oligomerization of TatA and subsequently membrane thinning and distortion of the bilayer to form a pore channel [257, 264, 266]. Hence, we assume that the structural rearrangement of the hydrophobic domain of LdPEX14 would distort and rupture the glycosomal membrane in a similar manner to form a transient pore that can pave the way for expanding the waistline to transport the cargo into the glycosomal lumen.

Membrane proteins that do not span the bilayer but still perturb it were classified as a new class of membrane proteins. These proteins challenged the conventional concept of membrane proteins and it was demonstrated that the membrane proteins that do not span the membrane bilayer can perturb the bilayer structure to form transmembrane channels [267]. This concept was used to explain the formation of lipid pores in amyloid disease, the action of antimicrobial peptides, and the assembly of the membrane-attack complexes of the immune system and could be adapted for solving the mystery of trafficking of cargo loaded receptors across membranes. Hence, we postulate that the conformational changes occurring in the LdPEX14 hydrophobic region result in membrane perturbation, and formation of a lipidic pore that could act as a foundation for expansion by the cargo loaded receptors.

Acknowledgements

This work was supported by operating grants from the Canadian Institutes of Health Research (AJ) and an FQRNT Regroupement Strategique grant to the Centre for Host-Parasite Interactions. NC was supported by a doctoral research scholarship from FQRNT. We thank Dr. C. Salsse (U. Laval) for help with the discussion on the analysis of the biophysical structure of the LdPEX14 hydrophobic region and D. Reinhardt (McGill U.) for providing access to the spectropolarimeter for the circular dichroism experiments.

Supplementary Figures

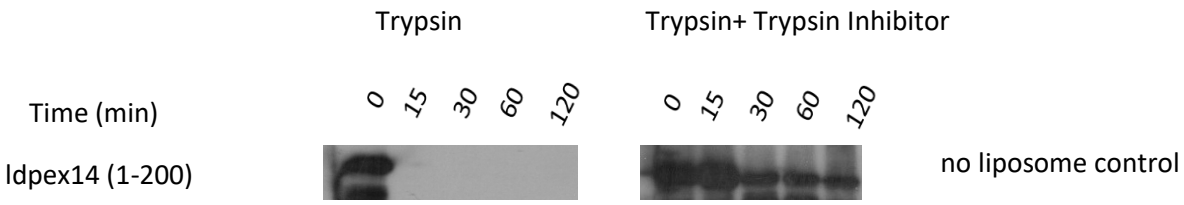

Figure S1: Trypsin digestion of ldpex14 (1-200) in the absence of LUV's

Complete digestion of ldpex14 (1-200) was observed within 15 minutes of addition of trypsin compared to full recovery of the protein in the presence of a trypsin plus trypsin inhibitor.

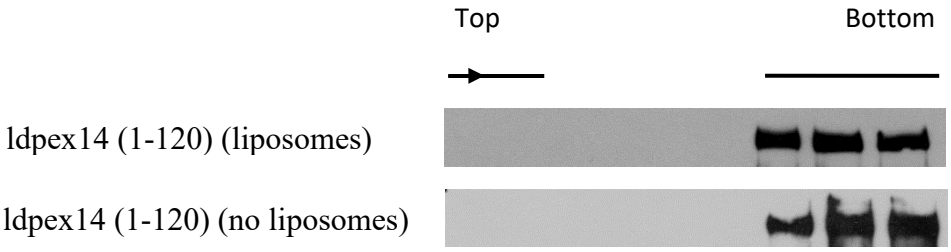

Figure S2: Sucrose density floatation of ldpex14 (1-120)

LUVs were loaded with the ldpex14 (1-120) and bound protein was separated by sucrose density floatation and proteins were detected by Western blot analysis using anti-LdPEX14. Sucrose density flotation demonstrated that ldpex14 (1-120), the N-terminal fragment of LdPEX14, were unable to bind the LUV's.

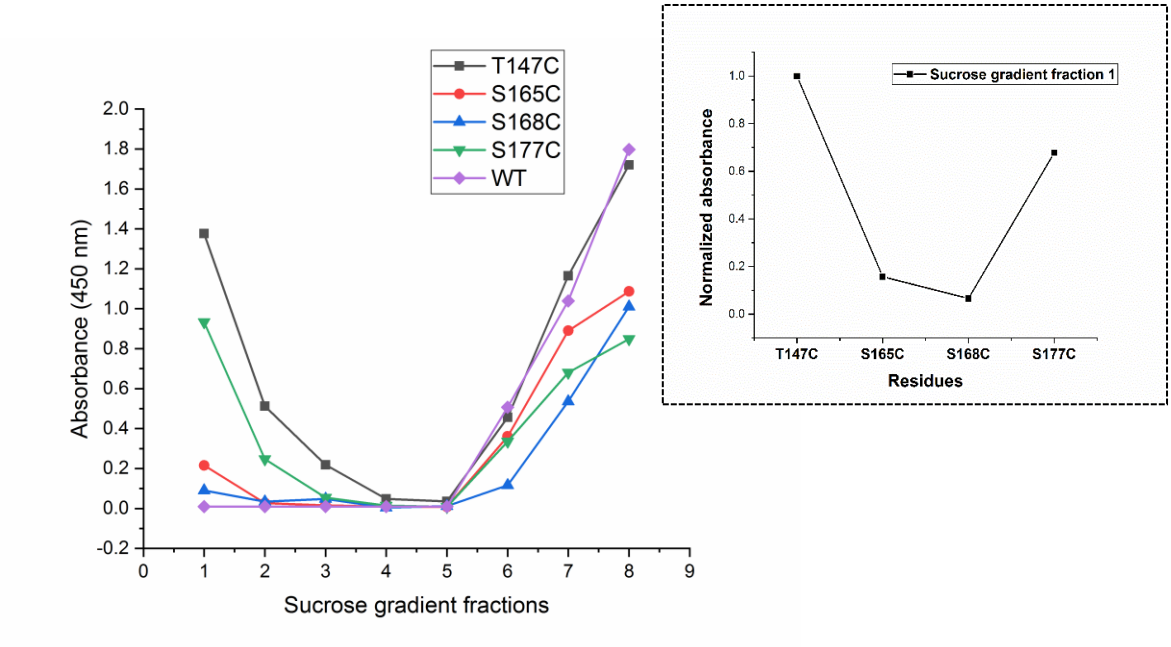

Figure S3: Interaction of biotinylated ldpex14 (120-200) mutants with SUVs

Orientation of the hydrophobic domain of ldpex14 was assessed in floated LUVs utilizing the interaction between biotinylated ldpex14 (120-200) cysteine mutants and streptavidin-HRP. The accessibility of residues inserted into LUVs was monitored as absorbance and residue having highest absorbance is the most accessible residue from outside the membrane bilayer.

Connecting Statement

In **Chapter 3**, we investigated the topology of hydrophobic region of LdPEX14 inserted into unilamellar vesicles. We found that the hydrophobic region exhibits a shallow penetration in WT LdPEX14 compared to a deeper penetration in ldpex14 (120-200). Also, insertion of the hydrophobic region of ldpex14 (120-200) was able to perturb the membrane and form a short pore. Even though there was structural rearrangement of the hydrophobic region in WT LdPEX14 in the presence of ldPEX5 (203-391), it was unable to induce a pore in the membrane.

We assume that the recruitment of other PEX14 interacting proteins such as LdPEX7, LdPEX13 and RING finger proteins would be needed to bring conformational changes to induce a pore. In the absence of accessory proteins, we altered pH as a surrogate method to induce conformational changes and determine whether LdPEX14 has the potential to induce the formation of a short pore. In Chapter 4, we discovered that conformational changes triggered by pH can perturb the membrane and form a short pore. This chapter demonstrates that conformational changes in the hydrophobic region of LdPEX14 can contribute to the formation of a membrane pore.

Chapter 4

Study of conformational changes in the hydrophobic region of LdPEX14 induced by low pH

Anwer Hasil Kottarampatel[1,2*], Normand Cyr[1,2], and Armando Jardim[1,2‡]

From the [1]Institute of Parasitology and [2]Centre for Host-Parasite Interactions, Macdonald Campus of McGill University, Ste-Anne-de-Bellevue QC, Canada,

Running Title: Conformational changes in Ld*PEX14*

Keywords: *Leishmania,* glycosome, PEX5, PEX14, protein targeting, membrane binding, liposome.

‡ To whom correspondence should be addressed: Institute of Parasitology, Macdonald Campus of McGill University, 21, 111 Lakeshore Road, Ste-Anne-de-Bellevue, Québec, Canada H9X 3V9. Phone: (514) 398-7727; Fax: (514) 398-7857, email: armando.jardim@mcgill.ca.

Abbreviations – ANS, 8-Anilinonaphthalene-1-sulfonic acid, IPTG, isopropylthiogalactoside; PBS, phosphate buffered saline, PEX, peroxin; LdPEX5, *L. donovani* peroxin 5; LdPEX14, *L. donovani* peroxin 14

Abstract

Transport of PTS-1 cargo protein across the glycosomal membrane in *Leishmania* requires the binding of the cargo loaded peroxin 5 (LdPEX5) receptor to the peroxin 14 (LdPEX14) docking complex on the glycosome surface. Analysis of LdPEX14 membrane interactions using vesicles that mimic the phospholipid composition of the *L. donovani* glycosome lipid bilayer showed that membrane insertion was dependent on an amphipathic helix spanning residues 149-179 of LdPEX14. Dye leakage assays revealed that pore formation by the full length LdPEX14 required conformational changes that could be triggered by a pH shift. Rearrangement of the LdPEX14 hydrophobic region was necessary to form the pore by LdPEX14.

Introduction

Leishmaniasis is considered as a neglected tropical disease caused by the parasites of *Leishmania* genus [268-270]. The various clinical manifestation of the disease are cutaneous, mucocutaneous, and visceral leishmaniasis, the latter of which is caused by *L. donovani* [55, 271] and if left untreated, is fatal for the patient [7, 272]. Cases of leishmaniasis have been reported in over 88 countries, primarily in tropical and subtropical areas around the globe. The World Health Organization (WHO) estimated that around 350 million people are at risk and 10 million people are currently infected [4, 8].

Leishmania parasites have a digenetic life cycle, a promastigote form residing in the sand-fly midgut and an amastigote form residing in the macrophages of human host [11, 12, 59]. *Leishmania spp*. contain a unique organelle, called the glycosome which compartmentalizes a variety of metabolic pathways that include glycolysis, pyrimidine biosynthesis [18], ether-lipid biosynthesis, β-oxidation of fatty acids [20] pentose-phosphate pathway, and purine salvage [21, 131].

Glycosomes do not contain genetic material or protein translation machinery. Hence, nascent luminal proteins are synthesized in the cytosol and transported across the glycosomal membrane. Glycosomes are evolutionarily related to peroxisomes of higher eukaryotes. Similarly folded and oligomeric proteins are transported across the peroxisomal membrane [26, 163]. Proteins destined for the glycosome contain one of the two topogenic signal sequences, a C-terminal PTS-1 (peroxisomal targeting sequence 1) or the N-terminal PTS2 (peroxisomal targeting sequence 2) [273]. Proteins with a PTS1 or PTS2 signal are bound by cytosolic peroxin receptors peroxin 5 (PEX5) and peroxin 7 (PEX7), respectively, and transported into the

glycosome with the help of a glycosomal peripheral membrane protein, peroxin 14 (PEX14) [29, 33, 135, 150].

Electrophysiology experiments have demonstrated the presence of distinct pores in the peroxisomal/glycosomal membrane [35, 143]. In yeast, PEX14 and PEX5p assemble into a large complex ~800 kDa that form pores in the liposome with a diameter of around 0.6 nm. [35, 36, 162]. It has been reported that the pores formed in the peroxisome are large enough to pass a PTS1-decorated gold particle [163]. A distinct PTS2 pore with co-receptor PEX18 and the PEX14/PEX17-docking complex has been identified in yeast possessing an estimated diameter of ~4.7 nm [34]. PEX14 was found to be a common ingredient in both the PTS1 and PTS2 pores and is thought be play a key role in building the translocation pore.

PEX14 is an essential component for kinetoplastid parasite viability [23, 31]. *L. donovani* PEX14 exhibits characteristics of a peripheral membrane protein with interacting domains distinguished as the PEX5 binding domain, PEX7 binding domain, leucine zipper, and a hydrophobic region spanning residues 149-179 [33, 138, 144]. Sucrose density centrifugation and fluorescence-activated cell sorting (FACS) have demonstrated that membrane-binding activity was dependent on a predicted hydrophobic transmembrane-like helix found within residues 149-179. A fragment of PEX14 spanning from 120-200 amino acid residues, ldpex14(120-200) was able to bind to the LUVs. Thus the hydrophobic region was found to mediate the binding of PEX14 with the LUVs that mimics the glycosomal membrane [32]. Also, by dye leakages assay it was demonstrated that ldpex14 (120-200) has the propensity to form pores in the liposomal membrane. Surprisingly the full length PEX14 was unable form a pore in the membrane by itself [32, 33]. It was demonstrated that binding of ldpex5 (203-391)

to PEX14 resulted in movement of the hydrophobic region deeper into the bilayer as described in **Chapter 3**. But still PEX14 was unable to form a transient pore in the presence of ldpex5 (203-391) or PEX5. It is possible that recruitment of other PEX14 interacting proteins is required to form a functional pore.

In the absence of PEX14 interacting partners like PEX5, LdPEX7, RING finger proteins etc., we adopted a surrogate method to induce conformational changes by altering the pH. Here we demonstrate that conformational changes triggered by changes in pH caused the hydrophobic region to penetrate the membrane bilayer which resulted in the formation of a pore. These studies provide a molecular insight for understanding how the conformational changes at the hydrophobic region could contribute to transient transmembrane pore formation that is involved in the transport of folded proteins into the glycosome lumen.

Materials and Methods

Chemicals and reagents – All restriction endonucleases and DNA-modifying enzymes were purchased from Invitrogen or New England Biolabs. Horseradish peroxidase (HRP)-conjugated goat anti-rabbit IgG was purchased from GE Healthcare. Synthetic phospholipids and cholesterol (Chl) were obtained from Avanti Polar Lipids. All other reagents were of the highest commercially available quality.

Protein expression and purification – The *L. donovani PEX14* coding sequence and an internal deletion mutant lacking the amino acids 149-179 (ldpex*14Δ149-179)*, 138-165 (ldpex*14Δ138-165),* 160-179 ((ldpex*14Δ160-179),* or 179-200 ((ldpex*14Δ179-200)* were generated by PCR

based mutagenesis using the C-terminal hexahistidine-tagged pET30-Ld*PEX14-His$_6$* to construct pET30-ldpex*14Δ149-179-His$_6$*, ldpex*14Δ138-165-His$_6$*, ldpex*14Δ160-179-His$_6$*, ldpex*14Δ179-200-His$_6$* expression vectors. A fragment encompassing amino acids 120-200 of the LdPEX14 was amplified by PCR and cloned into the *Nde*I/*Xho*I sites of pET30b (+) to generate pET30b-ldpex*14 (120-200)-His$_6$* expression construct. LdPEX14/ldpex14 proteins were expressed in the *E. coli* strain ER2566 and purified as previously described [33], except for ldpex14 (120-200) which was extracted from inclusion bodies prior to purification. Purified proteins were concentrated and buffer exchanged for 40 mM Tris-HCl pH 8.0 150 mM NaCl (TBS150) using an Amicon Ultra filter 3K or 10K MWCO unit (Millipore) and the protein concentration measured spectrophotometrically at 280 nm by the method of Pace *et al.* [200]. Purified proteins were stored at -80 °C.

Liposome preparation – Individual phospholipids of DOPE:DOPC:DOPG:PI:Chl (55:25:15:2.5:2.5) were dissolved in chloroform and thin films were prepared by evaporation of the solvent under a nitrogen stream. The lipid film was kept under vacuum for 16 h to remove any residual chloroform. Multilamellar vesicles were prepared by re-suspending the lipid film in PBS at a concentration of 5 mg/ml. The suspension was then extruded through a 0.2 μm polycarbonate membrane (Millipore) to generate large unilamellar vesicles (LUV) with a diameter of 200 nm, a size comparable to *Leishmania* glycosomes [274].

LUV leakage assay – DOPE:DOPC:DOPG:PI:Chl (55:25:15:2.5:2.5) lipid films were re-suspended in PBS containing 100 mM 5(6)-carboxyfluorescein (CF) (Sigma Aldrich) or 50 mM sulforhodamine B (SRB) (Sigma Aldrich) and the multilamellar vesicles extruded through a 200

nm polycarbonate membrane to generate large unilamellar liposomes (LUVs). Dye loaded LUVs were purified by gel filtration on Sephadex G-50 column equilibrated in PBS and aliquots of CF or SRB loaded LUVs were titrated with increasing concentrations of ldpex14 (120-200), LdPEX14, ldpex14 deletion mutants and dye release was monitored using excitation and emission wavelengths of 492 nm and 515 nm for CF or 565 nm and 586 nm for SRB. The total CF or SRB content of the LUVs was determined by addition of Triton X-100. All dye leakage assays were performed at 25 °C.

For leakage assays performed at varying pH values, a universal buffer containing 50 mM sodium acetate, 50 mM MOPS, and 50 mM Tris-HCl was prepared and the pH was adjusted using HCl or NaOH. Aliquots of SRB loaded LUVs were diluted into the universal buffer of specific pH and dye leakage was monitored for 5 min prior to addition of LdPEX14/ldpex14 proteins. To estimate the diameter of the pores formed by LdPEX14, LUVs were loaded with 10 mg/ml of 10, or 45 kDa fluorescein-isothiocyanate (FITC) conjugated-dextran (FD4, FD10, or FD45) and extravesicular dextran was removed by gel filtration on Sephadex G-200 column. To assess dextran leakage, LUVs (400 µg) were incubated with LdPEX14 (LdPEX14:phosphlipid ratio 1:250 to 1:2,000) in 50 mM sodium acetate, 100 mM NaCl, pH 4.5 buffer and incubated at 25 °C for 15 min and were pelleted at 100,000 x *g* for 45 min at 4 °C in a Beckman-Coulter tabletop centrifuge using a TLA100.3 rotor. The supernatant was carefully removed, and LUV pellet was solubilized in 0.5 % Triton X-100, 50 mM Tris pH 7.5 and the fluorescence intensity for the supernatant and pellet measured using excitation and emission wavelengths of 495 and 515 nm, respectively.

Leakage was calculated by the following equation:

$$\% \text{ leakage} = (F_{con}-F_{LdPEX14})/F_{con} \times 100$$

Where, F_{con} is total fluorescence in the control LUVs and $F_{LdPEX14}$ is the total fluorescence in LUVs treated with LdPEX14.

Sucrose density flotation centrifugation – LUVs were incubated with proteins (1:500 LdPEX14:phospholipid) in 300 µl of PBS for 40 min at 25 °C, mixed with 1.2 ml of 66 % sucrose in PBS (w/v), transferred to a 5.2 ml ultracentrifuge tube and overlaid with 3.0 ml of 40 % sucrose in PBS, and then 1.0 ml of PBS. Samples were subjected to centrifugation at 75,000 x *g* for 16 h at 4 °C in a Beckman-Coulter SW55 rotor. The gradient was fractionated (0.65 ml/fraction) and the proteins precipitated with trichloroacetic acid (15%) prior to Western blot analysis.

Size exclusion chromatography – Chromatographic analysis was performed on a Phenomenex BioSep S3000 column using a Beckman-Coulter System Gold high performance liquid chromatography system with a UV/Vis photodiode array detector. For each run, 50 µg of LdPEX14 was injected and the column was developed using either a 40 mM Tris-HCl pH 7.8, 150 mM NaCl, 50 mM sodium acetate, 150 mM NaCl pH 5.5 or 50 mM sodium acetate, 150 mM NaCl pH 4.5 as a mobile phase at a flow rate of 0.2 ml min^{-1}. The column was calibrated using a protein standard mixture containing thyroglobulin (660 & 330 kDa), IgG (160 kDa), ovalbumin (45 kDa), and horse heart myoglobin (17 kDa).

Fluorescence spectroscopy –Fluorescence measurements were performed on a Varian Cary Eclipse spectrofluorometer at 25 °C using an excitation wavelength of 290 nm. The effect of pH on the LdPEX14 (5 μM) structure was examined by recording the emission spectra from 305-400 nm at various pH levels using a universal buffer containing 50 mM sodium acetate, 50 mM MOPS, and 50 mM Tris-HCl and the pH was adjusted using HCl or NaOH. Insertion of Trp152 in the lipid bilayer was monitored by recording emission spectra from 305-400 nm at a scan rate of 120 nm/min with slit widths of 5 nm. A 5 μM solution of ldpex14 (120-200) in 40 mM Tris pH 8.0, 150 mM NaCl, was titrated with SUVs to a final concentration of 1.0 mM phospholipids. Solvent accessibility of tryptophan residues was assessed using acrylamide as a fluorescence quenching reagent. ldpex14 (120-200) (5.0 μM in PBS) was titrated with acrylamide in the presence or absence of SUVs (1.0 mM phospholipids). Changes in fluorescence intensity were monitored at an emission wavelength of 325 nm and an excitation wavelength of 290 nm. Forster Resonance Energy Transfer (FRET) experiments were performed by incubating 10 μM of LdPEX14 alone or in the presence of 5 μM 1-anilino-8-naphthalene sulfonate (ANS) at pH 4.5 or 7.5 and recording the emission spectra from 305-550 nm.

Circular dichroism (CD) analysis – LdPEX14 or ldpex14 (Δ149-179) preparations were dialyzed against 10 mM sodium phosphate, 10 mM NaCl pH 7.5 or 10 mM sodium acetate pH 4.5, 10 mM NaCl pH 7.5 and the concentration adjusted to 10 μM with spectra recorded at 23 °C on a JASCO 810 instrument using a 1 mm cuvette at a scan rate of 100 nm/min and a bandwidth of 1 nm. CD spectra were recorded from 195 nm to 260 nm recorded at 23 °C. Five spectra were collected and averaged.

Results

Multiple sequence alignment of predicted PEX14 hydrophobic regions

Primary structure analysis of LdPEX14 reveals various domains, a conserved transmembrane domain is observed among all these species indicating the potential importance of this region. The transmembrane region in PEX14 from phylogenetically diverse organisms was predicted using EMBOSS and residues in the transmembrane region were aligned using the PRALINE multiple sequence alignment software (**Figure 1**). Even though the PEX14 sequences shared only ~10% identity, the hydrophobic region was more conserved and the potential transmembrane domain was predicted by the TMAP program [275, 276].

Organism	Multiple sequence alignment of predicted PEX14 transmembrane region
Homo sapiens	- S R W R D - - Y G A L A I I M A G I - A F - G F - H Q L Y K K Y L
Mus musculus	- S R W R D - - Y G A L A I I M A G I - A F - G F - H Q L Y K R Y L
Trypanosoma brucei	- - - W R D L V I G A G A A V I G G F A A F - K A - F Q L Y S P Y E
Leishmania donovani	- V D W R D V V I G A G A A M L S G F S A Y - K L - F N R Y S - - -
Arabidopsis thaliana	R F R W Y H - - - - - - A I L A V G V L A A S G A G T A V F I K R S
Consistency	0 2 3 * 6 7 0 1 3 6 6 2 * 6 7 5 4 * 6 1 * 5 0 5 4 0 3 5 5 8 4 3 3 2

Figure 1: Comparison of predicted PEX14 protein transmembrane

The transmembrane region in PEX14 among various species was predicted by using EMBOSS- TMAP, after inserting multiple sequences of PEX14 and the residues in this transmembrane region were aligned using the PRALINE multiple sequence alignment program which uses the BLOSSUM 62 residue exchange matrix, where 0 represents the least conserved and 10 is the most conserved.

LdPEX14 induces dye leakage from encapsulated liposome at pH 4.5

We postulate that docking of the cargo loaded LdPEX5 and LdPEX7 receptor proteins in addition to other integral membrane proteins of the translocation complex may facilitate the structural changes that promote pore formation by LdPEX14. However, the interactions driving these events have not been defined; consequently, we used a pH shift to mediate subtle potential conformational changes that would promote membrane penetration. For these dye leakage assays, sulforhodamine B (SRB), a pH insensitive fluorescent dye loaded into LUVs were mixed with LdPEX14 at various pH values and the dye release was monitored. These experiments showed that LdPEX14 triggers an increasing amount of dye release as a function of decreasing pH that typically resulted in ~50-60% SRB leakage at pH 4.5 with an LdPEX14:phospholipid ratio of 1:1000 (**Figure 2A**). SRB loaded LUVs alone showed nonsignificant dye leakage even at pH 4.5.

Previous studies have demonstrated that despite LdPEX14 binding to LUVs at pH 7.5, this membrane active protein failed to induce pore formation and dye leakage. To confirm that a conformational change induced by an acidic pH was sufficient for membrane insertion, LUVs were loaded with an increasing concentration of LdPEX14 at pH 7.5 and subjected to a rapid shift to pH to 4.5. These experiments revealed that exposure of membrane bound LdPEX14 to an acidic pH caused a protein concentration dependent SRB leakage with an LdPEX14:phospholipid ratio of 1:10,000 promoting ~28% leakage (**Figure 2B**). Interestingly, adding increasing concentrations of LdPEX14 to LUVs at pH 4.5 also caused SRB leakage. However, higher concentrations of LdPEX14 were required which suggest that the conformations adopted by this protein at acidic pH had a restricted capacity for membrane insertions and pore formation (**Figure 2B**). Dye loaded liposomes alone showed negligible leakage as a function of pH.

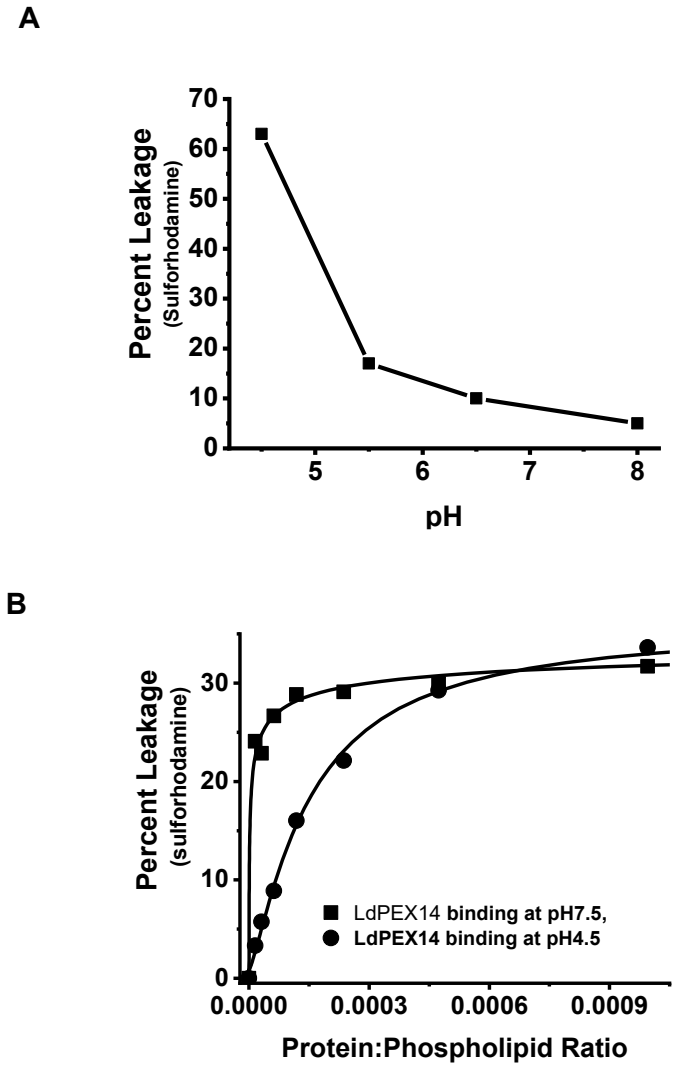

Figure 2: Dye leakage activity of LdPEX14/ldpex14

(**A**) The effect of pH on LdPEX14 mediated release of sulforhodamine B (SRB) loaded DOPE:DOPC:DOPG:PI:Chl LUVs was monitored by performing dye leakage assays at various pH. (**B**) The effect of pH on protein binding and pore formation was examined by incubating SRB loaded LUVs with increasing concentration of LdPEX14 at pH 7.5 and after 5 min the pH was shifted to 4.5 (squares) and dye release monitored. Alternatively, increasing concentrations of LdPEX14 were added to SRB loaded LUVs at pH 4.5 (circles) and monitored. Total dye release was plotted as a function of the LdPEX14:phospholipid ratio.

Effect of pH on LdPEX14 conformation

The effect of pH on LdPEX14 conformation was examined in solution using the intrinsic fluorescence of Trp152 as a structural probe. At pH 8.0, Trp152 showed emission maxima (λ_{max}) centered at ~327 nm, consistent with this residue being located in a nonpolar environment (**Figure 3A**). However, decreasing the pH induced a red shift in the emission λ_{max} to 337 nm characteristic of Trp152 relocating to a more polar, solvent exposed environment. The mobilization of the amphipathic domain was further investigated by Forster Resonance Energy Transfer (FRET) experiments using the extrinsic fluorescence probe 8-Anilinonaphthalene-1 Sulfonic Acid **(**ANS). The binding of ANS to a hydrophobic surface results in a dramatic increase in the fluorescence intensity and a blue shift in the emission λ_{max} to 475 nm at an excitation wavelength of ~340 nm which overlaps the emission spectra of Trp152. Consequently, when Trp152 is excited at a wavelength of 290 nm the fluorescence emission energy will be absorbed by neighbouring ANS molecules causing a quenching in the emission fluorescence ~340 nm and the appearance of a new fluorescence emission band at ~475 nm. Addition of ANS to LdPEX14 at pH 7.5 resulted in a FRET effect and the emergence of an emission λ_{max} centered at 475 nm (**Figure 3B**) suggesting that this extrinsic fluorescence reporter associated with a hydrophobic domain. Shifting the pH from 7.5 to 4.5 induced a conformational change that resulted in a ~4-fold increase in the ANS fluorescence; a finding that substantiated the intrinsic fluorescence data suggesting that the amphipathic region containing Trp152 relocated to a more surface exposed environment (**Figure 3B**). It is tempting to speculate that this re-arrangement allows the LdPEX14 amphipathic region to penetrate deeper into the lipid bilayer to facilitate pore formation. That ANS preferentially bound to the amphipathic domain was supported by the finding that ldpex14 (Δ149-179) showed a significantly lower ANS fluorescence at pH 4.5 or 7.5 (**Figure 3C**).

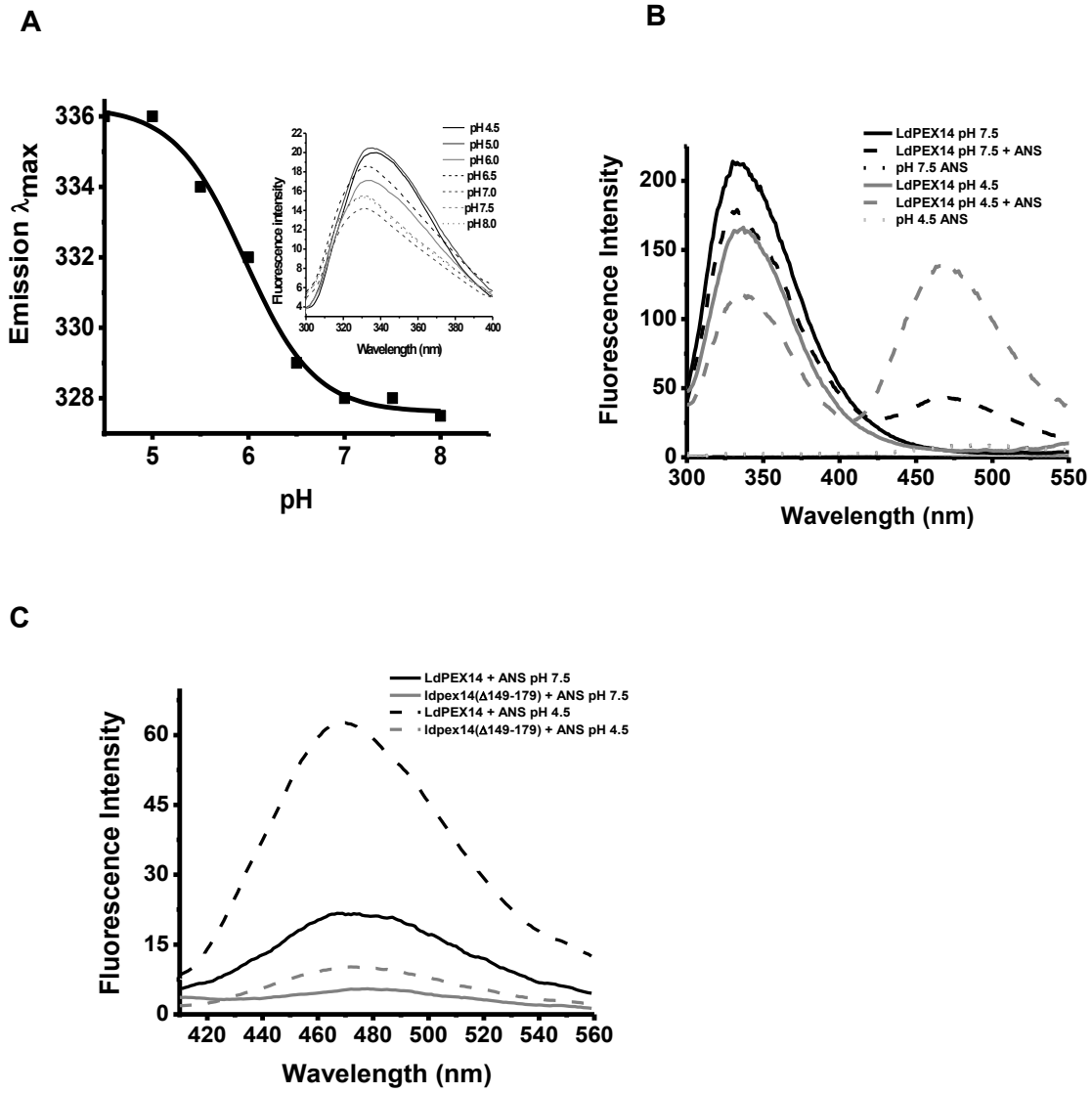

Figure 3: Effect of pH on LdPEX14 conformation

(**A**) The effect of pH on LdPEX14 conformation was monitored by intrinsic fluorescence at an excitation wavelength of 290 nm and recording the emission spectra was recorded from 300-420 nm (inset) and the changes in the emission λ_{max} plotted as a function of pH. (**B**) Exposure of the LdPEX14 amphipathic domain in response to pH was analyzed by FRET between Trp152 and ANS. LdPEX14 (10 μM) at pH 4.5 or 7.5 or with LdPEX14 plus 5 μM ANS using an excitation wavelength of 290 nm and recording the emission spectra from 300-550 nm. (**C**) Binding of ANS to LdPEX14 and ldpex14 (Δ149-179) was assessed at pH 4.5 and 7.5 in the presence of 5 μM ANS at an excitation wavelength of 350 nm.

Effect of pH on the LdPEX14 structure bound to liposomes

To assess if pH affects the LdPEX14 oligomeric state [33], size exclusion chromatography (SEC) analysis was performed at pH 4.5, 5.5, and 7.5. Surprisingly, no notable change in the LdPEX14 quaternary structure was observed, suggesting that changes in pH induced a localized conformational alteration that did not disrupt the LdPEX14 homomeric structure (**Figure 4A**). The slight differences in the elution position were attributed to variations in the hydrodynamic volume of the complex. Circular dichroism (CD) analysis of wild type LdPEX14 also demonstrated that acidic pH induced minor variations in the minima at 208 nm and 220 nm, consistent with modest changes in the α-helical content of LdPEX14 (**Figure 4B**).

To establish that SRB leakage induced by LdPEX14 was mediated through a discrete pore rather than a more general disruption of membrane integrity, leakage experiments were also performed with LUVs using SRB or FITC labelled dextrans (4 kDa, 10 kDa, or 45 kDa) with Stokes radii of 0.65, 1.4, 2.3, and 3.2 nm, respectively. Addition of LdPEX14 to LUVs at a pH of 4.5 triggered a robust leakage of only SRB and confirmed the formation of a pore with an inner diameter of ~1.0 nm that did not permit the transit of the larger dextran molecules (**Figure 4C**). No SRB or FITC-dextran release was detected at pH 7.5.

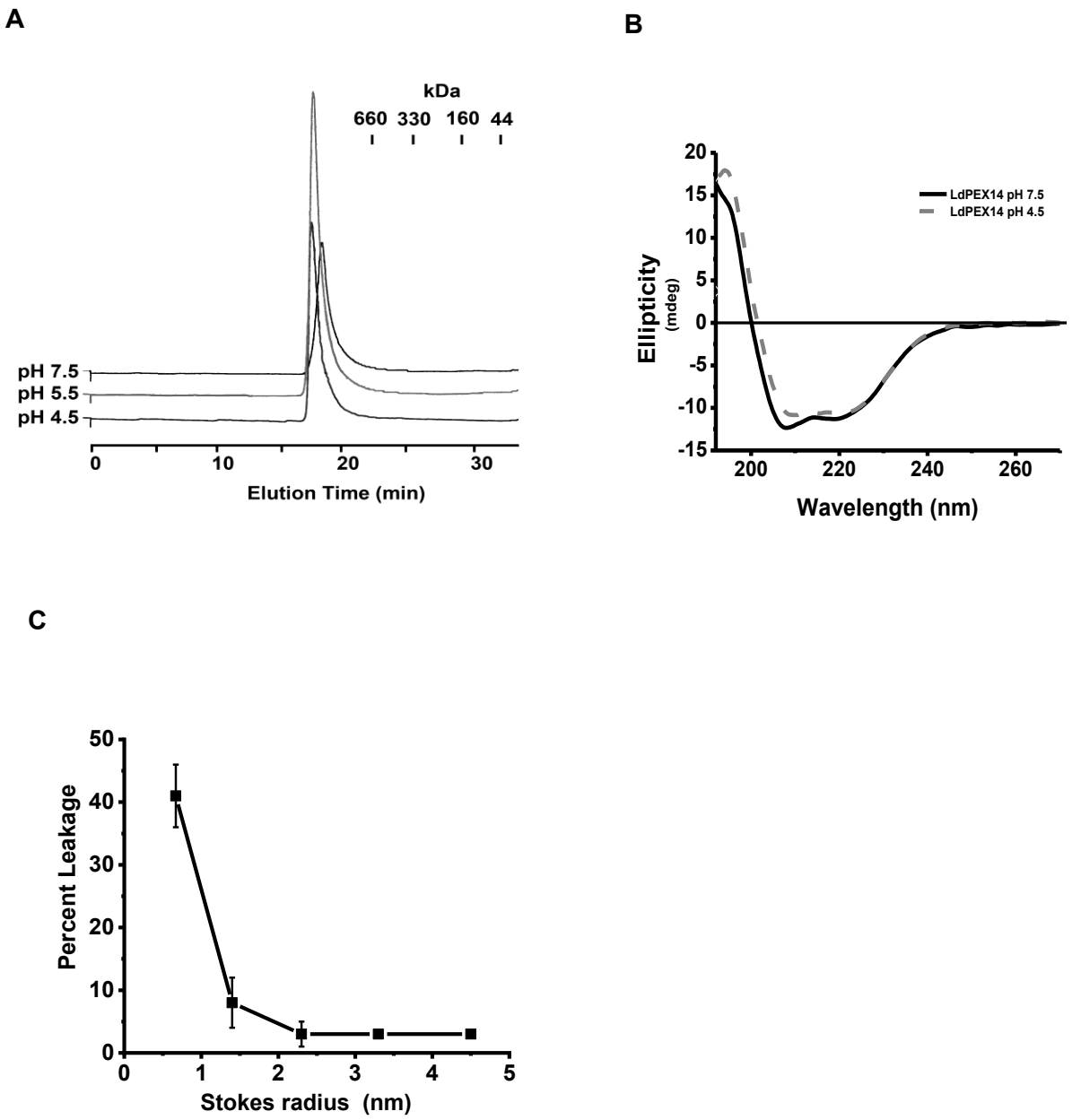

Figure 4: Effect of pH on structure of LdPEX14 and the interacting liposomes.

(**A**) Changes in the LdPEX14 structure induced by pH were analyzed by size exclusion chromatography using mobile phases with pH 4.5, 5.5, or 7.5 and protein elution monitored at a wavelength of 280 nm or (**B**) circular dichroism spectroscopy. (**C**) DOPE:DOPC:DOPG:PI:Chl LUVs loaded with carboxyfluorescein or fluorescein isothiocyanate labelled dextrans with increasing Stokes radii were treated with LdPEX14 and the percent of dye release determined following sedimentation of LUVs.

Ld*PEX14 hydrophobic region is required for pore formation*

Leakage assays were performed at pH 7.5 with the deletion mutants ldpex14 (Δ138-165), ldpex14 (Δ160-179), ldpex14 (Δ179-200), and ldpex14 (Δ149-179) (**Figure 5A)**. Like wild type LdPEX14, the deletion mutants showed no notable dye release (**Figure 5B**). However, a robust leakage of ~52% was observed for the wild-type LdPEX14 when the pH was shifted from 7.5 to 4.5. A similar degree of dye leakage was observed with ldpex14 (Δ179-200) suggesting that residues 179-200 may not be essential for binding or pore formation (**Figure 5B**). In contrast, ldpex14 (Δ138-165) and ldpex14 (Δ160-179) induced a decreased dye leakage of 18% and 21%, respectively, indicating that loss of residues 138-165 or 160-179 partially impaired pore formation. Deletion of residues 149-179, however, reduced dye leakage to ~5% confirming that this region was important for pore formation (**Figure 5B**). The latter result was not surprising since flotation studies showed that ldpex14 (Δ149-179) failed to bind lipid bilayers [32]. Leakage assays with ldpex14 (120-200) revealed that this fragment was pH insensitive and induced comparable levels of dye leakage activity at pH 4.5 and 7.5 (**Figure 5B)**. The phospholipid composition also impacted the capacity of LdPEX14 to trigger SRB leakage from DOPE:DOPC:PI:Chl LUVs. Omitting phosphatidylglycerol from LUVs abrogated the capacity of LdPEX14 to promote dye release at pH 4.5 or 7.5 (**Figure 5B**), confirming the results from flotation studies showing that incorporation of anionic phospholipids into lipid bilayers was required for LdPEX14 binding.

Since sucrose density flotation and dye release experiments suggested that residues 149-179 were important for LdPEX14-membrane interaction [32], we further investigated this interaction using ldpex14 (120-200). Titration of ldpex14 (120-200) with increasing concentration of DOPE:DOPC:DOPG:PI:Chl SUV triggered a concentration dependent blue shift of 28 nm

(**Figure 5C,** inset) in the Trp152 emission λ_{max} at protein:phospholipid ratio of 1:250 (**Figure 5C**), a shift which was consistent with the insertion of Trp152 into the hydrophobic core of the lipid bilayer.

The insertion of ldpex14 (120-200) into the membrane was verified by fluorescence quenching experiments. Stern-Volmer plots obtained with ldpex14 (120-200) in solution titrated with acrylamide exhibited an upward trending curve characteristic of quenching, arising from both dynamic and static quenching components [212] that has Stern-Volmer constants (K_{sv}) of 9.1 and 0.8 M^{-1}, respectively (**Figure 5D**). In contrast, ldpex14 (120-200) bound to SUVs exhibited a linear response consistent with dynamic quenching with a K_{sv} constant of 3.2 M^{-1}. The decrease in the K_{sv} value, together with the blue shift in the emission λ_{max}, confirms that Trp152 inserts into the lipid bilayer becoming less accessible to acrylamide quenching. Similar attempts to monitor the insertion of Trp152 in LdPEX14 were confounded by the fact that in the absence of membranes this residue exhibits an emission λ_{max} at 327 nm which is consistent with this tryptophan residue being sequestered in a nonpolar environment prior to membrane insertion.

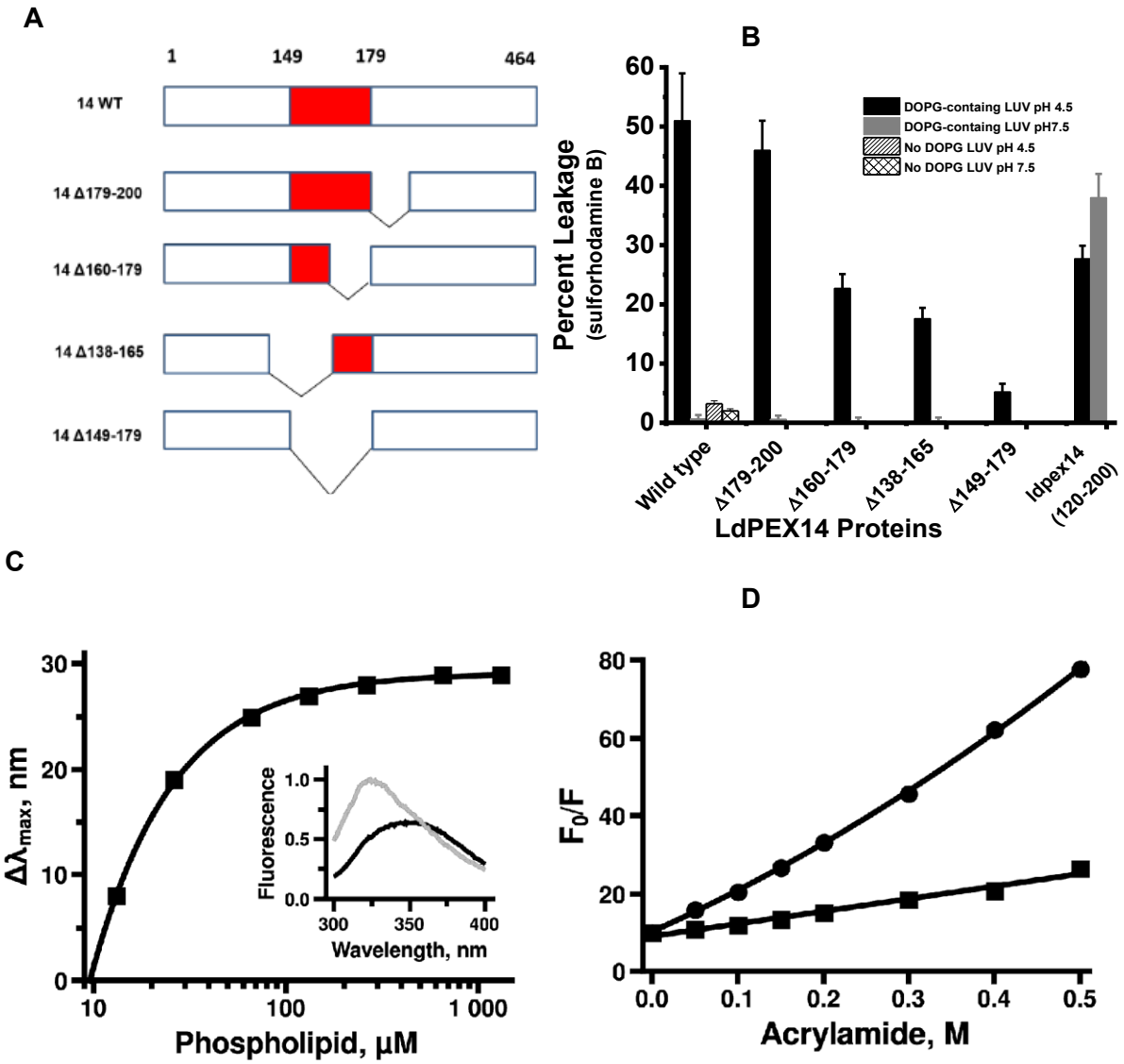

Figure 5: LdPEX14 hydrophobic region is required for membrane binding and pore formation

(**A**) Deletion mutants of the LdPEX14 protein. Schematic structures of LdPEX14 WT and four site-specific deletion mutants around the hydrophobic region spanning149-179 (red). (**B**) The pore forming activity of LdPEX14, ldpex14 (Δ138-165), ldpex14 (Δ160-179), ldpex14 (Δ179-200), or ldpex14 (Δ149-179) with sulforhodamine B loaded DOPE:DOPC:DOPG:PI:Chl or DOPE:DOPC:DOPI:Chl LUVs was examined at pH 4.5 and 7.5. Dye release was monitored at excitation and emission wavelengths of 565 and 586, respectively. (**C**) The emission spectra for ldpex14 (120-200) in the absence (*inset, black line*) and presence (*inset, gray line*) of SUVs was recorded at an excitation wavelength of 290 nm. This hypsochromic shift was dependent on phospholipid concentration. (**D**) The accessibility of Trp152 of ldpex14 (120-200) in the absence (circles) or presence (squares) of SUVs to the aqueous environment was assessed by acrylamide quenching.

Discussion

Proteins are considered to have dynamic rather than a static structure, changing their shape or conformation in response to the environmental conditions in which it is exposed and influenced by neighboring interacting partners [277-279]. Proteins can have various conformations, each one performing a specific role, such as converting itself from active to inactive form; examples include, (i) the active conformation of pepsin is formed around pH 2. which has a native-like catalytically inactive conformation around pH 4.0-6.5 and is denatured at neutral pH [280], (ii) Opsin which is a apoprotein formed after decay of metarhodopsin II (signaling state of visual pigment rhodopsin) exists in two conformations depending on pH, a low pH state similar to metarhodopsin II and a high pH state similar to inactive metarhodopsin I [281]. Some conformational changes help the proteins to participate in protein-protein interactions; for example SPE7, a monoclonal immunoglobulin E (IgE) raised against a 2,4-dinitrophenyl (DNP) hapten was found to adopt different conformations that allowed it to bind unrelated antigens [282, 283], while few others are known to mediate membrane-protein interactions; examples include, (i) membrane interactions induces an open conformation for bacterial cell division regulator MiniE, (ii) sarco(endo)plasmic reticulum Ca^{2+}–ATPase (SERCA), a membrane protein, adapts to membranes of different thickness by undergoing conformational changes and inducing local deformations in the lipid bilayer [284-286]. Also there are conformational changes associated with enzyme catalysis; examples include, (i) A conformational change is accompanied when Ribonuclease A binds to its substrate (RNA), (ii) A conformational change is accompanied when chymotrypsin forms an initial enzyme-substrate complex and this reaction is followed by formation of free enzyme and product[287-289]).

It has been demonstrated that pH can bring structural changes in proteins including , (i) influenza virus hemagglutinin, where the ectodomain of hemagglutinin (HA) undergoes conformational change at low pH (≤ 5.8) resulting in an increase of binding event with liposome and this structural rearrangement is thought to be responsible for the membrane fusion event and eventual release of the viral genome into the host [290, 291], (ii) transferrin binds to ferric ions and low pH (pH 5.3) induces conformational change in the N-terminal half of transferrin, resulting in the physiological release of iron in cells [292, 293], (iii) retinol binding protein (RBP), where low pH induces conformational changes in the RBP and releases hydrophobic retinol from the deep pocket of RBP [294], (iv) pheromone binding protein, where low pH induces conformational changes in Pheromone-binding proteins (PBPs) and release the bound hydrophobic pheromones on or near the target cell membranes [295, 296].

Low pH can bring conformational changes in proteins, exposing hydrophobic regions thereby revealing the membrane interacting region, for example, low pH (pH ~5.0) induces conformational change in the herpes simplex virus (HSV) fusion protein gB containing cytoplasmic tail sequences (s-gB) and these structural changes expose the hydrophobic fusion peptide sequences that bind with the target lipid membranes [297, 298]. We used a similar strategy of exploiting low pH as a method to bring about conformational changes in LdPEX14 and expose its hydrophobic region. A hyperchromic shift in the λ_{max} of a single tryptophan indicated a conformational change in LdPEX14[299], and was enough for the formation of a pore in the membrane and leak the dye out of encapsulated liposomes. . Far-UV CD spectra reflects the secondary structure content of the protein [300], and we observed slight differences between the two pH conditions indicating that there was no major change in the secondary structure. The quaternary structure was also preserved indicating that the overall structure of

LdPEX14 is preserved at low pH. A change in the microenvironment surrounding the tryptophan may be due to slight changes in helicity and tertiary contacts of the protein resulting in a more flexible conformation at low pH. The movement of the hydrophobic region to a more exposed location was confirmed by its substantial increase in the fluorescence intensity after probing with ANS.

Low pH triggered conformational changes have been reported for various proteins and is thought to be mediated through various mechanisms like protonation of histidine [301-303] or acidic amino acids such as aspartate or glutamate [304] or characterized by the presence of multiple hydrophobic residues or residues that form salt bridges [305]. LdPEX14 has a single histidine at position 136 just upstream of the hydrophobic region (His 1), and multiple acidic residues (Glu 31, Asp). All of these residues are located outside the hydrophobic region spanning 149-179 of LdPEX14 except for two aspartate residues. The hydrophobic residues are distributed throughout the LdPEX14 protein and a hydrophobic patch spans the region between 149-179 amino acids. We have shown that deletion of a part of the hydrophobic region diminished the leakage and deletion of the whole region abolishing the leakage. This indicates that a conformational change resulted in the movement of the hydrophobic element into the membrane, resulting in the dye leakage. Although a precise mechanism for conformational change at low pH for LdPEX14 is unknown, it may be contributed mostly by hydrophobic residues or a combined effect of protonation of the histidine (located just upstream of the hydrophobic region causing a bend in the structure acting like a hinge) [302], acidic residues, or the multiple hydrophobic residues.

Liposome binding studies have previously established that recombinant LdPEX14 spontaneously inserted into model membranes. This association was critically dependent upon

residues 149-179, a segment calculated to adopt an amphipathic helix containing a nonpolar and polar face [32]. Amphipathic helices are known to mediate membrane binding by inserting the nonpolar face of the helix, in parallel geometry, into the outer leaflet of the bilayer [306, 307]. The amphipathic helix is predicted to stabilize the LdPEX14-membrane association in a similar configuration; an interaction that in the absence of an LdPEX14 structural rearrangement failed to disrupt membrane integrity as suggested by the dye release assay performed at pH 7.5. This is critical since the leakage of small metabolites from the glycosome is a lethal for kinetoplastid parasites [23, 151, 308]. Surprisingly, deletions that eliminated a smaller portion of the amphipathic domain were not sufficient to abolish the membrane binding activity of ldpex14 (Δ138-165) or ldpex14 (Δ160-179), possibly due to an avidity effect that allows weak interaction from the 16-20 subunits in the ~800 kDa homomeric complex formed by LdPEX14/ldpex14 to synergize and stabilize membrane binding. Functional analysis, however, showed that these deletions impaired pore formation causing a reduction in sulforhodamine dye leakage.

These observations suggest that the LdPEX14 amphipathic segment probably participates directly in the assembly of a transient pore [33, 35, 309] which is supported by the finding that ldpex14 (120-200) can form stable oligomers in LUVs that trigger dye release [refer to Chapter 3]. Homologous transmembrane regions in the mammalian PEX14 protein have been demonstrated to homo-oligomerize. However, the capacity of this transmembrane peptide to form pores was not examined [309]. In order to further explore the role of LdPEX14 in the formation of the translocation pore and transport across the membrane, studies have to be designed and carried out in the presence of accessory proteins such as LdPEX13 and RING finger proteins LdPEX2, LdPEX10, and LdPEX12.

Connecting Statement

In the previous two chapters, we investigated the interaction of LdPEX14 with unilamellar vesicles mimicking the glycosomal membrane. We demonstrated that the hydrophobic region of LdPEX14 plays a crucial role in governing the interactions with the glycosome. To further investigate the role of PEX14 in glycosome biogenesis and protein translocation, we created a knock out the LdPEX14 gene from *Leishmania* using CRISPR/Cas9.

In chapter 5, we demonstrated that the expression of Cas9 could be regulated in *Leishmania* promastigotes by fusing the Cas9 with a destabilizing domain of the FKBP12 protein. We used this regulatable Cas9 to knock out LdPEX14 gene and found that the PEX14 is an essential gene for the viability of the *L. donovani* parasite.

Chapter 5

Destabilization domain mediated regulatable expression of Cas9 in *Leishmania donovani* and CRISPR/Cas9 for knocking out LdPEX14

Anwer Hasil Kottarampatel[1,2], Phil Yates[3], Anand Vardhan[1,2], and Armando Jardim[1,2]*

*[1]Institute of Parasitology and [2]Centre for Host-Parasite Interactions, Macdona*ld *Campus of McGill University, Ste-Anne-de-Bellevue QC, Canada. Departments of Biochemistry and Molecular Biology, Oregon Health & Science University, Portland, Oregon, USA*[3].

Running Title: CRISPR-Cas9 knock out *Leishmania* XPRT and PEX14

Keywords: *Leishmania*, glycosome, LdPEX14, peroxin, CRISPR/Cas9, ddFKBP

Abbreviations:

LdPEX, *Leishmania donovani* peroxin; PTS, peroxisomal targeting signal, ddFKBP, FKBP protein destabilization domain, CRISPR, Clustered Regularly Interspaced Short Palindromic Repeats, Cas9, CRISPR associated protein 9, PAM, Protospacer adjacent motif

*To whom correspondence should be addressed: Institute of Parasitology, Macdonald Campus of McGill University, 21, 111 Lakeshore Road, Ste. Anne-de-Bellevue, Québec, Canada H9X 3V9. Phone: (514) 398-7727; Fax: (514) 398-7857, email: armando.jardim@mcgill.ca.

Abstract

CRISPR/Cas9 is a powerful genome editing tool used for the study of gene function. Here we employed a system that allows regulatable expression of Cas9 in *L. donovani* promastigotes. We fused the destabilizing domain of FKBP 12 (ddFKBP) to both the N-terminus and C-terminus flanks of Cas9. The N-terminal ddFKBP fusion provided conditional destabilization of Cas9 and in the presence of the drug rapamycin, increased levels of the ddFKBP-Cas9 protein were detectable in promastigotes. This regulatable Cas9 was used to knockout the genes LdXPRT and LdPEX14 in *L. donovani*. This technology can be expanded to characterize functions of other genes in *Leishmania spp*.

Introduction

Leishmaniasis is a neglected tropical disease mostly affecting people in developing countries [310, 311]. The disease is characterized by various clinical manifestations such as cutaneous, muco-cutaneous and visceral leishmaniasis. Visceral leishmaniasis caused by *L. donovani* is one of the more dangerous forms of this disease and if left untreated can be fatal for the patient [48, 272, 312]. The parasite has a digenetic life cycle, a flagellated promastigote form residing in the sandfly vector and a non-flagellated amastigote form that survives in the macrophages of human host [12, 64].

Leishmania spp. contain a unique organelle called the glycosome that is evolutionarily related to peroxisomes of yeast, fungi, plants, and mammalian cells [313]. Glycosome compartmentalizes various metabolic pathways including glycolysis, ether lipid biosynthesis, purine salvage and pentose phosphate pathway [16, 17, 102]. Glycosomal proteins are synthesized in the cytosol and post translationally translocated into the cytosol with the help of peroxin receptor proteins. There are two main glycosomal targeting sequences, peroxisomal targeting signal sequence 1 (PTS-1) and peroxisomal targeting signal sequence 2 (PTS-2). PTS-1 typically is a C-terminal consensus sequence [A, S] / [K, R, N, H] / [L, M, V, Y] and PTS-2 is a N-terminal consensus sequence [RK]-[LVI]-[X]5-[HQ]-[LA]. Proteins bearing the PTS1 and PTS2 motifs are recognized by the cytosolic receptor proteins, peroxin5 (LdPEX5) or peroxin7 (LdPEX7), respectively and then this complex docks to the peripheral membrane associated protein LdPEX14 and with the help of LdPEX14, the cargo gets unloaded in the glycosomal lumen [27, 28, 141].

Leishmania genomes have high plasticity and attempts to knock out essential genes by classical approaches may give rise to the emergence of additional copies of the targeted gene

[314] on extrachromosomal elements. RNA interference is routinely used to knock down genes in related kinetoplastids such as *T. brucei,* but the absence of dicer and argonaute proteins make the use of RNA interference difficult in *L. donovani*, *L. major*, and *L. mexicana* strains of *Leishmania* [315, 316]. The knockdown of PEX14 in *T. brucei* impeded glycosomal import of PTS-1and PTS-2 proteins and resulted in mistargeting of glycosomal enzymes to the cytosol, an event that was lethal to these parasites [23, 31]. PEX14 was also important in mediating crucial protein-protein interactions in kinetoplastids, as it was recently demonstrated that small molecular inhibitors blocking the interaction of PEX5 with PEX14 were able to kill the parasite *in vitro* [155, 156]. It has been demonstrated that CRISPR/Cas9 based gene knock out can produce double stranded breaks in targeted DNA and isolating *Leishmania* null mutants was possible in one round of transfection [317]. To expand our knowledge and explore the functions of PEX14 in the protein translocation machinery, we decided to create a knock out cell line of *L. donovani* devoid of LdPEX14 utilizing the CRISPR-Cas9 approach. Since previous studies have reported that LdPEX14 is essential for the viability in other related kinetoplastid parasites, we used a slightly different approach of complementing an ectopic copy of LdPEX14 to rescue the parasite devoid of the endogenous LdPEX14 [31].

CRISPR (clustered regularly interspaced short palindromic repeat)-Cas9 knock out based methods need two major components, (1) Cas9 nuclease, a RNA-guided endonuclease shown to specifically digest DNA and (2) a gRNA (guide RNA) bearing 20 nucleotides (seed sequence) at its 5’ end. These 20 nucleotides of the gRNA hybridize to its complementary base on the target site forming a RNA-DNA hybrid and directs the Cas9 to the specific target site producing a double stranded break in the DNA. The target site lies 5’ to a PAM (Protospacer Adjacent Motif) sequence typically a 5′-NGG canonical sequence [318, 319].

CRISPR-Cas9 based knock out approaches have been successfully tested in *Leishmania spp.*; However, these systems lack regulatable expression of the Cas9 protein [317, 320, 321]. It has been demonstrated previously by Wandless lab that conditional regulation of protein is possible when it is fused to a destabilization domain of the FKBP protein [322, 323]. Fusion of ddFKBP to the protein of interest has been successfully used to regulate the expression of various proteins. Proteins fused to the ddFKBP are rapidly degraded, but addition of a ligand such as Shield 1 or rapamycin can bind with the destabilizing domain and protect the protein from degradation [322-324]. To regulate the expression of Cas9 in *Leishmania* we fused a destabilization domain of the FKBP protein to the Cas9. Here we show that fusion of ddFKBP to the N-terminus of the Cas9 allows temporal control of Cas9 expression in *Leishmania*.

Materials and Methods

Chemicals and reagents –All restriction endonucleases and DNA-modifying enzymes were purchased from Invitrogen or New England Biolabs. Horseradish peroxidase (HRP)-conjugated goat anti-rabbit IgG was purchased from GE Healthcare. Cas9 monoclonal antibody and In-fusion HD Cloning Kit was purchased from Clonetech laboratories. All other reagents were of the highest commercially available quality.

Leishmania donovani cultures – L. donovani promastigotes were cultured in M199 media (Sigma Aldrich) supplemented with penicillin/streptomycin, and 10% dialyzed heat-inactivated FBS at 26 $^{\circ}$C in 5% CO_2 incubators and grown to late logarithmic stage before passage.

Construction of Cas9 in pRP Plasmids – For N-terminal ddfkbp-Cas9 fusion, the hSpCas9 was amplified from plasmid PX330 (Addgene plasmid # 42230), pX330-U6-Chimeric_BB-CBh-hSpCas9 and cloned in the medium expression pRP plasmid [325], between NdeI and BamHI restriction sites (**Figure 1A**). For C-terminal Cas9-ddfkbp fusion, the hSpCas9 was cloned in the medium expression pRP plasmid between HindIII and BamHI restriction sites (figure not shown). The fused hSpCas9 is flanked by 5' and 3' UTRs, and the RNA expression is under the control of a *L. donovani* ribosomal RNA (rRNA) promoter (**Figure 1B**). The plasmids were linearized with AvrII before transfection to the parasite.

A

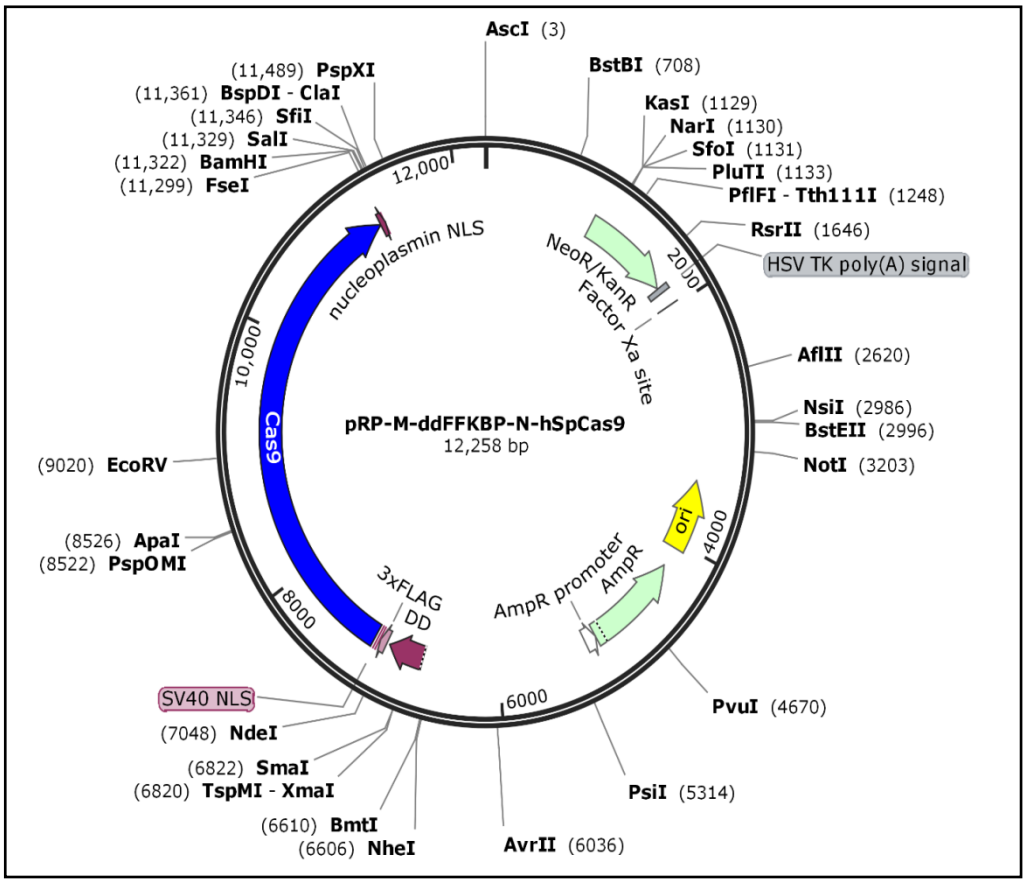

B

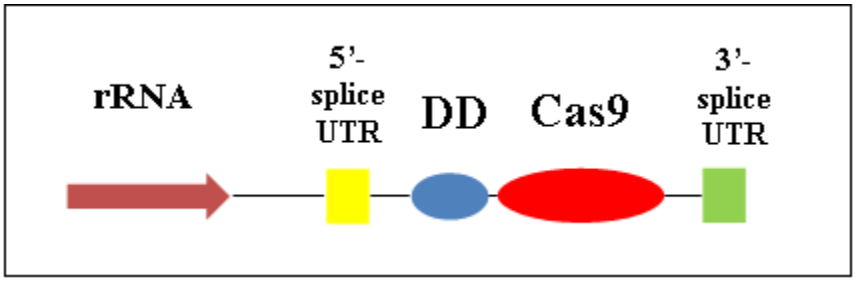

Figure 1: Map of pRP plasmid with ddFKBP-Cas9 fusion partner

(**A**) A map of medium expression pRP plasmid having a ddFKBP fused to N-terminus of hSpCas9 (pRP-M-ddFKBP-N-hspCas9), ampicillin resistance gene (Amp^R) is for drug selection in *E. coli* and Neomycin resistance gene (Neo^R) is for drug selection in eukaryotic cells. (**B**) Schematic of the pRP vector construct having ddFKBP fused Cas9 under the control of *L. donovani* rRNA promoter (rRNA).

Construction of in PLS6 plasmids – The 20 nucleotide seed which is part of the gRNA for LdPEX14 (region between 1047-1067 bp) and LdXPRT (region between 22-42 bp) were selected using the webtool, Eukaryotic Pathogen gRNA Design Tool (EuPaGDT; available at http://grna.ctegd.uga.edu) and the DNA segment encoding this region was cloned into the BsgI site of the pLS6 plasmid using In-fusion HD Cloning Kit. The homology donor regions (HR1 and HR2) of around 500 bp DNA sequence flanking the gene were selected and cloned into KpnI/XbaI and HpaI/MfeI restriction sites of pLS6 plasmid (**Figure 2A** and **Figure 2B**).

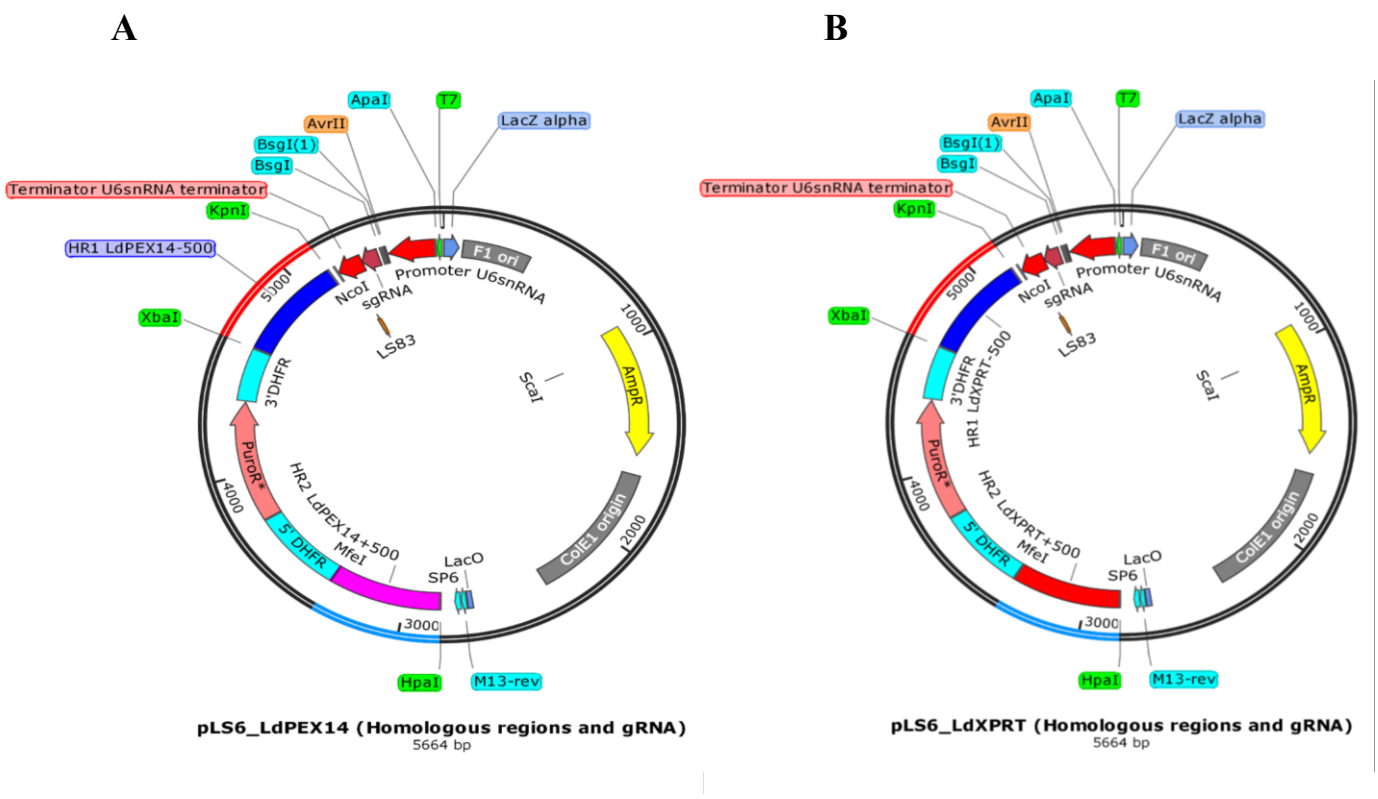

Figure 2: pLS6 plasmid bearing the homology donor regions and gRNA expression cassette

pLS6 donor plasmid with puromycin resistance cassette flanked by homology donor regions of 500 bp DNA sequence flanking the gene, and the sgRNA expression cassette under the control of a U6snRNA promoter. 20 nucleotide seed sequence for sgRNA was selected for (**A**) LdPEX14 (region between 1047-1067 bp) and (**B**) LdXPRT (region between 22-42 bp).

Construction of LdPEX14 *in pRP plasmids* –FLAG-LdPEX14 open reading frame was cloned into the SFiI site of the pRP high expression plasmid with BSD drug cassette (pRP-H-BSD-FLAG-LdPEX14) (**Figure 3A**) [325]. The ectopic plasmid bearing the N-terminal FLAG tagged LdPEX14 had a change in the nucleotide sequence of the coding region to eliminate hybridization with the gRNA (the 20 nucleotides and the 5'-NGG-3' Protospacer adjacent motif) used for the deletion of the Ld*PEX14* gene. Modification of FLAG-LdPEX14 was performed to hide the ectopic copy of PEX14 from recognition by the gRNA and Cas9 nuclease directed against the genomic copy of LdPEX14 (**Figure 3B**).

A

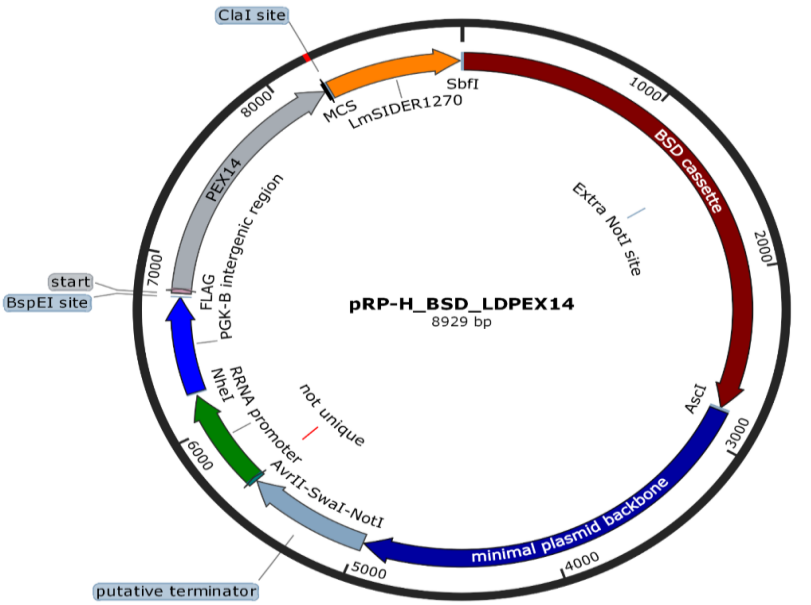

B

Nucleotide sequence

20 nucleotide and PAM

```
WT-LdPEX14              1045    GAGCAGGCGCGAAATTCACCAGAGGTG 1068
Codon optimized PEX14   1045    GAACAAGCTCGTAACTCGCCGGAAGTG 1068
                                **.**.** **:**.**.**.**.***
```

ExPASy translate tool

Protein sequence

```
WT-LdPEX14                      348 EQARNSPEV 357
Codon optimized PEX14           348 EQARNSPEV 357
                                    *********
```

Figure 3: Map of pRP plasmid with flag-LdPEX14 (pRP-H-BSD-Flag-LdPEX14)

(**A**) An ectopic flag-LdPEX14 was cloned into the pRP high expression plasmid between the SFiI sites. Blasticidin resistance gene (BSD^R) is for drug selection in eukaryotic cells (pRP-H-BSD-flag-LdPEX14) and the construct is under the control of *L. donovani* rRNA promoter (rRNA). (**B**) The redundancy in codon usage for *L. donovani* were used to modify the nucleotide sequence of LdPEX14 in the ectopic plasmid (pRP-H-BSD-flag-LdPEX14) that translate into LdPEX14 protein with the same amino acid sequence.

Transfection and cloning – Plasmids for Cas9 were linearized with the AvrII restriction endonuclease and was electroporated with a Bio-Rad gene pulser II electroporator into *L.*

donovani 1S2D promastigotes, using the following conditions 25 µF, 1500V (3.75 kV/cm) pausing 10 s between pulses [315]. Clones containing the integrated constructs were selected for in bulk culture by the presence of 25 µg/ml G418. A limiting dilution to isolate clones was performed in 96 well plates. The first column of the 96 well plate received $1X10^6$ cells per well and a 10-fold dilution was performed across the plate to obtain single clones in wells 7 or 8. The cells in 96 well plate were allowed to grow between one to two weeks and then expanded to a 24 well plate followed by a transfer to T-25 flasks. The promastigotes expressing Cas9 were subjected to another round of electroporation (same procedure as above) with pLS6 plasmids containing gRNA and homologous regions for LdPEX14 and LdXPRT. Positive clones were selected for in bulk culture using 20 µg/ml puromycin and 25 µg/ml G418.

Western blot – L. donovani promastigote culture densities were determined using a hemocytometer and parasites were harvested and washed with warm PBS. Cell pellets were resuspended in an appropriate amount of 2X SDS PAGE buffer and proteins were resolved and transferred to PVDF membranes. Membranes were blocked with 2% w/v non-fat dry milk in 1 × TBST (0.1% Tween20) for 1 h at 20 °C then incubated with primary antibodies diluted in 2% w/v non-fat dry milk TBST as follows: anti-Cas9 (1:1,000), anti-tubulin (1:5,000) as equal loading control, anti-LdPEX14 (1:10,000), anti-LdXPRT (1:2,000). Membranes with primary antibody were incubated overnight at 4 °C. Membranes were washed with TBST to remove unbound antibodies and then probed with the secondary antibody, anti-rabbit HRP (GE Healthcare). The membranes were developed using Amersham ECL Western Blotting Detection reagents (GE Healthcare).

Results

Regulated expression of Cas9 in L. donovani

Constitutive expression of Cas9 can cause off target mutations in genomic DNA of *L. donovani* and also make it a daunting task to isolate the knockout clones for essential genes. To overcome possible developmental defects and off target effects of constitutive knockdown of an essential gene, we fused a destabilizing domain (dd) to the Cas9. It has been demonstrated that fusion of a destabilizing domain of human FKBP12 protein to a protein of interest (POI) results in degradation of the entire fusion protein and the addition of a ligand like rapamycin or Shield-1 which binds to the ddFKBP domain protects the fused protein from degradation [322]**.** We used the plasmid pRP for cloning Cas9, as it can be integrated into the ribosomal RNA (rRNA) locus and provide stable expression in the absence of drug selection. Also, a wide range of constitutive transgene expression options from very high to very low expression levels were available among pRP plasmids [325]. We observed that the pRP-M-Cas9 (medium expression plasmid) devoid of the destabilizing fusion partner (ddFKBP) resulted in the constitutive expression of Cas9 in the absence of rapamycin (**Figure 4A**). Fusion of the ddFKBP domain to the N-terminus of Cas9 showed that this protein could not be detected in *L. donovani* promastigotes. However, the addition of 1 μM rapamycin caused a notable increase in the levels of ddFKBP-Cas9. Fusion of the ddFKBP domain to the C-terminus of Cas9 elicited no change in the Cas9 expression before or after addition of 1 μM rapamycin ligand. This indicates that the fusion of ddFKBP to Cas9 achieved a more regulatable expression of the fusion protein analyzed after 24 hours (**Figure 4B**). However, the clones for Cas9-ddFKBP fusion (6 to 8), had strong expression of the protein in presence or absence of rapamycin (**Figure 4C**).

For analyzing the kinetics of Cas9 degradation, cells were harvested at 0, 2, and 24 h after treatment with 1 μM rapamycin. Protein accumulation was detected within 2 h and robust levels were observed within 24 h of rapamycin treatment (**Figure 4D**). A decrease in the level of protein expression was seen in at 48 hours of ligand withdrawal from the media. These data demonstrated that fusion of ddFKBP to the N-terminus of Cas9 provides a tunable system with rapid control of protein levels by decreasing the rate of protein degradation in the presence of rapamycin.

Expression of Flag-Ld*PEX14 in L. donovani*

The challenge was to protect the ectopic copy of PEX14 from the Cas9 cleavage designed to target genomic LdPEX14. The specificity of Cas9/gRNA is determined by components including the protospacer-adjacent motif (PAM), the 20 nucleotide seed, Cas9/gRNA abundance, sequence of the gRNA and various other factors [326]. The PAM must lie 3′ of the target sequence and it is typically an NGG. PAM binding and the 10-12 bases proximal to PAM were found to be necessary for cleavage of target DNA [326-328]. In our study, the ectopic PEX14 had a modification at the 20 bp region and the gRNA recognition site of PAM. We exploited redundancy of the genetic code to modify the 20 bp sequence in the ectopic copy of LdPEX14 [329, 330], thereby having a very different nucleotide sequence but translating the same amino acids as the wild-type PEX14. We observed robust expression of the FLAG-LdPEX14 in *Leishmania* parasites grown to log phase (**Figure 4E**).

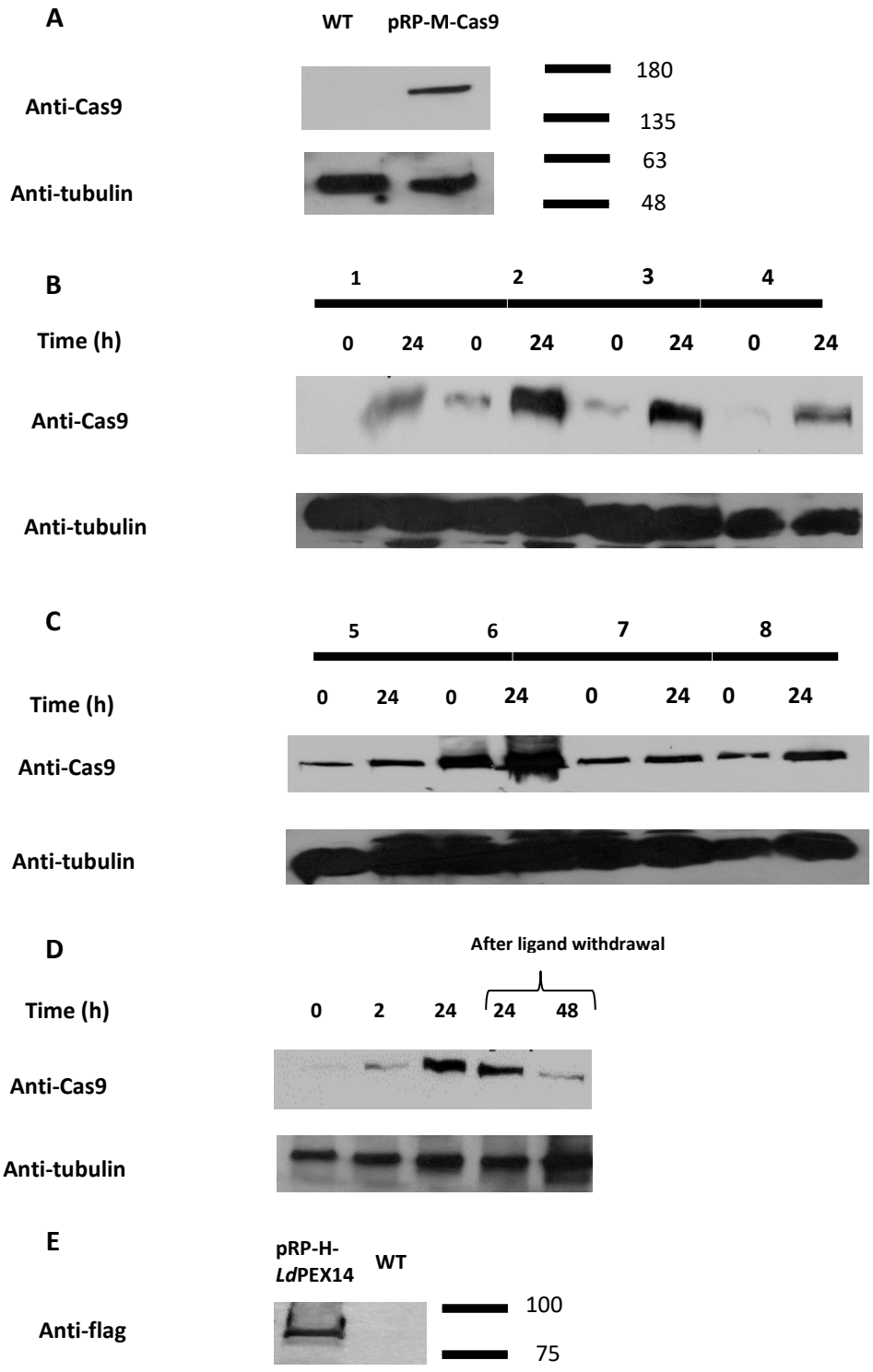

Figure 4: Inducible system for Cas9 expression based on conditionally destabilized Cas9

The *L. donovani* cells transfected with plasmids expressing Cas9 were lysed using RIPA buffer and 20 µg of total protein was loaded on SDS-PAGE gel, transferred to a PVDF membrane and probed with Cas9 monoclonal

antibody. (**A**) Robust expression of Cas9 was found in *L. donovani* transfected with medium expression pRP-plasmid devoid of a destabilization domain fusion partner (ddFKBP) compared to the mock treated WT *L. donovani* cells. (**B**) Expression of Cas9 by various clones (1-4) of *L. donovani* transfected with P-M-N-ddFKBP-Cas9 (N-terminus ddFKBP fusion partner). Cas9 was either not detected or negligible levels were detected in the zero minute or before addition of rapamycin. Cells treated with 1μM rapamycin demonstrated strong expression of the fusion protein analyzed after 24 hours. (**C**) Expression of Cas9 by various clones (5-9) of *L. donovani* transfected with P-M-C-Cas9-ddFKBP (C-terminus ddFKBP fusion partner). Robust expression of Cas9 was detected even before the addition of the ligand (1 μM rapamycin). (**D**) Regulation of expression by the destabilized DD-Cas9 was observed. Increased expression of Cas9 was found for the Clone-1 (**Figure 4B**) over time in presence of 1 μM rapamycin. After 24 hours rapamycin was removed from the media and the amount of Cas9 was monitored until 48 hours. (**E**) *L. donovani* cells transfected with pRP-H-BSD-flag-LdPEX14 plasmid were lysed using RIPA buffer and 20 μg of total protein was loaded on SDS-PAGE gel, transferred to a PVDF membrane and probed with FLAG antibody. Robust expression of flag-LdPEX14 was detected compared to the WT *L. donovani* cells.

Knockout of LdPEX14 *and* LdXPRT *genes from L. donovani*

We were able to knockout XPRT from *L. donovani* in one round of transfection, confirmed by Western blotting using anti-XPRT antibodies (**Figure 5A**). In contrast, *L. donovani* receiving the knock out plasmid PLS6_LdPEX14 were mostly dead within 3 weeks, indicating that knocking out of LdPEX14 was lethal to the parasite., indicating that LdPEX14 knockout was lethal to the parasite (**Figure 5B**). Even complementing the genomic LdPEX14 with an ectopic copy of plasmid expressing flag-LdPEX14 was unable to rescue the survival of the parasite. The inability of the ectopically expressed LdPEX14 to rescue the parasite survival may be contributed by various factors such as (i) Cas9 was still able to access and cleave the ectopic copy of flag-LdPEX14 bearing the modifications, (ii) overexpression of ectopic copy of gene without proper regulation may have resulted in incorrect targeting of the over expressed protein. We were unable to isolate any colonies of *L. donovani* positive for knockout of the genomic LdPEX14. These results reiterate that LdPEX14 is an essential gene for the viability of *L. donovani*.

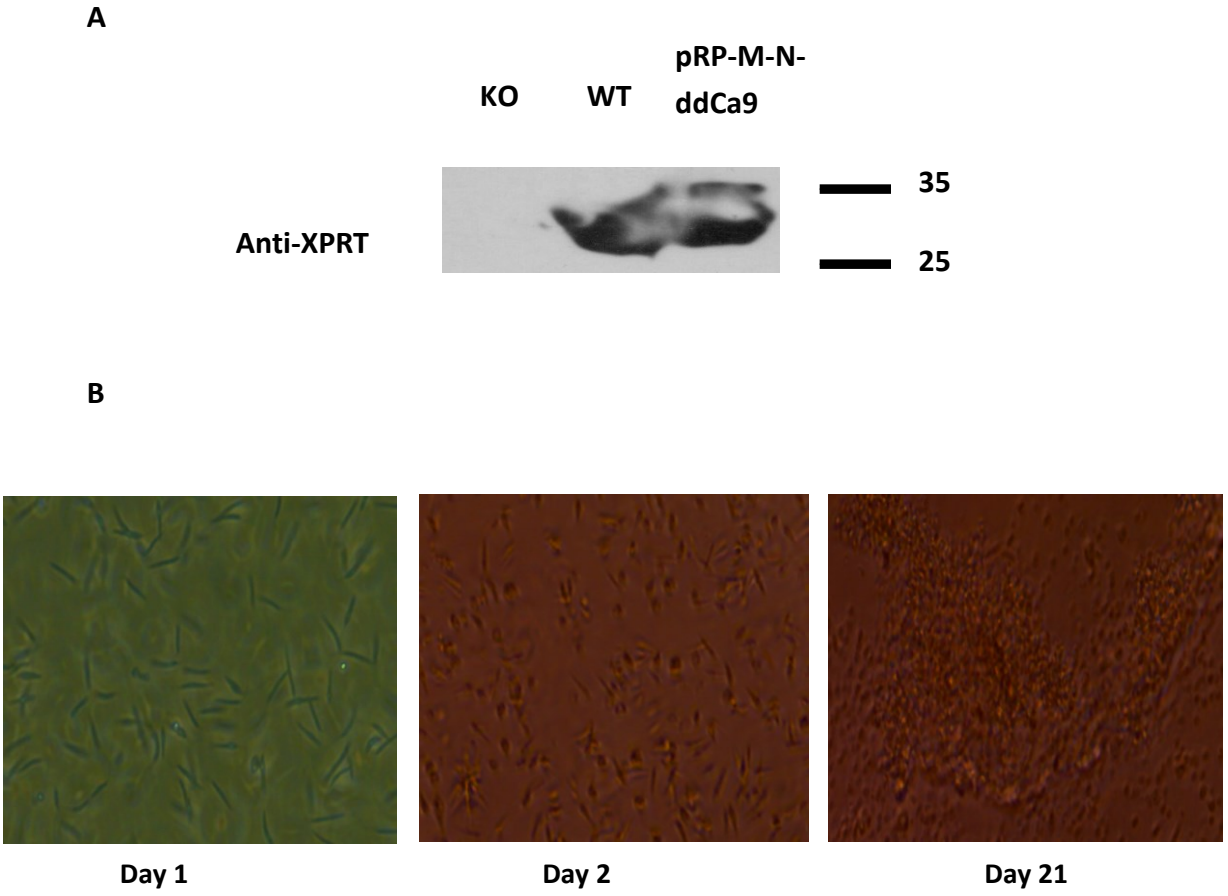

Figure 5: Gene editing using CRISPR/Cas9 in *L. donovani* enables identification of essential genes

(**A**) *L. donovani* cells transfected with pRP-M-N-ddCas9 plasmid were lysed using RIPA buffer and 20 µg of total protein was loaded on a SDS-PAGE gel, transferred to a PVDF membrane, and probed with XPRT antibody. XPRT protein expression was absent in the knockout cell (KO) compared to the WT *L. donovani* cells and cells transfected with pRP-M-N-ddCas9. (**B**) Images taken with an Evos XL core microscope showing that disruption of *L. donovani* PEX14 gene is lethal to the parasite. *L. donovani* expressing Cas9 in presence of rapamycin were transfected with the PLS6 plasmid having the gRNA and homologous donor region for recombination. The cells were then cloned in a 96 well plate, and their growth was monitored. Image showing cells expressing Cas9 in the presence of rapamycin after 1, 2 and 21 days of cloning.

Discussion

If knocking out a gene is a lethal event, it is a definitive phenotype indicating that the targeted gene is essential for the survival of an organism. A conditionally regulated system will be an option for studying the essential gene and recently, methods have been developed to conditionally regulate the CRISPR/Cas9 based genome editing tool. These include methods such as Shield-I regulated ddFKBP-Cas9 induction [324], doxycycline regulated Cas9 induction [331] and a split Cas9 based system fused to FRB and FKBP dimerization domain [332].

Overexpression of RNA guided Endonucleases (RGNs) like Cas9 can continuously scan genomic DNA and cleave even imperfectly matched RNA-DNA interfaces causing off-target mutations [333-335]. A regulatable Cas9 in *L. donovani* was an attractive option, as it provides a way to control the level of the Cas9 endonuclease within the cell, thereby minimizing the likelihood of off-target mutations in the absence of ligand. The Shield-I regulated ddFKBP-Cas9 expression system was shown to be very efficient for the temporal regulation of Cas9 and gene editing in mammalian cells [324]. In our study, we utilized this approach of fusing ddFKBP to Cas9 and we could achieve specific conditional regulation of Cas9 expression (**Figure 4B**).

Recently, using CRISPR/Cas9 approach, it has been demonstrated that the RAD51 gene is essential for *L. donovani* [321]. We observed similar proportion of death of the parasite after they receive the plasmid containing the gRNA and the homology donor regions (**Figure 5B**).

PEX14 was found to be essential for survival of *T. brucei*, [31, 336] and the challenge was to rescue a parasite devoid of the essential LdPEX14 gene. For this purpose, we expressed an ectopic copy of PEX14 and despite a robust expression of the protein. Still, we were unable to rescue parasite survival. There may be one or a combination of factors responsible for this. For example, modifications of the 20 nucleotides and PAM sequences may not have been enough to

hide the ectopic copy from the Cas9 cleavage or overexpression of the ectopic copy without proper regulation may have resulted in incorrect targeting of the over expressed protein. Also, for our study we altered the PAM from a typical NGG to NAG. But this may not be enough to protect the ectopic copy as there are reports that Cas9 can cleave target DNA even with a NAG PAM sequence. Cas9 is known to cleave target DNA with lower efficiency if at least one of the two G's (NNG or NGN) are present at positions 2 and 3 [326, 337].

In short, our work demonstrated that conditionally regulating the Cas9 approach is robust and can be used for characterization and identification of essential genes. Various approaches can be adopted to improve our method of gene editing such as, (1) using a more efficient and strong promoter like the *Leishmania* rRNA promoter for the gRNA expression cassette compared to the U6snRNA promoter used in our study, (2) sequentially transfecting L. donovani expressing Cas9/gRNA with single stranded oligonucleotide donors to enhance DNA repair by micro homology mediated end joining and gene editing efficiency [321], (3) expression of an ectopic copy of the gene that can be regulated by a ligand, and (4) replacing only a part of the essential gene rather than the entire gene and studying the functions of each domain separately.

Acknowledgements

We thank Feng Zhang (Massachusetts Institute of Technology) for providing us with pX330-U6-Chimeric_BB-CBh-hSpCas9 plasmids, Philip Yates (Oregon Health & Science University) for pRP plasmids and Dr. Yvon Sterkers (University of Montpellier) for PLS6 plasmids. We thank Dr. Jan Boitz (Oregon Health and Science University) for the helpful discussion on the electroporation of plasmids into *Leishmania.*

Chapter 6

Summary and Conclusions

Summary and conclusions

Leishmaniasis is a neglected tropical disease which affects millions of people around the globe and unfortunately the pool of infection is mainly localized in developing areas of the world like India, the Middle East, Africa, and Latin America [40, 311]. According to the World Health Organization (WHO), it is estimated that around 30,000 deaths occur annually from leishmaniasis [54]. The total number of current infections is mostly underestimated due to the lack of accurate diagnostic tools and surveillance programs [338, 339]. Treatment for leishmaniasis relies on a limited number of chemotherapeutics but most of the available drugs are facing problems of toxicity and resistance issues [13, 47, 271]. Pharmaceutical research in finding new chemical leads for treatment of leishmaniasis is quite sluggish and there is an urgent need to find new therapeutic targets and chemical leads to eradicate leishmaniasis from endemic areas.

This thesis aimed to investigate the mechanistic details about the interaction of LdPEX14 with the glycosomal membrane. Our investigations were focused to answer specific questions, viz, (i) What is the role of PEX14 in the formation of the transient pore? (ii) Are there any conserved regions in PEX14 responsible for the formation of this pore? (iii) What are the possible conformational changes that PEX14 has to undergo to form a pore? (iv) Is the pore formed by PEX14 large enough to let oligomeric proteins pass or a short one? To answer these questions, we investigated the interactions of PEX14 with glycosomal membrane mimicking unilamellar vesicles.

Previous studies demonstrated that a hydrophobic region spanning amino acids 149-179 of LdPEX14 was crucial for mediating the interaction between LdPEX14 and large unilamellar vesicles (LUVs). Sucrose density flotation experiments demonstrated that a deletion mutant

lacking the hydrophobic region, LdPEX14 (Δ149-179), was unable to bind the LUVs and that ldpex14 (120-200), a fragment of LdPEX14 encompassing the hydrophobic region were able to restore the membrane binding with unilamellar vesicles. These sucrose density flotation experiments in addition to dye leakage assays demonstrated that the hydrophobic region of ldpex14 (120-200) can bind and form pores in the membrane [32, 33]. My goal was to expand these previous studies to determine the topology of this hydrophobic region inserted in the membrane anticipating that these studies can reveal vital clues behind the formation of the translocation pore.

In the first manuscript, to better understand the interaction of the hydrophobic region of LdPEX14 with the membrane, a series of tryptophan and cysteine mutants for the hydrophobic region were constructed. Studies conducted with various fluorescence quenchers revealed the depth and orientation of the inserted hydrophobic region of LdPEX14 in unilamellar vesicles. Dual fluorescence quenching analysis (DQA) performed to examine the topology and orientation of the hydrophobic region in the lipid bilayer revealed that the hydrophobic region in ldpex14 (120-200) has a deeper penetration compared to more of a shallow penetration observed for the WT LdPEX14. Forster Resonance Energy Transfer (FRET) experiments between tryptophan mutants and dansyl as donor and acceptor showed a parabolic response with residues 147 and 177 having the largest values. These data suggested that following insertion of ldpex14 (120-200), this fragment most likely adopts a helix-turn-helix configuration that exposes both the N- and C-termini extra-luminal space of the SUVs. Two other independent experiments, viz, (i) trypsinization of the peptides inserted into the bilayer and (ii) probing biotin labelled peptides inserted into bilayer with streptavidin-Horseradish Peroxidase (HRP) from aqueous side, both

confirmed that the N- and C-termini of the inserted hydrophobic region is exposed to the extra luminal space of liposomes.

Studies with ldpex14 (120-200) demonstrated that the hydrophobic region has a propensity to oligomerize and adopt an α-helical conformation in the presence of unilamellar vesicles. Studies performed with ldpex5 (203-391), a fragment shown to induce conformational changes in LdPEX14 [33], were able to trigger insertion of the hydrophobic region deeper into the bilayer. Experiments performed with dye encapsulated liposomes demonstrated that ldpex14 (120-200) has the potential to form pores in the membrane and that the pore formed was discrete with a pore diameter of ~1.0 nm.

In the second manuscript, our studies demonstrated that conformational changes induced in LdPEX14 at a low pH, was enough to form discrete pores in the membrane. Earlier studies demonstrated that the hydrophobic region of ldpex14 can form a discrete pore in the membrane, but LdPEX14 WT was unable to form a pore by itself. In the absence of LdPEX14-interacting partners like LdPEX13, LdPEX5, LdPEX7 and RING finger proteins, we altered pH as a surrogate method to induce conformational changes in LdPEX14. Studies performed utilizing the fluorescence of intrinsic tryptophan located in the hydrophobic domain and an extrinsic probe 1-anilino-8-naphthalene sulfonate (ANS) confirmed that low pH induced rearrangement of the hydrophobic region of LdPEX14. CD (Circular dichroism) and Size exclusion chromatography-HPLC (SEC-HPLC) confirmed that the low pH did not alter the quaternary or the secondary structure of LdPEX14.

In the third manuscript, to gain more insights into the functions of PEX14, we decided to knockout the PEX14 gene from *L. donovani* using CRISPR/Cas9. We developed a regulatable Cas9 expression system in *L. donovani* where the fusion of ddFKBP (destabilization domain of

FKBP12 protein) to the N-terminus of Cas9 provided controlled destabilization of Cas9 in the absence of a rapamycin ligand and an increase in the level of protein expression was detected in the presence of the rapamycin ligand. Studies were conducted with this system and it was used to knock out LdPEX14 and LdXPRT genes in *L. donovani* and can be exploited to characterize other genes in *Leishmania*. Our observations that those parasites receiving the knockout plasmids were unable to survive indicate that LdPEX14 is an essential gene.

In summary, our first manuscript demonstrated that the hydrophobic region of ldpex14 (120-200) inserts into the membrane in a helix-turn-helix conformation forming discrete pores in the membrane, similar to the peptide/lipid pores formed by the short hydrophobic domain (TMH) of TatA (Twin arginine translocase A subunit). We were able to shed light on mechanistic details of how a transient pore can be formed in the glycosomal membrane and we postulate that these discrete pores formed by the hydrophobic region can act as a foundation for the insertion of cargo loaded receptors PEX5 and PEX7 and further expand the pore to translocate the fully folded glycosomal matrix proteins.

Our second manuscript demonstrated that pH-induced structural rearrangement of the hydrophobic region of LdPEX14, which can form discrete pores in the unilamellar vesicles mimicking the glycosomal lipid membrane composition. This rearrangement of the hydrophobic region in LdPEX14 might be a crucial event in the formation of discrete pores similar to the one formed by ldpex14 (120-200).

Our third manuscript demonstrated that expression of Cas9 can be regulated in *L. donovani* by utilizing the ddFKBP-Cas9 fusion construct. Our study also confirmed that LdPEX14 is an essential gene for the viability of *L. donovani*.

Future perspectives

Studying membrane proteins is still a major challenge for biochemists and structural biologists across the globe. To gain a better understanding of translocation process across the glycosomal membrane, interactions of LdPEX14 with the glycosomal membrane mimicking liposomes should be characterized in the presence of accessory membrane proteins such as LdPEX13, RING finger proteins LdPEX2, LdPEX10, and LdPEX12. These studies could be conducted in proteoliposomes by reconstituting membrane proteins in liposomes [340-342]. The real challenge for this type of experiments would be expressing and purifying these membrane proteins in their native conformation. Once the proteoliposomes are made ready, experiments can be designed to study the interactions of cargo loaded receptors PEX5 and PEX7 in the presence of LdPEX14. Trial and error methods like addition of one protein at a time or one after the other or a mixture of proteins to the proteoliposome in different combinations can be used to determine critical components needed to form the translocation pore to translocate the protein cargo into the glycosomal lumen.

Electrophysiological experiments by isolating and reconstituting the glycosomal membrane proteins in lipid mono/bilayers can be used to investigate the channel forming activity of these membrane proteins. The challenge here would be separating large complexes of membrane proteins into individual components. Recently, we published a manuscript detailing an excellent procedure to isolate the glycosome with high purity form *L. donovani* [172]. Future attempts could be made to isolate glycosomes and reconstitute the membrane proteins in lipids for electrophysiological studies.

We have demonstrated that the hydrophobic region of *L. donovani* PEX14 has the potential to insert and form pores in the glycosomal membrane mimicking liposomes. It would be interesting to extrapolate these studies to higher eukaryotes and test them to see if the hydrophobic domain of human or yeast PEX14 has the same potential to form pores in the lipid membranes. These future studies could pave a path to solve the mystery behind the protein transport across peroxisomes.

In our study, we have also demonstrated that in *L. donovani* the expression of Cas9 could be regulated by fusing a ddFKBP domain to its N-terminus. Similar strategies could be employed to engineer an ddFKBP-Cas9 construct, that can be used for regulating the expression of Cas9 in related kinetoplastid parasites such as *T. brucei* or *T. cruzi*.

Bibliography

1. Herwaldt, B.L. *Leishmaniasis.* The Lancet, 1999. **354**(9185): p. 1191-1199.
2. World Health Organization. *Neglected tropical diseases : Prevention, control, elimination and eradication* 2012 [cited 2018, 23 May]; Available from: http://apps.who.int/gb/ebwha/pdf_files/EB132/B132_19-en.pdf.
3. Kuhls, K., M.Z. Alam, E. Cupolillo, G.E.M. Ferreira, I.L. Mauricio, R. Oddone, M.D. Feliciangeli, T. Wirth, M.A. Miles, and G. Schönian. *Comparative microsatellite typing of new world Leishmania infantum reveals low heterogeneity among populations and its recent old world origin.* PLoS Neglected Tropical Diseases, 2011. **5**(6): p. e1155.
4. World Health Organization. *Leishmaniasis: Magnitude of problem*. 2018 [cited 2018, 23 May]; Available from: http://www.who.int/leishmaniasis/burden/magnitude/burden_magnitude/en/.
5. McCall, L.-I., W.-W. Zhang, and G. Matlashewski. *Determinants for the development of visceral leishmaniasis disease.* PLoS Pathogens, 2013. **9**(1): p. e1003053.
6. Thakur, C., P. Olliaro, S. Gothoskar, S. Bhowmick, B. Choudhury, S. Prasad, M. Kumar, and B. Verma. *Treatment of visceral leishmaniasis (kala-azar) with aminosidine (= paromomycin)-antimonial combinations, a pilot study in Bihar, India.* Transactions of the Royal Society of Tropical Medicine and Hygiene, 1992. **86**(6): p. 615-616.
7. Reithinger, R., J.-C. Dujardin, H. Louzir, C. Pirmez, B. Alexander, and S. Brooker. *Cutaneous leishmaniasis.* The Lancet Infectious Diseases, 2007. **7**(9): p. 581-596.
8. World Health Organization. *Leishmaniasis: Epidemiological situation*. 2018 [cited 2018, 5 May]; Available from: http://www.who.int/leishmaniasis/burden/en/.
9. Hasker, E., S.P. Singh, P. Malaviya, A. Picado, K. Gidwani, R.P. Singh, J. Menten, M. Boelaert, and S. Sundar. *Visceral leishmaniasis in rural Bihar, India.* Emerging Infectious Diseases, 2012. **18**(10): p. 1662.
10. Centers for Disease Control and Prevention. *Leishmaniasis: Biology*. 2013 [cited 2018, 24 May]; Available from: https://www.cdc.gov/parasites/leishmaniasis/biology.html.
11. Dostálová, A. and P. Volf. *Leishmania development in sand flies: parasite-vector interactions overview.* Parasites & Vectors, 2012. **5**(1): p. 276.
12. Bates, P.A. *Transmission of Leishmania metacyclic promastigotes by phlebotomine sand flies.* International Journal for Parasitology, 2007. **37**(10): p. 1097-1106.
13. Sundar, S. and A. Singh. *Chemotherapeutics of visceral leishmaniasis: present and future developments.* Parasitology, 2017: p. 1-7.
14. Sundar, S., J. Chakravarty, D. Agarwal, M. Rai, and H.W. Murray. *Single-dose liposomal amphotericin B for visceral leishmaniasis in India.* New England Journal of Medicine, 2010. **362**(6): p. 504-512.
15. Bhandari, V., A. Kulshrestha, D.K. Deep, O. Stark, V.K. Prajapati, V. Ramesh, S. Sundar, G. Schonian, J.C. Dujardin, and P. Salotra. *Drug susceptibility in Leishmania isolates following miltefosine treatment in cases of visceral leishmaniasis and post kala-azar dermal leishmaniasis.* PLoS Neglected Tropical Diseases, 2012. **6**(5): p. e1657.
16. Moyersoen, J., J. Choe, E. Fan, W.G. Hol, and P.A. Michels. *Biogenesis of peroxisomes and glycosomes: trypanosomatid glycosome assembly is a promising new drug target.* FEMS Microbiology Reviews, 2004. **28**(5): p. 603-643.
17. Gualdrón-López, M., A. Brennand, V. Hannaert, W. Quiñones, A.J. Cáceres, F. Bringaud, J.L. Concepción, and P.A. Michels. *When, how and why glycolysis became compartmentalised in the Kinetoplastea. A new look at an ancient organelle.* International Journal for Parasitology, 2012. **42**(1): p. 1-20.
18. Hammond, D.J. and W.E. Gutteridge. *Purine and pyrimidine metabolism in the Trypanosomatidae.* Molecular and Biochemical Parasitology, 1984. **13**(3): p. 243-261.

19. Lux, H., N. Heise, T. Klenner, D. Hart, and F.R. Opperdoes. *Ether–lipid (alkyl-phospholipid) metabolism and the mechanism of action of ether–lipid analogues in Leishmania.* Molecular and Biochemical Parasitology, 2000. **111**(1): p. 1-14.
20. Lee, S.H., J.L. Stephens, and P.T. Englund. *A fatty-acid synthesis mechanism specialized for parasitism.* Nature Reviews Microbiology, 2007. **5**(4): p. 287.
21. Maugeri, D.A., J.J. Cazzulo, R.J. Burchmore, M.P. Barrett, and P.O. Ogbunude. *Pentose phosphate metabolism in Leishmania mexicana.* Molecular and Biochemical Parasitology, 2003. **130**(2): p. 117-125.
22. Parsons, M. *Glycosomes: parasites and the divergence of peroxisomal purpose.* Molecular Microbiology, 2004. **53**(3): p. 717-724.
23. Furuya, T., P. Kessler, A. Jardim, A. Schnaufer, C. Crudder, and M. Parsons. *Glucose is toxic to glycosome-deficient trypanosomes.* Proceedings of the National Academy of Sciences, 2002. **99**(22): p. 14177-14182.
24. Fairlamb, A.H. *Chemotherapy of human African trypanosomiasis: current and future prospects.* Trends in Parasitology, 2003. **19**(11): p. 488-494.
25. Häusler, T., Y.-d. Stierhof, E. Wirtz, and C. Clayton. *Import of a DHFR hybrid protein into glycosomes in vivo is not inhibited by the folate-analogue aminopterin.* The Journal of Cell Biology, 1996. **132**(3): p. 311-324.
26. Léon, S., J.M. Goodman, and S. Subramani. *Uniqueness of the mechanism of protein import into the peroxisome matrix: transport of folded, co-factor-bound and oligomeric proteins by shuttling receptors.* Biochimica et Biophysica Acta (BBA)-Molecular Cell Research, 2006. **1763**(12): p. 1552-1564.
27. Holroyd, C. and R. Erdmann. *Protein translocation machineries of peroxisomes.* FEBS Letters, 2001. **501**(1): p. 6-10.
28. Subramani, S., A. Koller, and W.B. Snyder. *Import of peroxisomal matrix and membrane proteins.* Annual Review of Biochemistry, 2000. **69**(1): p. 399-418.
29. Jardim, A., N. Rager, W. Liu, and B. Ullman. *Peroxisomal targeting protein 14 (PEX14) from Leishmania donovani: molecular, biochemical, and immunocytochemical characterization.* Molecular and Biochemical Parasitology, 2002. **124**(1-2): p. 51-62.
30. Galland, N. and P.A. Michels. *Comparison of the peroxisomal matrix protein import system of different organisms. Exploration of possibilities for developing inhibitors of the import system of trypanosomatids for anti-parasite chemotherapy.* European Journal of Cell Biology, 2010. **89**(9): p. 621-637.
31. Moyersoen, J., J. Choe, A. Kumar, F.G. Voncken, W.G. Hol, and P.A. Michels. *Characterization of Trypanosoma brucei PEX14 and its role in the import of glycosomal matrix proteins.* The FEBS Journal, 2003. **270**(9): p. 2059-2067.
32. Cyr, N., T.K. Smith, É. Boisselier, L.-P. Leroux, A.H. Kottarampatel, A. Davidsen, C. Salesse, and A. Jardim. *The hydrophobic region of the Leishmania peroxin 14: requirements for association with a glycosome mimetic membrane.* Biochemical Journal, 2018. **475**(2): p. 511-529.
33. Cyr, N., K.P. Madrid, R. Strasser, M. Aurousseau, R. Finn, J. Ausio, and A. Jardim. *Leishmania donovani peroxin 14 undergoes a marked conformational change following association with peroxin 5.* Journal of Biological Chemistry, 2008. **283**(46): p. 31488-31499.
34. Montilla-Martinez, M., S. Beck, J. Klümper, M. Meinecke, W. Schliebs, R. Wagner, and R. Erdmann. *Distinct pores for peroxisomal import of PTS1 and PTS2 proteins.* Cell Reports, 2015. **13**(10): p. 2126-2134.
35. Meinecke, M., C. Cizmowski, W. Schliebs, V. Krüger, S. Beck, R. Wagner, and R. Erdmann. *The peroxisomal importomer constitutes a large and highly dynamic pore.* Nature Cell Biology, 2010. **12**(3): p. 273.
36. Erdmann, R. and W. Schliebs. *Peroxisomal matrix protein import: the transient pore model.* Nature Reviews Molecular Cell Biology, 2005. **6**(9): p. 738.

37. Pearson, R.D. and A. de Queiroz Sousa. *Clinical spectrum of leishmaniasis.* Clinical Infectious Diseases, 1996: p. 1-11.
38. Kimutai, A., P. Ngure, W. Tonui, M. Gicheru, and L. Nyamwamu. *Leishmaniasis in Northern and Western Africa: a review.* African Journal of Infectious Diseases, 2009. **3**(1).
39. Novais, F.O., A.C. Wong, D.O. Villareal, D.P. Beiting, and P. Scott. *CD8+ T Cells Lack Local Signals To Produce IFN-γ in the Skin during Leishmania Infection.* The Journal of Immunology, 2018. **200**(5): p. 1737-1745.
40. World Health Organiztion. *Leishmaniasis: The disease and its epidemiology*. 2018 [cited 2018, 5 Feb]; Available from: http://www.who.int/leishmaniasis/disease_epidemiology/en/.
41. World Health Organization. *Leishmaniasis: Vector control*. 2018 [cited 2018, 03 Aug]; Available from: http://www.who.int/leishmaniasis/vector-control/en/.
42. Alvar, J., P. Aparicio, A. Aseffa, M. Den Boer, C. Canavate, J.-P. Dedet, L. Gradoni, R. Ter Horst, R. López-Vélez, and J. Moreno. *The relationship between leishmaniasis and AIDS: the second 10 years.* Clinical Microbiology Reviews, 2008. **21**(2): p. 334-359.
43. Centers for Disease Control and Prevention. *Leishmaniasis*. 2013 [cited 2018, 23 May]; Available from: https://www.cdc.gov/parasites/leishmaniasis/gen_info/faqs.html.
44. de Vries, H.J., S.H. Reedijk, and H.D. Schallig. *Cutaneous leishmaniasis: recent developments in diagnosis and management.* American Journal of Clinical Dermatology, 2015. **16**(2): p. 99-109.
45. Palumbo, E. *Treatment strategies for mucocutaneous leishmaniasis.* Journal of Global Infectious Diseases, 2010. **2**(2): p. 147.
46. Amato, V.S., F.F. Tuon, H.A. Bacha, V.A. Neto, and A.C. Nicodemo. *Mucosal leishmaniasis: current scenario and prospects for treatment.* Acta Tropica, 2008. **105**(1): p. 1-9.
47. Goto, H. and J.A.L. Lindoso. *Current diagnosis and treatment of cutaneous and mucocutaneous leishmaniasis.* Expert Review of Anti Infective Therapy, 2010. **8**(4): p. 419-433.
48. David, C.V. and N. Craft. *Cutaneous and mucocutaneous leishmaniasis.* Dermatologic Therapy, 2009. **22**(6): p. 491-502.
49. Perez-Franco, J.E., M.L. Cruz-Barrera, M.L. Robayo, M.C. Lopez, C.D. Daza, A. Bedoya, M.L. Mariño, C.H. Saavedra, and M.C. Echeverry. *Clinical and parasitological features of patients with American cutaneous leishmaniasis that did not respond to treatment with meglumine antimoniate.* PLoS Neglected Tropical Diseases, 2016. **10**(5): p. e0004739.
50. Lima, Á.L., I.D. de Lima, J.F. Coutinho, Ú.P. de Sousa, M.A. Rodrigues, M.E. Wilson, R.D. Pearson, J.W. Queiroz, and S.M. Jerônimo. *Changing epidemiology of visceral leishmaniasis in northeastern Brazil: a 25-year follow-up of an urban outbreak.* Transactions of The Royal Society of Tropical Medicine and Hygiene, 2017. **111**(10): p. 440-447.
51. Mondal, D., K.N. Nasrin, M.M. Huda, M. Kabir, M.S. Hossain, A. Kroeger, T. Thomas, and R. Haque. *Enhanced case detection and improved diagnosis of PKDL in a Kala-azar-endemic area of Bangladesh.* PLoS Neglected Tropical Diseases, 2010. **4**(10): p. e832.
52. Musa, A., E. Khalil, F. Mahgoub, S. Hamad, A. Elkadaru, and A. El Hassan. *Efficacy of liposomal amphotericin B (AmBisome®) in the treatment of persistent post-kala-azar dermal leishmaniasis (PKDL).* Annals of Tropical Medicine & Parasitology, 2005. **99**(6): p. 563-569.
53. Addy, M. and A. Nandy. *Ten years of kala-azar in west Bengal, Part I. Did post-kala-azar dermal leishmaniasis initiate the outbreak in 24-Parganas?* Bulletin of the World Health Organization, 1992. **70**(3): p. 341.
54. World Health Organization. *Leishmaniasis: Key facts*. 2018 [cited 2018, 03 Aug]; Available from: http://www.who.int/news-room/fact-sheets/detail/leishmaniasis.
55. Singh, R., H. Pandey, and S. Sundar. *Visceral leishmaniasis (kala-azar): challenges ahead.* Indian Journal of Medical Research, 2006. **123**(3): p. 331.
56. Das, P., S. Samuels, P. Desjeux, A. Mittal, R. Topno, N.A. Siddiqui, D. Sur, A. Pandey, and R. Sarnoff. *Annual incidence of visceral leishmaniasis in an endemic area of Bihar, India.* Tropical Medicine & International Health, 2010. **15**(s2): p. 4-11.

57. Bora, D. *Epidemiology of visceral leishmaniasis in India.* National Medical Journal of India, 1999. **12**: p. 62-68.
58. World Health Organization. *Leishmaniasis in the WHO european region*. [cited 2018, 03 Aug]; Available from: http://www.euro.who.int/__data/assets/pdf_file/0007/246166/Fact-sheet-Leishmaniasis-Eng.pdf?ua=1.
59. Silva, A.M., A. Cordeiro-da-Silva, and G.H. Coombs. *Metabolic variation during development in culture of Leishmania donovani promastigotes.* PLoS Neglected Tropical Diseases, 2011. **5**(12): p. e1451.
60. Liu, D. and J.E. Uzonna. *The early interaction of Leishmania with macrophages and dendritic cells and its influence on the host immune response.* Frontiers in Cellular and Infection Microbiology, 2012. **2**: p. 83.
61. Peters, N.C., J.G. Egen, N. Secundino, A. Debrabant, N. Kimblin, S. Kamhawi, P. Lawyer, M.P. Fay, R.N. Germain, and D. Sacks. *In vivo imaging reveals an essential role for neutrophils in leishmaniasis transmitted by sand flies.* Science, 2008. **321**(5891): p. 970-974.
62. Antoine, J.-C., E. Prina, T. Lang, and N. Courret. *The biogenesis and properties of the parasitophorous vacuoles that harbour Leishmania in murine macrophages.* Trends in Microbiology, 1998. **6**(10): p. 392-401.
63. Van Assche, T., M. Deschacht, R.A.I. da Luz, L. Maes, and P. Cos. *Leishmania–macrophage interactions: Insights into the redox biology.* Free Radical Biology and Medicine, 2011. **51**(2): p. 337-351.
64. Gluenz, E., M.L. Ginger, and P.G. McKean. *Flagellum assembly and function during the Leishmania life cycle.* Current Opinion in Microbiology, 2010. **13**(4): p. 473-479.
65. Kaye, P. and P. Scott. *Leishmaniasis: complexity at the host–pathogen interface.* Nature Reviews Microbiology, 2011. **9**(8): p. 604.
66. Salam, M., M.G. Khan, and D. Mondal. *Urine antigen detection by latex agglutination test for diagnosis and assessment of initial cure of visceral leishmaniasis.* Transactions of the Royal Society of Tropical Medicine and Hygiene, 2011. **105**(5): p. 269-272.
67. Boelaert, M., S. Rijal, S. Regmi, R. Singh, B. Karki, D. Jacquet, F. Chappuis, L. Campino, P. Desjeux, and D. LE RAY. *A comparative study of the effectiveness of diagnostic tests for visceral leishmaniasis.* The American Journal of Tropical Medicine and Hygiene, 2004. **70**(1): p. 72-77.
68. Siddig, M., H. Ghalib, D.C. Shillington, and E.A. Petersen. *Visceral leishmaniasis in the Sudan: comparative parasitological methods of diagnosis.* Transactions of the Royal Society of Tropical Medicine and Hygiene, 1988. **82**(1): p. 66-68.
69. Burns, J.M., W.G. Shreffler, D.R. Benson, H.W. Ghalib, R. Badaro, and S.G. Reed. *Molecular characterization of a kinesin-related antigen of Leishmania chagasi that detects specific antibody in African and American visceral leishmaniasis.* Proceedings of the National Academy of Sciences, 1993. **90**(2): p. 775-779.
70. Zijlstra, E., N. Daifalla, P. Kager, E. Khalil, A. El-Hassan, S. Reed, and H. Ghalib. *rK39 enzyme-linked immunosorbent assay for diagnosis of Leishmania donovani infection.* Clinical and Diagnostic Laboratory Immunology, 1998. **5**(5): p. 717-720.
71. Ashford, D.A., J.R. David, M. Freire, R. David, I. Sherlock, M.d.C. Eulálio, D.P. Sampaio, and R. Badaro. *Studies on control of visceral leishmaniasis: impact of dog control on canine and human visceral leishmaniasis in Jacobina, Bahia, Brazil.* The American Journal of Tropical Medicine and Hygiene, 1998. **59**(1): p. 53-57.
72. Coleman, M., G.M. Foster, R. Deb, R.P. Singh, H.M. Ismail, P. Shivam, A.K. Ghosh, S. Dunkley, V. Kumar, and M. Coleman. *DDT-based indoor residual spraying suboptimal for visceral leishmaniasis elimination in India.* Proceedings of the National Academy of Sciences, 2015. **112**(28): p. 8573-8578.
73. Kaul, S., R. Sharma, K. Dey, R. Rai, and T. Verghese. *Impact of DDT indoor residual spraying on Phlebotomus argentipes in a kala-azar endemic village in eastern Uttar Pradesh.* Bulletin of the World Health Organization, 1994. **72**(1): p. 79.

74. Singh, R., R. Das, and S. Sharma. *Resistance of sandflies to DDT in Kala-azar endemic districts of Bihar, India.* Bulletin of the World Health Organization, 2001. **79**: p. 793-793.
75. Astellas Pharma US. *Ambisome: Amphotericin B liposome for injection*. 2018 [cited 2018, 25 May]; Available from: http://www.ambisome.com/.
76. Davies, T., L. Field, P. Usherwood, and M. Williamson. *DDT, pyrethrins, pyrethroids and insect sodium channels.* International Union of Biochemistry and Molecular Biology Life, 2007. **59**(3): p. 151-162.
77. Ritmeijer, K., C. Davies, R. Van Zorge, S.J. Wang, J. Schorscher, S.I. Dongu'du, and R.N. Davidson. *Evaluation of a mass distribution programme for fine-mesh impregnated bednets against visceral leishmaniasis in eastern Sudan.* Tropical Medicine & International Health, 2007. **12**(3): p. 404-414.
78. Mondal, D., M.M. Huda, M.K. Karmoker, D. Ghosh, G. Matlashewski, S.G. Nabi, and A. Kroeger. *Reducing visceral leishmaniasis by insecticide impregnation of bed-nets, Bangladesh.* Emerging Infectious Diseases, 2013. **19**(7): p. 1131.
79. Picado, A., S.P. Singh, S. Rijal, S. Sundar, B. Ostyn, F. Chappuis, S. Uranw, K. Gidwani, B. Khanal, and M. Rai. *Longlasting insecticidal nets for prevention of Leishmania donovani infection in India and Nepal: paired cluster randomised trial.* British Medical Journal, 2010. **341**: p. c6760.
80. Veeken, H., K. Ritmeijer, J. Seaman, and R. Davidson. *A randomized comparison of branded sodium stibogluconate and generic sodium stibogluconate for the treatment of visceral leishmaniasis under field conditions in Sudan.* Tropical Medicine & International Health, 2000. **5**(5): p. 312-317.
81. Berman, J.D., D. Waddell, and B. Hanson. *Biochemical mechanisms of the antileishmanial activity of sodium stibogluconate.* Antimicrobial Agents and Chemotherapy, 1985. **27**(6): p. 916-920.
82. Chawla, B., A. Jhingran, A. Panigrahi, K.D. Stuart, and R. Madhubala. *Paromomycin affects translation and vesicle-mediated trafficking as revealed by proteomics of paromomycin–susceptible–resistant Leishmania donovani.* PLoS One, 2011. **6**(10): p. e26660.
83. Berman, J. *Miltefosine to treat leishmaniasis.* Expert Opinion on Pharmacotherapy, 2005. **6**(8): p. 1381-1388.
84. Bhattacharya, S.K., P.K. Sinha, S. Sundar, C.P. Thakur, T.K. Jha, K. Pandey, V.R. Das, N. Kumar, C. Lal, and N. Verma. *Phase 4 trial of miltefosine for the treatment of Indian visceral leishmaniasis.* The Journal of Infectious Diseases, 2007. **196**(4): p. 591-598.
85. Sundar, S. and J. Chakravarty. *Liposomal amphotericin B and leishmaniasis: dose and response.* Journal of Global Infectious Diseases, 2010. **2**(2): p. 159.
86. Saravolatz, L.D., C. Bern, J. Adler-Moore, J. Berenguer, M. Boelaert, M. den Boer, R.N. Davidson, C. Figueras, L. Gradoni, and D.A. Kafetzis. *Liposomal amphotericin B for the treatment of visceral leishmaniasis.* Clinical Infectious Diseases, 2006. **43**(7): p. 917-924.
87. Purkait, B., A. Kumar, N. Nandi, A.H. Sardar, S. Das, S. Kumar, K. Pandey, V. Ravidas, M. Kumar, and T. De. *Mechanism of amphotericin B resistance in clinical isolates of Leishmania donovani.* Antimicrobial Agents and Chemotherapy, 2012. **56**(2): p. 1031-1041.
88. Moore, E. and D. Lockwood. *Treatment of visceral leishmaniasis.* Journal of Global Infectious Diseases, 2010. **2**(2): p. 151.
89. Mohapatra, S. *Drug resistance in leishmaniasis: Newer developments.* Tropical Parasitology, 2014. **4**(1): p. 4.
90. Sundar, S., A. Singh, M. Rai, and J. Chakravarty. *Single-dose indigenous liposomal amphotericin B in the treatment of Indian visceral leishmaniasis: a phase 2 study.* The American Journal of Tropical Medicine and Hygiene, 2015. **92**(3): p. 513-517.
91. Jha, S., N. Singh, and T. Jha. *Changing response to diamidine compounds in cases of kala-azar unresponsive to antimonial.* The Journal of the Association of Physicians of India, 1991. **39**(4): p. 314-316.

92. Hughes, A.L. and H. Piontkivska. *Phylogeny of Trypanosomatidae and Bodonidae (Kinetoplastida) based on 18S rRNA: evidence for paraphyly of Trypanosoma and six other genera.* Molecular Biology and Evolution, 2003. **20**(4): p. 644-652.
93. Hughes, A.L. and H. Piontkivska. *Molecular phylogenetics of Trypanosomatidae: contrasting results from 18S rRNA and protein phylogenies.* Kinetoplastid Biology and Disease, 2003. **2**(1): p. 15.
94. Maslov, D.A., S.A. Podlipaev, and J. Lukes. *Phylogeny of the kinetoplastida: taxonomic problems and insights into the evolution of parasitism.* Memórias do Instituto Oswaldo Cruz, 2001. **96**(3): p. 397-402.
95. Hannaert, V., F. Bringaud, F.R. Opperdoes, and P.A. Michels. *Evolution of energy metabolism and its compartmentation in Kinetoplastida.* Kinetoplastid Biology and Disease, 2003. **2**(1): p. 11.
96. Simpson, L., S. Sbicego, and R. Aphasizhev. *Uridine insertion/deletion RNA editing in trypanosome mitochondria: a complex business.* RNA, 2003. **9**(3): p. 265-276.
97. Carter, N.S., S.M. Landfear, and B. Ullman. *Nucleoside transporters of parasitic protozoa.* Trends in Parasitology, 2001. **17**(3): p. 142-145.
98. Stuart, K., T.E. Allen, S. Heidmann, and S.D. Seiwert. *RNA editing in kinetoplastid protozoa.* Microbiology and Molecular Biology Reviews, 1997. **61**(1): p. 105-120.
99. Opperdoes, F.R., P. Baudhuin, I. Coppens, C. De Roe, S.W. Edwards, P.J. Weijers, and O. Misset. *Purification, morphometric analysis, and characterization of the glycosomes (microbodies) of the protozoan hemoflagellate Trypanosoma brucei.* The Journal of Cell Biology, 1984. **98**(4): p. 1178-1184.
100. Sommer, J.M. and C. Wang. *Targeting proteins to the glycosomes of African trypanosomes.* Annual Reviews in Microbiology, 1994. **48**(1): p. 105-138.
101. Michels, P.A., J. Moyersoen, H. Krazy, N. Galland, M. Herman, and V. Hannaert. *Peroxisomes, glyoxysomes and glycosomes.* Molecular Membrane Biology, 2005. **22**(1-2): p. 133-145.
102. Plewes, K.A., S.D. Barr, and L. Gedamu. *Iron superoxide dismutases targeted to the glycosomes of Leishmania chagasi are important for survival.* Infection and Immunity, 2003. **71**(10): p. 5910-5920.
103. Opperdoes, F.R. and J.-P. Szikora. *In silico prediction of the glycosomal enzymes of Leishmania major and trypanosomes.* Molecular and Biochemical Parasitology, 2006. **147**(2): p. 193-206.
104. Parsons, M., T. Furuya, S. Pal, and P. Kessler. *Biogenesis and function of peroxisomes and glycosomes.* Molecular and Biochemical Parasitology, 2001. **115**(1): p. 19-28.
105. Schrader, M. and H.D. Fahimi. *The peroxisome: still a mysterious organelle.* Histochemistry and Cell Biology, 2008. **129**(4): p. 421-440.
106. Li, X., E. Baumgart, G.-X. Dong, J.C. Morrell, G. Jimenez-Sanchez, D. Valle, K.D. Smith, and S.J. Gould. *PEX11α is required for peroxisome proliferation in response to 4-phenylbutyrate but is dispensable for peroxisome proliferator-activated receptor alpha-mediated peroxisome proliferation.* Molecular and Cellular Biology, 2002. **22**(23): p. 8226-8240.
107. Nagotu, S., V.C. Kalel, R. Erdmann, and H.W. Platta. *Molecular basis of peroxisomal biogenesis disorders caused by defects in peroxisomal matrix protein import.* Biochimica et Biophysica Acta (BBA)-Molecular Basis of Disease, 2012. **1822**(9): p. 1326-1336.
108. Michels, P., V. Hannaert, and F. Bringaud. *Metabolic aspects of glycosomes in trypanosomatidae–new data and views.* Parasitology Today, 2000. **16**(11): p. 482-489.
109. Opperdoes, F.R. *Compartmentation of carbohydrate metabolism in trypanosomes.* Annual Reviews in Microbiology, 1987. **41**(1): p. 127-151.
110. Gualdron-Lopez, M., A. Brennand, L. Avilan, and P.A. Michels. *Translocation of solutes and proteins across the glycosomal membrane of trypanosomes; possibilities and limitations for targeting with trypanocidal drugs.* Parasitology, 2013. **140**(1): p. 1-20.

111. Bakker, B.M., P.A. Michels, F.R. Opperdoes, and H.V. Westerhoff. *What controls glycolysis in bloodstream form Trypanosoma brucei?* Journal of Biological Chemistry, 1999. **274**(21): p. 14551-14559.
112. Blum, J.J. *Energy metabolism inLeishmania.* Journal of Bioenergetics and Biomembranes, 1994. **26**(2): p. 147-155.
113. Guerra, D.G., A. Decottignies, B.M. Bakker, and P.A. Michels. *The mitochondrial FAD-dependent glycerol-3-phosphate dehydrogenase of Trypanosomatidae and the glycosomal redox balance of insect stages of Trypanosoma brucei and Leishmania spp.* Molecular and Biochemical Parasitology, 2006. **149**(2): p. 155-169.
114. Albert, M.-A., J.R. Haanstra, V. Hannaert, J. Van Roy, F.R. Opperdoes, B.M. Bakker, and P.A. Michels. *Experimental and in silico analyses of glycolytic flux control in bloodstream form Trypanosoma brucei.* Journal of Biological Chemistry, 2005. **280**(31): p. 28306-28315.
115. Haanstra, J.R., E.J. Kerkhoven, A. Van Tuijl, M. Blits, M. Wurst, R. Van Nuland, M.A. Albert, P.A. Michels, J. Bouwman, and C. Clayton. *A domino effect in drug action: from metabolic assault towards parasite differentiation.* Molecular Microbiology, 2011. **79**(1): p. 94-108.
116. Bakker, B.M., F.I. Mensonides, B. Teusink, P. van Hoek, P.A. Michels, and H.V. Westerhoff. *Compartmentation protects trypanosomes from the dangerous design of glycolysis.* Proceedings of the National Academy of Sciences, 2000. **97**(5): p. 2087-2092.
117. Michels, P.A. and V. Hannaert. *The evolution of kinetoplastid glycosomes.* Journal of Bioenergetics and Biomembranes, 1994. **26**(2): p. 213-219.
118. Bringaud, F., L. Rivière, and V. Coustou. *Energy metabolism of trypanosomatids: adaptation to available carbon sources.* Molecular and Biochemical Parasitology, 2006. **149**(1): p. 1-9.
119. Bakker, B.M., H.V. Westerhoff, and P.A. Michels. *Regulation and control of compartmentalized glycolysis in bloodstream formTrypanosoma brucei.* Journal of Bioenergetics and Biomembranes, 1995. **27**(5): p. 513-525.
120. Blattner, J., S. Helfert, P. Michels, and C. Clayton. *Compartmentation of phosphoglycerate kinase in Trypanosoma brucei plays a critical role in parasite energy metabolism.* Proceedings of the National Academy of Sciences, 1998. **95**(20): p. 11596-11600.
121. Thevelein, J.M. and S. Hohmann. *Trehalose synthase: guard to the gate of glycolysis in yeast?* Trends in Biochemical Sciences, 1995. **20**(1): p. 3-10.
122. Hohmann, S., M.J. Neves, W. de Koning, R. Alijo, J. Ramos, and J.M. Thevelein. *The growth and signalling defects of the ggs1 (fdp1/byp1) deletion mutant on glucose are suppressed by a deletion of the gene encoding hexokinase PII.* Current Genetics, 1993. **23**(4): p. 281-289.
123. Haanstra, J.R., A. van Tuijl, P. Kessler, W. Reijnders, P.A. Michels, H.V. Westerhoff, M. Parsons, and B.M. Bakker. *Compartmentation prevents a lethal turbo-explosion of glycolysis in trypanosomes.* Proceedings of the National Academy of Sciences, 2008. **105**(46): p. 17718-17723.
124. Davies, M.J., A. Ross, and W. Gutteridge. *The enzymes of purine salvage in Trypanosoma cruzi, Trypanosoma brucei and Leishmania mexicana.* Parasitology, 1983. **87**(2): p. 211-217.
125. Jardim, A., S.E. Bergeson, S. Shih, N. Carter, R.W. Lucas, G. Merlin, P.J. Myler, K. Stuart, and B. Ullman. *Xanthine Phosphoribosyl transferase from Leishmania donovani : Molecular cloning, biochemical characterization, and genetic analysis.* Journal of Biological Chemistry, 1999. **274**(48): p. 34403-34410.
126. Allen, T.E., H.-Y. Hwang, A. Jardim, R. Olafson, and B. Ullman. *Cloning and expression of the hypoxanthine-guanine phosphoribosyltransferase from Leishmania donovani.* Molecular and Biochemical Parasitology, 1995. **73**(1-2): p. 133-143.
127. Ullman, B. and D. Carter. *Hypoxanthine-guanine phosphoribosyltransferase as a therapeutic target in protozoal infections.* Infectious Agents and Disease, 1995. **4**(1): p. 29-40.
128. Allen, T., H.-Y. Hwang, K. Wilson, S. Hanson, A. Jardim, and B. Ullman. *Cloning and expression of the adenine phosphoribosyltransferase gene from Leishmania donovani.* Molecular and Biochemical Parasitology, 1995. **74**(1): p. 99-103.

129. Shih, S., H.-Y. Hwang, D. Carter, P. Stenberg, and B. Ullman. *Localization and Targeting of the Leishmania donovaniHypoxanthine-Guanine Phosphoribosyltransferase to the Glycosome.* Journal of Biological Chemistry, 1998. **273**(3): p. 1534-1541.
130. Zarella-Boitz, J.M., N. Rager, A. Jardim, and B. Ullman. *Subcellular localization of adenine and xanthine phosphoribosyltransferases in Leishmania donovani.* Molecular and Biochemical Parasitology, 2004. **134**(1): p. 43-51.
131. Boitz, J.M., B. Ullman, A. Jardim, and N.S. Carter. *Purine salvage in Leishmania: complex or simple by design?* Trends in Parasitology, 2012. **28**(8): p. 345-352.
132. McNew, J.A. and J.M. Goodman. *An oligomeric protein is imported into peroxisomes in vivo.* The Journal of Cell Biology, 1994. **127**(5): p. 1245-1257.
133. Glover, J.R., D.W. Andrews, and R.A. Rachubinski. *Saccharomyces cerevisiae peroxisomal thiolase is imported as a dimer.* Proceedings of the National Academy of Sciences, 1994. **91**(22): p. 10541-10545.
134. Islinger, M., K.W. Li, J. Seitz, A. Völkl, and G.H. Lüers. *Hitchhiking of Cu/Zn superoxide dismutase to peroxisomes–evidence for a natural piggyback import mechanism in mammals.* Traffic, 2009. **10**(11): p. 1711-1721.
135. Jardim, A., W. Liu, E. Zheleznova, and B. Ullman. *Peroxisomal Targeting Signal-1 Receptor Protein PEX5 from Leishmania donovani: Molecular cloning, biochemical characterization, and genetic analysis.* Journal of Biological Chemistry, 2000. **275**(18): p. 13637-13644.
136. Shiozawa, K., P.V. Konarev, C. Neufeld, M. Wilmanns, and D.I. Svergun. *Solution structure of human Pex5· Pex14· PTS1 protein complexes obtained by small angle X-ray scattering.* Journal of Biological Chemistry, 2009. **284**(37): p. 25334-25342.
137. Choe, J., J. Moyersoen, C. Roach, T.L. Carter, E. Fan, P.A. Michels, and W.G. Hol. *Analysis of the sequence motifs responsible for the interactions of peroxins 14 and 5, which are involved in glycosome biogenesis in Trypanosoma brucei.* Biochemistry, 2003. **42**(37): p. 10915-10922.
138. Hojjat, H. and A. Jardim. *Identification of Leishmania donovani peroxin 14 residues required for binding the peroxin 5 receptor proteins.* Biochemical Journal, 2015. **465**(2): p. 247-257.
139. Neuhaus, A., H. Kooshapur, J. Wolf, N.H. Meyer, T. Madl, J. Saidowsky, E. Hambruch, A. Lazam, M. Jung, and M. Sattler. *A novel Pex14 protein-interacting site of human Pex5 is critical for matrix protein import into peroxisomes.* Journal of Biological Chemistry, 2014. **289**(1): p. 437-448.
140. Emmanouilidis, L., M. Gopalswamy, D.M. Passon, M. Wilmanns, and M. Sattler. *Structural biology of the import pathways of peroxisomal matrix proteins.* Biochimica et Biophysica Acta (BBA)-Molecular Cell Research, 2016. **1863**(5): p. 804-813.
141. Lazarow, P.B. *.1. 7. The import receptor Pex7p and the PTS2 targeting sequence.* Biochimica et Biophysica Acta (BBA)-Molecular Cell Research, 2006. **1763**(12): p. 1599-1604.
142. Pilar, A.V.C., K.P. Madrid, and A. Jardim. *Interaction of Leishmania PTS2 receptor peroxin 7 with the glycosomal protein import machinery.* Molecular and Biochemical Parasitology, 2008. **158**(1): p. 72-81.
143. Pan, D., T. Nakatsu, and H. Kato. *Crystal structure of peroxisomal targeting signal-2 bound to its receptor complex Pex7p–Pex21p.* Nature Structural and Molecular Biology, 2013. **20**(8): p. 987.
144. Pilar, A.V.C., R. Strasser, J. McLean, E. Quinn, N. Cyr, H. Hojjat, A.H. Kottarampatel, and A. Jardim. *Analysis of the Leishmania peroxin 7 interactions with peroxin 5, peroxin 14 and PTS2 ligands.* Biochemical Journal, 2014. **460**(2): p. 273-282.
145. Heiland, I. and R. Erdmann. *Biogenesis of peroxisomes.* The FEBS Journal, 2005. **272**(10): p. 2362-2372.
146. Sparks, A.B., J.E. Rider, N.G. Hoffman, D.M. Fowlkes, L. Quillam, and B.K. Kay. *Distinct ligand preferences of Src homology 3 domains from Src, Yes, Abl, cortactin, p53bp2, PLCgamma, Crk, and Grb2.* Proceedings of the National Academy of Sciences, 1996. **93**(4): p. 1540-1544.

147. Cohen, G.B., R. Ren, and D. Baltimore. *Modular binding domains in signal transduction proteins.* Cell, 1995. **80**(2): p. 237-248.
148. Stein, K., A. Schell-Steven, R. Erdmann, and H. Rottensteiner. *Interactions of Pex7p and Pex18p/Pex21p with the peroxisomal docking machinery: implications for the first steps in PTS2 protein import.* Molecular and Cellular Biology, 2002. **22**(17): p. 6056-6069.
149. Schliebs, W. and W.-H. Kunau. *PTS2 co-receptors: diverse proteins with common features.* Biochimica et Biophysica Acta (BBA)-Molecular Cell Research, 2006. **1763**(12): p. 1605-1612.
150. Galland, N., F. Demeure, V. Hannaert, E. Verplaetse, D. Vertommen, P. Van Der Smissen, P.J. Courtoy, and P.A. Michels. *Characterization of the role of the receptors PEX5 and PEX7 in the import of proteins into glycosomes of Trypanosoma brucei.* Biochimica et Biophysica Acta (BBA)-Molecular Cell Research, 2007. **1773**(4): p. 521-535.
151. Guerra-Giraldez, C., L. Quijada, and C.E. Clayton. *Compartmentation of enzymes in a microbody, the glycosome, is essential in Trypanosoma brucei.* Journal of Cell Science, 2002. **115**(13): p. 2651-2658.
152. Hajduk, P.J., J.R. Huth, and S.W. Fesik. *Druggability indices for protein targets derived from NMR-based screening data.* Journal of Medicinal Chemistry, 2005. **48**(7): p. 2518-2525.
153. Rickert, M., X. Wang, M.J. Boulanger, N. Goriatcheva, and K.C. Garcia. *The structure of interleukin-2 complexed with its alpha receptor.* Science, 2005. **308**(5727): p. 1477-1480.
154. Villoutreix, B.O., M.A. Kuenemann, J.L. Poyet, H. Bruzzoni-Giovanelli, C. Labbé, D. Lagorce, O. Sperandio, and M.A. Miteva. *Drug-Like Protein□ Protein Interaction Modulators: Challenges and Opportunities for Drug Discovery and Chemical Biology.* Molecular Informatics, 2014. **33**(6-7): p. 414-437.
155. Dawidowski, M., L. Emmanouilidis, V. Kalel, K. Tripsianes, K. Schorpp, K. Hadian, M. Kaiser, P. Mäser, M. Kolonko, and S. Tanghe. *Inhibitors of PEX14 disrupt protein import into glycosomes and kill Trypanosoma parasites.* Science, 2017. **355**(6332): p. 1416-1420.
156. Kalel, V.C., L. Emmanouilidis, M. Dawidowski, W. Schliebs, M. Sattler, G.M. Popowicz, and R. Erdmann. *Inhibitors of glycosomal protein import provide new leads against trypanosomiasis.* Microbial Cell, 2017. **4**(7): p. 229.
157. Rapp, S., U. Soto, and W. Just. *Import of firefly luciferase into peroxisomes of permeabilized Chinese hamster ovary cells: a model system to study peroxisomal protein import in vitro.* Experimental Cell Research, 1993. **205**(1): p. 59-65.
158. Dammai, V. and S. Subramani. *The human peroxisomal targeting signal receptor, Pex5p, is translocated into the peroxisomal matrix and recycled to the cytosol.* Cell, 2001. **105**(2): p. 187-196.
159. Kunau, W.-H. *Peroxisomes: the extended shuttle to the peroxisome matrix.* Current Biology, 2001. **11**(16): p. R659-R662.
160. Kim, P. and E. Hettema. *Multiple pathways for protein transport to peroxisomes.* Journal of Molecular Biology, 2015. **427**(6): p. 1176-1190.
161. Nair, D.M., P.E. Purdue, and P.B. Lazarow. *Pex7p translocates in and out of peroxisomes in Saccharomyces cerevisiae.* The Journal of Cell Biology, 2004. **167**(4): p. 599-604.
162. Stanley, W.A. and M. Wilmanns. *Dynamic architecture of the peroxisomal import receptor Pex5p.* Biochimica et Biophysica Acta (BBA)-Molecular Cell Research, 2006. **1763**(12): p. 1592-1598.
163. Walton, P.A., P. Hill, and S. Subramani. *Import of stably folded proteins into peroxisomes.* Molecular Biology of the Cell, 1995. **6**(6): p. 675-683.
164. Albertini, M., P. Rehling, R. Erdmann, W. Girzalsky, J.A. Kiel, M. Veenhuis, and W.-H. Kunau. *Pex14p, a peroxisomal membrane protein binding both receptors of the two PTS-dependent import pathways.* Cell, 1997. **89**(1): p. 83-92.
165. Kunze, M., N. Malkani, S. Maurer-Stroh, C. Wiesinger, J.A. Schmid, and J. Berger. *Mechanistic Insights into PTS2-mediated Peroxisomal Protein Import: The co-receptor PEX5L drastically*

increases the interaction strength between the cargo protein and the receptor PEX7. Journal of Biological Chemistry, 2015. **290**(8): p. 4928-4940.
166. Grunau, S., W. Schliebs, R. Linnepe, C. Neufeld, C. Cizmowski, B. Reinartz, H.E. Meyer, B. Warscheid, W. Girzalsky, and R. Erdmann. *Peroxisomal Targeting of PTS2 Pre-Import Complexes in the Yeast Saccharomyces cerevisiae.* Traffic, 2009. **10**(4): p. 451-460.
167. Ma, C. and S. Subramani. *Peroxisome matrix and membrane protein biogenesis.* International Union of Biochemistry and Molecular Biology Life, 2009. **61**(7): p. 713-722.
168. Rodrigues, T.A., C.P. Grou, and J.E. Azevedo. *Revisiting the intraperoxisomal pathway of mammalian PEX7.* Scientific Reports, 2015. **5**: p. 11806.
169. Verplaetse, E., D.J. Rigden, and P.A. Michels. *Identification, characterization and essentiality of the unusual peroxin 13 from Trypanosoma brucei.* Biochimica et Biophysica Acta (BBA)-Molecular Cell Research, 2009. **1793**(3): p. 516-527.
170. Huhse, B., P. Rehling, M. Albertini, L. Blank, K. Meller, and W.-H. Kunau. *Pex17p of Saccharomyces cerevisiae is a novel peroxin and component of the peroxisomal protein translocation machinery.* The Journal of Cell Biology, 1998. **140**(1): p. 49-60.
171. Brennand, A., D.J. Rigden, and P.A. Michels. *Trypanosomes contain two highly different isoforms of peroxin PEX13 involved in glycosome biogenesis.* FEBS Letters, 2012. **586**(13): p. 1765-1771.
172. Jardim, A., D.B. Hardie, J. Boitz, and C.H. Borchers. *Proteomic Profiling of Leishmania donovan i Promastigote Subcellular Organelles.* Journal of Proteome Research, 2018.
173. Prestele, J., G. Hierl, C. Scherling, S. Hetkamp, C. Schwechheimer, E. Isono, W. Weckwerth, G. Wanner, and C. Gietl. *Different functions of the C3HC4 zinc RING finger peroxins PEX10, PEX2, and PEX12 in peroxisome formation and matrix protein import.* Proceedings of the National Academy of Sciences, 2010. **107**(33): p. 14915-14920.
174. Saveria, T., P. Kessler, B.C. Jensen, and M. Parsons. *Characterization of glycosomal RING finger proteins of trypanosomatids.* Experimental Parasitology, 2007. **116**(1): p. 14-24.
175. Chang, C.-C., D.S. Warren, K.A. Sacksteder, and S.J. Gould. *PEX12 interacts with PEX5 and PEX10 and acts downstream of receptor docking in peroxisomal matrix protein import.* The Journal of Cell Biology, 1999. **147**(4): p. 761-774.
176. Matsuzono, Y. and Y. Fujiki. *In vitro transport of membrane proteins to peroxisomes by shuttling receptor Pex19p.* Journal of Biological Chemistry, 2006. **281**(1): p. 36-42.
177. Jones, J.M., J.C. Morrell, and S.J. Gould. *Multiple distinct targeting signals in integral peroxisomal membrane proteins.* The Journal of Cell Biology, 2001. **153**(6): p. 1141-1150.
178. Honsho, M. and Y. Fujiki. *Topogenesis of peroxisomal membrane protein requires a short, positively charged intervening-loop sequence and flanking hydrophobic segments study using human membrane protein PMP34.* Journal of Biological Chemistry, 2001. **276**(12): p. 9375-9382.
179. Pinto, M.P., C.P. Grou, I.S. Alencastre, M.E. Oliveira, C. Sá-Miranda, M. Fransen, and J.E. Azevedo. *The import competence of a peroxisomal membrane protein is determined by Pex19p before the docking step.* Journal of Biological Chemistry, 2006. **281**(45): p. 34492-34502.
180. Shibata, H., Y. Kashiwayama, T. Imanaka, and H. Kato. *Domain architecture and activity of human Pex19p, a chaperone-like protein for intracellular trafficking of peroxisomal membrane proteins.* Journal of Biological Chemistry, 2004. **279**(37): p. 38486-38494.
181. van der Zand, A., J. Gent, I. Braakman, and H.F. Tabak. *Biochemically distinct vesicles from the endoplasmic reticulum fuse to form peroxisomes.* Cell, 2012. **149**(2): p. 397-409.
182. van der Zand, A., I. Braakman, and H.F. Tabak. *Peroxisomal membrane proteins insert into the endoplasmic reticulum.* Molecular Biology of the Cell, 2010. **21**(12): p. 2057-2065.
183. Neufeld, C., F.V. Filipp, B. Simon, A. Neuhaus, N. Schüller, C. David, H. Kooshapur, T. Madl, R. Erdmann, and W. Schliebs. *Structural basis for competitive interactions of Pex14 with the import receptors Pex5 and Pex19.* The EMBO Journal, 2009. **28**(6): p. 745-754.

184. Giannopoulou, E.-A., L. Emmanouilidis, M. Sattler, G. Dodt, and M. Wilmanns. *Towards the molecular mechanism of the integration of peroxisomal membrane proteins.* Biochimica et Biophysica Acta (BBA)-Molecular Cell Research, 2016. **1863**(5): p. 863-869.
185. Saveria, T., A. Halbach, R. Erdmann, R. Volkmer-Engert, C. Landgraf, H. Rottensteiner, and M. Parsons. *Conservation of PEX19-binding motifs required for protein targeting to mammalian peroxisomal and trypanosome glycosomal membranes.* Eukaryotic Cell, 2007. **6**(8): p. 1439-1449.
186. Fransen, M., I. Vastiau, C. Brees, V. Brys, G.P. Mannaerts, and P.P. Van Veldhoven. *Analysis of human Pex19p's domain structure by pentapeptide scanning mutagenesis.* Journal of Molecular Biology, 2005. **346**(5): p. 1275-1286.
187. Fransen, M., T. Wylin, C. Brees, G.P. Mannaerts, and P.P. Van Veldhoven. *Human pex19p binds peroxisomal integral membrane proteins at regions distinct from their sorting sequences.* Molecular and Cellular Biology, 2001. **21**(13): p. 4413-4424.
188. Rayapuram, N. and S. Subramani. *The importomer—a peroxisomal membrane complex involved in protein translocation into the peroxisome matrix.* Biochimica et Biophysica Acta (BBA)-Molecular Cell Research, 2006. **1763**(12): p. 1613-1619.
189. Baker, A., T.L. Hogg, and S.L. Warriner. *Peroxisome protein import: a complex journey.* Biochemical Society Transactions, 2016. **44**(3): p. 783-789.
190. Waterham, H.R. and M.S. Ebberink. *Genetics and molecular basis of human peroxisome biogenesis disorders.* Biochimica et Biophysica Acta (BBA)-Molecular Basis of Disease, 2012. **1822**(9): p. 1430-1441.
191. Kal, A.J., A.J. van Zonneveld, V. Benes, M. van den Berg, M.G. Koerkamp, K. Albermann, N. Strack, J.M. Ruijter, A. Richter, and B. Dujon. *Dynamics of gene expression revealed by comparison of serial analysis of gene expression transcript profiles from yeast grown on two different carbon sources.* Molecular Biology of the Cell, 1999. **10**(6): p. 1859-1872.
192. Hailu, A., A.M. Musa, C. Royce, and M. Wasunna. *Visceral leishmaniasis: new health tools are needed.* PLoS Medicine, 2005. **2**(7): p. e211.
193. Shimizu, N., R. Itoh, Y. Hirono, H. Otera, K. Ghaedi, K. Tateishi, S. Tamura, K. Okumoto, T. Harano, and S. Mukai. *The peroxin Pex14p cDNA cloning by functional complementation on a Chinese hamster ovary cell mutant, characterization, and functional analysis.* Journal of Biological Chemistry, 1999. **274**(18): p. 12593-12604.
194. Will, G.K., M. Soukupova, X. Hong, K.S. Erdmann, J.A. Kiel, G. Dodt, W.-H. Kunau, and R. Erdmann. *Identification and characterization of the human orthologue of yeast Pex14p.* Molecular and Cellular Biology, 1999. **19**(3): p. 2265-2277.
195. Komori, M., S.W. Rasmussen, J.A. Kiel, R.J. Baerends, J.M. Cregg, I.J. van der Klei, and M. Veenhuis. *The Hansenula polymorpha PEX14 gene encodes a novel peroxisomal membrane protein essential for peroxisome biogenesis.* The EMBO Journal, 1997. **16**(1): p. 44-53.
196. Fransen, M., S.R. Terlecky, and S. Subramani. *Identification of a human PTS1 receptor docking protein directly required for peroxisomal protein import.* Proceedings of the National Academy of Sciences, 1998. **95**(14): p. 8087-8092.
197. Johnson, M.A., W.B. Snyder, J. Lin Cereghino, M. Veenhuis, S. Subramani, and J.M. Cregg. *Pichia pastoris Pex14p, a phosphorylated peroxisomal membrane protein, is part of a PTS–receptor docking complex and interacts with many peroxins.* Yeast, 2001. **18**(7): p. 621-641.
198. Girzalsky, W., P. Rehling, K. Stein, J. Kipper, L. Blank, W.-H. Kunau, and R. Erdmann. *Involvement of Pex13p in Pex14p localization and peroxisomal targeting signal 2–dependent protein import into peroxisomes.* The Journal of Cell Biology, 1999. **144**(6): p. 1151-1162.
199. Dias, A.F., T.A. Rodrigues, A.G. Pedrosa, A. Barros-Barbosa, T. Francisco, and J.E. Azevedo. *The peroxisomal matrix protein translocon is a large cavity-forming protein assembly into which PEX5 protein enters to release its cargo.* Journal of Biological Chemistry, 2017: p. jbc. M117. 805044.

200. Pace, C.N., F. Vajdos, L. Fee, G. Grimsley, and T. Gray. *How to measure and predict the molar absorption coefficient of a protein.* Protein Science, 1995. **4**(11): p. 2411-2423.
201. Musse, A.A., J. Wang, G.A. Prentice, E. London, and A.R. Merrill. *Scanning the membrane-bound conformation of helix 1 in the colicin E1 channel domain by site-directed fluorescence labeling.* Journal of Biological Chemistry, 2006. **281**(2): p. 885-895.
202. Hachmann, J.P. and J.W. Amshey. *Models of protein modification in Tris–glycine and neutral pH Bis–Tris gels during electrophoresis: effect of gel pH.* Analytical Biochemistry, 2005. **342**(2): p. 237-245.
203. Caputo, G.A. and E. London. *Using a Novel Dual Fluorescence Quenching Assay for Measurement of Tryptophan Depth within Lipid Bilayers To Determine Hydrophobic α-Helix Locations within Membranes.* Biochemistry, 2003. **42**(11): p. 3265-3274.
204. Caputo, G.A. and E. London. *Analyzing transmembrane protein and hydrophobic helix topography by dual fluorescence quenching*, in *Lipid-Protein Interactions*. 2013, Springer. p. 279-295.
205. Dennison, S.M., S.M. Stewart, K.C. Stempel, H.-X. Liao, B.F. Haynes, and S.M. Alam. *Stable docking of neutralizing human immunodeficiency virus type 1 gp41 membrane-proximal external region monoclonal antibodies 2F5 and 4E10 is dependent on the membrane immersion depth of their epitope regions.* Journal of Virology, 2009. **83**(19): p. 10211-10223.
206. Zimmermann, L., A. Stephens, S.-Z. Nam, D. Rau, J. Kübler, M. Lozajic, F. Gabler, J. Söding, A.N. Lupas, and V. Alva. *A completely Reimplemented MPI bioinformatics toolkit with a new HHpred server at its Core.* Journal of Molecular Biology, 2018. **430**(15): p. 2237-2243.
207. Gautier, R., D. Douguet, B. Antonny, and G. Drin. *HELIQUEST: a web server to screen sequences with specific α-helical properties.* Bioinformatics, 2008. **24**(18): p. 2101-2102.
208. Jmol. *An open-source Java viewer for chemical structures in 3D.* 2018 [cited 2018, 05 August]; Available from: http://www.jmol.org/
209. Pettersen, E.F., T.D. Goddard, C.C. Huang, G.S. Couch, D.M. Greenblatt, E.C. Meng, and T.E. Ferrin. *UCSF Chimera—a visualization system for exploratory research and analysis.* Journal of Computational Chemistry, 2004. **25**(13): p. 1605-1612.
210. Ulmschneider, M.B. and M.S. Sansom. *Amino acid distributions in integral membrane protein structures.* Biochimica et Biophysica Acta (BBA)-Biomembranes, 2001. **1512**(1): p. 1-14.
211. Krishnakumar, S.S. and E. London. *Effect of sequence hydrophobicity and bilayer width upon the minimum length required for the formation of transmembrane helices in membranes.* Journal of Molecular Biology, 2007. **374**(3): p. 671-687.
212. Lakowicz, J.R. *Principles of Fluorescence Spectroscopy*. third ed. 2006, New York: Springer. 43.
213. Hayashibara, M. and E. London. *Topography of Diphtheria Toxin A Chain Inserted into Lipid Vesicles.* Biochemistry, 2005. **44**(6): p. 2183-2196.
214. Mansoor, S.E., M.A. DeWitt, and D.L. Farrens. *Distance mapping in proteins using fluorescence spectroscopy: the tryptophan-induced quenching (TrIQ) method.* Biochemistry, 2010. **49**(45): p. 9722-9731.
215. Jones Brunette, A.M. and D.L. Farrens. *Distance mapping in proteins using fluorescence spectroscopy: tyrosine, like tryptophan, quenches bimane fluorescence in a distance-dependent manner.* Biochemistry, 2014. **53**(40): p. 6290-6301.
216. Weber, P.C., D. Ohlendorf, J. Wendoloski, and F. Salemme. *Structural origins of high-affinity biotin binding to streptavidin.* Science, 1989. **243**(4887): p. 85-88.
217. González, M.n., C.E. Argaraña, and G.D. Fidelio. *Extremely high thermal stability of streptavidin and avidin upon biotin binding.* Biomolecular Engineering, 1999. **16**(1-4): p. 67-72.
218. Ladokhin, A.S. *Analysis of Protein and Peptide Penetration into Membranes by Depth-Dependent Fluorescence Quenching: Theoretical Considerations.* Biophysical Journal, 1999. **76**(2): p. 946-955.
219. Kumar, A. *CFSSP: Chou and Fasman Secondary Structure Prediction server.* Wide Spectrum, 2013. **1**: p. 15-19.

220. Roccatano, D., G. Colombo, M. Fioroni, and A.E. Mark. *Mechanism by which 2,2,2-trifluoroethanol/water mixtures stabilize secondary-structure formation in peptides: A molecular dynamics study.* Proceedings of the National Academy of Sciences, 2002. **99**(19): p. 12179-12184.
221. Jasanoff, A. and A.R. Fersht. *Quantitative Determination of Helical Propensities from Trifluoroethanol Titration Curves.* Biochemistry, 1994. **33**(8): p. 2129-2135.
222. Bains, G., A.B. Patel, and V. Narayanaswami. *Pyrene: A Probe to Study Protein Conformation and Conformational Changes.* Molecules, 2011. **16**(9): p. 7909.
223. Bains, G.K., S.H. Kim, E.J. Sorin, and V. Narayanaswami. *The extent of pyrene excimer fluorescence emission is a reflector of distance and flexibility: analysis of the segment linking the LDL receptor-binding and tetramerization domains of apolipoprotein E3.* Biochemistry, 2012. **51**(31): p. 6207-6219.
224. Swamy, M., G.M. Siegers, S. Minguet, B. Wollscheid, and W.W.A. Schamel. *Blue Native Polyacrylamide Gel Electrophoresis (BN-PAGE) for the Identification and Analysis of Multiprotein Complexes.* Science STKE, 2006. **2006**(345): p. pl4-.
225. Chatterjee, A., C. Caballero-Franco, D. Bakker, S. Totten, and A. Jardim. *Pore-forming Activity of the Escherichia coli Type III Secretion System Protein EspD.* Journal of Biological Chemistry, 2015. **290**(42): p. 25579-25594.
226. Solomaha, E. and H.C. Palfrey. *Conformational changes in dynamin on GTP binding and oligomerization reported by intrinsic and extrinsic fluorescence.* Biochemical Journal, 2005. **391**(3): p. 601-611.
227. Pouny, Y., D. Rapaport, A. Mor, P. Nicolas, and Y. Shai. *Interaction of antimicrobial dermaseptin and its fluorescently labeled analogs with phospholipid membranes.* Biochemistry, 1992. **31**(49): p. 12416-12423.
228. Mudhakir, D. and H. Harashima. *Learning from the viral journey: how to enter cells and how to overcome intracellular barriers to reach the nucleus.* The AAPS Journal, 2009. **11**(1): p. 65.
229. Shai, Y. *Mechanism of the binding, insertion and destabilization of phospholipid bilayer membranes by α-helical antimicrobial and cell non-selective membrane-lytic peptides.* Biochimica et Biophysica Acta (BBA)-Biomembranes, 1999. **1462**(1): p. 55-70.
230. Meinecke, M., P. Bartsch, and R. Wagner. *Peroxisomal protein import pores.* Biochimica et Biophysica Acta (BBA) - Molecular Cell Research, 2016. **1863**(5): p. 821-827.
231. Duarte, A.M.S., E.R. de Jong, R.B.M. Koehorst, and M.A. Hemminga. *Conformational studies of peptides representing a segment of TM7 from H(+)-V(O)-ATPase in SDS micelles.* European Biophysics Journal, 2010. **39**(4): p. 639-646.
232. Therien, A.G., F.E. Grant, and C.M. Deber. *Interhelical hydrogen bonds in the CFTR membrane domain.* Nature Structural and Molecular Biology, 2001. **8**(7): p. 597.
233. Johnson, R.M., C.L. Heslop, and C.M. Deber. *Hydrophobic helical hairpins: design and packing interactions in membrane environments.* Biochemistry, 2004. **43**(45): p. 14361-14369.
234. Peng, S., L.-P. Liu, A.Q. Emili, and C.M. Deber. *Cystic fibrosis transmembrane conductance regulator: expression and helicity of a double membrane-spanning segment.* FEBS Letters, 1998. **431**(1): p. 29-33.
235. Arselin, G., M.F. Giraud, A. Dautant, J. Vaillier, D. Brethes, B. Coulary-Salin, J. Schaeffer, and J. Velours. *The GxxxG motif of the transmembrane domain of subunit e is involved in the dimerization/oligomerization of the yeast ATP synthase complex in the mitochondrial membrane.* European Journal of Biochemistry, 2003. **270**(8): p. 1875-1884.
236. Lee, S.-F., S. Shah, C. Yu, W.C. Wigley, H. Li, M. Lim, K. Pedersen, W. Han, P. Thomas, and J. Lundkvist. *A conserved GXXXG motif in APH-1 is critical for assembly and activity of the γ-secretase complex.* Journal of Biological Chemistry, 2004. **279**(6): p. 4144-4152.
237. Zhou, F.X., M.J. Cocco, W.P. Russ, A.T. Brunger, and D.M. Engelman. *Interhelical hydrogen bonding drives strong interactions in membrane proteins.* Nature Structural and Molecular Biology, 2000. **7**(2): p. 154.

238. Gratkowski, H., J.D. Lear, and W.F. DeGrado. *Polar side chains drive the association of model transmembrane peptides.* Proceedings of the National Academy of Sciences, 2001. **98**(3): p. 880-885.
239. Sulistijo, E.S. and K.R. MacKenzie. *Sequence dependence of BNIP3 transmembrane domain dimerization implicates side-chain hydrogen bonding and a tandem GxxxG motif in specific helix–helix interactions.* Journal of Molecular Biology, 2006. **364**(5): p. 974-990.
240. North, B., L. Cristian, X. Fu Stowell, J.D. Lear, J.G. Saven, and W.F. DeGrado. *Characterization of a Membrane Protein Folding Motif, the Ser Zipper, Using Designed Peptides.* Journal of Molecular Biology, 2006. **359**(4): p. 930-939.
241. Kim, T., K.I. Lee, P. Morris, R.W. Pastor, O.S. Andersen, and W. Im. *Influence of hydrophobic mismatch on structures and dynamics of gramicidin a and lipid bilayers.* Biophysical Journal, 2012. **102**(7): p. 1551-1560.
242. Matsuzaki, K., K.-i. Sugishita, N. Ishibe, M. Ueha, S. Nakata, K. Miyajima, and R.M. Epand. *Relationship of membrane curvature to the formation of pores by magainin 2.* Biochemistry, 1998. **37**(34): p. 11856-11863.
243. Wieprecht, T., M. Dathe, R.M. Epand, M. Beyermann, E. Krause, W.L. Maloy, D.L. MacDonald, and M. Bienert. *Influence of the angle subtended by the positively charged helix face on the membrane activity of amphipathic, antibacterial peptides.* Biochemistry, 1997. **36**(42): p. 12869-12880.
244. Voeltz, G.K., W.A. Prinz, Y. Shibata, J.M. Rist, and T.A. Rapoport. *A class of membrane proteins shaping the tubular endoplasmic reticulum.* Cell, 2006. **124**(3): p. 573-586.
245. Doucet, C.M. and M.W. Hetzer. *Nuclear pore biogenesis into an intact nuclear envelope.* Chromosoma, 2010. **119**(5): p. 469-477.
246. Vollmer, B., A. Schooley, R. Sachdev, N. Eisenhardt, A.M. Schneider, C. Sieverding, J. Madlung, U. Gerken, B. Macek, and W. Antonin. *Dimerization and direct membrane interaction of Nup53 contribute to nuclear pore complex assembly.* The EMBO Journal, 2012. **31**(20): p. 4072-4084.
247. Mészáros, N., J. Cibulka, M.J. Mendiburo, A. Romanauska, M. Schneider, and A. Köhler. *Nuclear pore basket proteins are tethered to the nuclear envelope and can regulate membrane curvature.* Developmental Cell, 2015. **33**(3): p. 285-298.
248. Barbot, M., D.C. Jans, C. Schulz, N. Denkert, B. Kroppen, M. Hoppert, S. Jakobs, and M. Meinecke. *Mic10 oligomerizes to bend mitochondrial inner membranes at cristae junctions.* Cell Metabolism, 2015. **21**(5): p. 756-763.
249. Helfrich, W. *Elastic properties of lipid bilayers: theory and possible experiments.* Zeitschrift für Naturforschung C, 1973. **28**(11-12): p. 693-703.
250. Helfrich, P. and E. Jakobsson. *Calculation of deformation energies and conformations in lipid membranes containing gramicidin channels.* Biophysical Journal, 1990. **57**(5): p. 1075-1084.
251. Jarsch, I.K., F. Daste, and J.L. Gallop. *Membrane curvature in cell biology: An integration of molecular mechanisms.* The Journal of Cell Biology, 2016. **214**(4): p. 375-387.
252. Kusumi, A., K.G. Suzuki, R.S. Kasai, K. Ritchie, and T.K. Fujiwara. *Hierarchical mesoscale domain organization of the plasma membrane.* Trends in Biochemical Sciences, 2011. **36**(11): p. 604-615.
253. Zhang, Y.-P., R.N. Lewis, G.D. Henry, B.D. Sykes, R.S. Hodges, and R.N. McElhaney. *Peptide models of helical hydrophobic transmembrane segments of membrane proteins. 1. Studies of the conformation, intrabilayer orientation, and amide hydrogen exchangeability of Ac-K2-(LA) 12-K2-amide.* Biochemistry, 1995. **34**(7): p. 2348-2361.
254. Arkin, I.T. and A.T. Brunger. *Statistical analysis of predicted transmembrane α-helices.* Biochimica et Biophysica Acta (BBA)-Protein Structure and Molecular Enzymology, 1998. **1429**(1): p. 113-128.
255. Gennis, R.B. *Biomembranes: Molecular structure and function*. 2013: Springer Science & Business Media.

256. Henderson, R., J.M. Baldwin, T. Ceska, F. Zemlin, E.a. Beckmann, and K. Downing. *Model for the structure of bacteriorhodopsin based on high-resolution electron cryo-microscopy.* Journal of Molecular Biology, 1990. **213**(4): p. 899-929.
257. Rodriguez, F., S.L. Rouse, C.E. Tait, J. Harmer, A. De Riso, C.R. Timmel, M.S. Sansom, B.C. Berks, and J.R. Schnell. *Structural model for the protein-translocating element of the twin-arginine transport system.* Proceedings of the National Academy of Sciences, 2013: p. 201219486.
258. Toniolo, C., C. Peggion, M. Crisma, F. Formaggio, X. Shui, and D.S. Eggleston. *Structure determination of racemic trichogin A IV using centrosymmetric crystals.* Nature Structural and Molecular Biology, 1994. **1**(12): p. 908.
259. Respondek, M., T. Madl, C. Göbl, R. Golser, and K. Zangger. *Mapping the orientation of helices in micelle-bound peptides by paramagnetic relaxation waves.* Journal of the American Chemical Society, 2007. **129**(16): p. 5228-5234.
260. Hohlweg, W., S. Kosol, and K. Zangger. *Determining the orientation and localization of membrane-bound peptides.* Current Protein and Peptide Science, 2012. **13**(3): p. 267-279.
261. Benke, S., D. Roderer, B. Wunderlich, D. Nettels, R. Glockshuber, and B. Schuler. *The assembly dynamics of the cytolytic pore toxin ClyA.* Nature Communications, 2015. **6**: p. 6198.
262. Rojko, N., M. Dalla Serra, P. Maček, and G. Anderluh. *Pore formation by actinoporins, cytolysins from sea anemones.* Biochimica et Biophysica Acta (BBA)-Biomembranes, 2016. **1858**(3): p. 446-456.
263. Gouffi, K., F. Gérard, C.-L. Santini, and L.-F. Wu. *Dual Topology of the Escherichia coli TatA Protein.* Journal of Biological Chemistry, 2004. **279**(12): p. 11608-11615.
264. Chan, C.S., M.R. Zlomislic, D.P. Tieleman, and R.J. Turner. *The TatA Subunit of Escherichia coli Twin-Arginine Translocase Has an N-in Topology.* Biochemistry, 2007. **46**(25): p. 7396-7404.
265. Hou, B., E.S. Heidrich, D. Mehner-Breitfeld, and T. Brüser. *The TatA component of the twin-arginine translocation system locally weakens the cytoplasmic membrane of Escherichia coli upon protein substrate binding.* Journal of Biological Chemistry, 2018.
266. Goosens, V.J. and J.M. van Dijl. *Twin-Arginine Protein Translocation*, in *Protein and Sugar Export and Assembly in Gram-positive Bacteria*, F. Bagnoli and R. Rappuoli, Editors. 2017, Springer International Publishing: Cham. p. 69-94.
267. Stoddart, D., M. Ayub, L. Höfler, P. Raychaudhuri, J.W. Klingelhoefer, G. Maglia, A. Heron, and H. Bayley. *Functional truncated membrane pores.* Proceedings of the National Academy of Sciences, 2014. **111**(7): p. 2425-2430.
268. Hotez, P.J., D.H. Molyneux, A. Fenwick, J. Kumaresan, S.E. Sachs, J.D. Sachs, and L. Savioli. *Control of neglected tropical diseases.* New England Journal of Medicine, 2007. **357**(10): p. 1018-1027.
269. Alvar, J., S. Yactayo, and C. Bern. *Leishmaniasis and poverty.* Trends in Parasitology, 2006. **22**(12): p. 552-557.
270. Bern, C., J.H. Maguire, and J. Alvar. *Complexities of assessing the disease burden attributable to leishmaniasis.* PLoS Neglected Tropical Diseases, 2008. **2**(10): p. e313.
271. Sundar, S. and M. Rai. *Treatment of visceral leishmaniasis.* Expert Opinion on Pharmacotherapy, 2005. **6**(16): p. 2821-2829.
272. Guerin, P.J., P. Olliaro, S. Sundar, M. Boelaert, S.L. Croft, P. Desjeux, M.K. Wasunna, and A.D. Bryceson. *Visceral leishmaniasis: current status of control, diagnosis, and treatment, and a proposed research and development agenda.* The Lancet Infectious Diseases, 2002. **2**(8): p. 494-501.
273. Subramani, S. *Protein translocation into peroxisomes.* Journal of Biological Chemistry, 1996. **271**(51): p. 32483-32486.

274. Hart, D.T. and F.R. Opperdoes. *The occurence of glycosomes (microbodies) in the promastigote stage of four major Leishmania species.* Molecular and Biochemical Parasitology, 1984. **13** p. 159-172.
275. Argos, P. and B. Persson. *Topology prediction of membrane proteins.* Protein Science, 1996. **5**(2): p. 363-371.
276. Persson, B. and P. Argos. Prediction of transmembrane segments in proteins utilising multiple sequence alignments. 1994, Elsevier.
277. Moree, B., K. Connell, R.B. Mortensen, C.T. Liu, S.J. Benkovic, and J. Salafsky. *Protein conformational changes are detected and resolved site specifically by second-harmonic generation.* Biophysical Journal, 2015. **109**(4): p. 806-815.
278. Goh, C.-S., D. Milburn, and M. Gerstein. *Conformational changes associated with protein–protein interactions.* Current Opinion in Structural Biology, 2004. **14**(1): p. 104-109.
279. Tompa, P. *Intrinsically disordered proteins: a 10-year recap.* Trends in Biochemical Sciences, 2012. **37**(12): p. 509-516.
280. Campos, L.A. and J. Sancho. *The active site of pepsin is formed in the intermediate conformation dominant at mildly acidic pH.* FEBS Letters, 2003. **538**(1-3): p. 89-95.
281. Vogel, R. and F. Siebert. *Conformations of the active and inactive states of opsin.* Journal of Biological Chemistry, 2001. **276**(42): p. 38487-38493.
282. Changeux, J.-P. and S. Edelstein. *Conformational selection or induced fit? 50 years of debate resolved.* F1000 Biology Reports, 2011. **3**.
283. James, L.C., P. Roversi, and D.S. Tawfik. *Antibody multispecificity mediated by conformational diversity.* Science, 2003. **299**(5611): p. 1362-1367.
284. Ayed, S.H., A.D. Cloutier, L.J. McLeod, A.C. Foo, A.M. Damry, and N.K. Goto. *Dissecting the role of conformational change and membrane binding by the bacterial cell division regulator MinE in the stimulation of MinD ATPase activity.* Journal of Biological Chemistry, 2017: p. jbc. M117. 805945.
285. Sonntag, Y., M. Musgaard, C. Olesen, B. Schiøtt, J.V. Møller, P. Nissen, and L. Thøgersen. *Mutual adaptation of a membrane protein and its lipid bilayer during conformational changes.* Nature Communications, 2011. **2**: p. 304.
286. Snyder, A.J. and P. Danthi. *Lipid membranes facilitate conformational changes required for reovirus cell entry.* Journal of Virology, 2015: p. JVI. 02997-15.
287. Hammes, G.G. *Multiple conformational changes in enzyme catalysis.* Biochemistry, 2002. **41**(26): p. 8221-8228.
288. Pan, R., X.-J. Zhang, Z.-J. Zhang, Y. Zhou, W.-X. Tian, and R.-Q. He. *Substrate-induced changes in protease active site conformation impact subsequent reactions with substrates.* Journal of Biological Chemistry, 2010: p. jbc. M110. 103549.
289. Gutteridge, A. and J. Thornton. *Conformational change in substrate binding, catalysis and product release: an open and shut case?* FEBS Letters, 2004. **567**(1): p. 67-73.
290. Doms, R.W., A. Helenius, and J. White. *Membrane fusion activity of the influenza virus hemagglutinin. The low pH-induced conformational change.* Journal of Biological Chemistry, 1985. **260**(5): p. 2973-2981.
291. Lin, X., J.K. Noel, N.R. Eddy, J. Ma, and J.N. Onuchic. *Investigation of the pH Induced Conformational Rearrangement of Influenza Hemagglutinin.* Biophysical Journal, 2016. **110**(3): p. 13a.
292. Jeffrey, P.D., M.C. Bewley, R.T. MacGillivray, A.B. Mason, R.C. Woodworth, and E.N. Baker. *Ligand-induced conformational change in transferrins: crystal structure of the open form of the N-terminal half-molecule of human transferrin.* Biochemistry, 1998. **37**(40): p. 13978-13986.
293. Dewan, J.C., B. Mikami, M. Hirose, and J.C. Sacchettini. *Structural evidence for a pH-sensitive dilysine trigger in the hen ovotransferrin N-lobe: implications for transferrin iron release.* Biochemistry, 1993. **32**(45): p. 11963-11968.

294. Ptitsyn, O., G. Zanotti, A. Denesyuk, and V. Bychkova. *Mechanism of pH-induced release of retinol from retinol-binding protein.* FEBS Letters, 1993. **317**(3): p. 181-184.
295. Wojtasek, H. and W.S. Leal. *Conformational Change in the Pheromone-binding Protein fromBombyx mori Induced by pH and by Interaction with Membranes.* Journal of Biological Chemistry, 1999. **274**(43): p. 30950-30956.
296. Zubkov, S., A.M. Gronenborn, I.-J.L. Byeon, and S. Mohanty. *Structural consequences of the pH-induced conformational switch in A. polyphemus pheromone-binding protein: mechanisms of ligand release.* Journal of Molecular Biology, 2005. **354**(5): p. 1081-1090.
297. Dollery, S.J., C.C. Wright, D.C. Johnson, and A.V. Nicola. *Low pH-dependent changes in the conformation and oligomeric state of the pre-fusion form of herpes simplex virus glycoprotein B are separable from fusion activity.* Journal of Virology, 2011: p. JVI. 05291-11.
298. Dollery, S.J., M.G. Delboy, and A.V. Nicola. *Low pH-induced conformational change in herpes simplex virus glycoprotein B.* Journal of Virology, 2010. **84**(8): p. 3759-3766.
299. Beechem, J.M. and L. Brand. *Time-resolved fluorescence of proteins.* Annual Review of Biochemistry, 1985. **54**(1): p. 43-71.
300. Martin, S.R. and M.J. Schilstra. *Circular dichroism and its application to the study of biomolecules.* Methods in Cell Biology, 2008. **84**: p. 263-293.
301. Dai, Z., J.H. Kim, M. Tonelli, I.K. Ali, and J.L. Markley. *pH-induced conformational change of IscU at low pH correlates with protonation/deprotonation of two conserved histidine residues.* Biochemistry, 2014. **53**(32): p. 5290-5297.
302. Kalani, M.R., A. Moradi, M. Moradi, and E. Tajkhorshid. *Characterizing a histidine switch controlling pH-dependent conformational changes of the influenza virus hemagglutinin.* Biophysical Journal, 2013. **105**(4): p. 993-1003.
303. Cao, L., X. Shi, H. Chang, Q. Zhang, and Y. He. *pH-dependent recognition of apoptotic and necrotic cells by the human dendritic cell receptor DEC205.* Proceedings of the National Academy of Sciences, 2015. **112**(23): p. 7237-7242.
304. Yeo, K.J., Y.-S. Hong, J.-G. Jee, J.K. Lee, H.J. Kim, J.-W. Park, E.-H. Kim, E. Hwang, S.-Y. Kim, and E.-G. Lee. *Mechanism of the pH-induced conformational change in the sensor domain of the DraK Histidine kinase via the E83, E105, and E107 residues.* PLoS One, 2014. **9**(9): p. e107168.
305. Hanč, P., O. Schulz, H. Fischbach, S.R. Martin, S. Kjær, and C.R. e Sousa. *A pH-and ionic strength-dependent conformational change in the neck region regulates DNGR-1 function in dendritic cells.* The EMBO Journal, 2016: p. e201694695.
306. Segrest, J.P., H. De Loof, J.G. Dohlman, C.G. Brouillette, and G. Anantharamaiah. *Amphipathic helix motif: classes and properties.* Proteins: Structure, Function, and Bioinformatics, 1990. **8**(2): p. 103-117.
307. Cornell, R.B. and S.G. Taneva. *Amphipathic helices as mediators of the membrane interaction of amphitropic proteins, and as modulators of bilayer physical properties.* Current Protein and Peptide Science, 2006. **7**(6): p. 539-552.
308. Gualdron-López, M., M.H. Vapola, I.J. Miinalainen, J.K. Hiltunen, P.A. Michels, and V.D. Antonenkov. *Channel-forming activities in the glycosomal fraction from the bloodstream form of Trypanosoma brucei.* PLoS One, 2012. **7**(4): p. e34530.
309. Itoh, R. and Y. Fujiki. *Functional domains and dynamic assembly of the peroxin Pex14p, the entry site of matrix proteins.* Journal of Biological Chemistry, 2006.
310. Trouiller, P., P. Olliaro, E. Torreele, J. Orbinski, R. Laing, and N. Ford. *Drug development for neglected diseases: a deficient market and a public-health policy failure.* The Lancet, 2002. **359**(9324): p. 2188-2194.
311. Alvar, J., I.D. Velez, C. Bern, M. Herrero, P. Desjeux, J. Cano, J. Jannin, M. den Boer, and W.L.C. Team. *Leishmaniasis worldwide and global estimates of its incidence.* PLoS One, 2012. **7**(5): p. e35671.

312. Chappuis, F., S. Sundar, A. Hailu, H. Ghalib, S. Rijal, R.W. Peeling, J. Alvar, and M. Boelaert. *Visceral leishmaniasis: what are the needs for diagnosis, treatment and control?* Nature Reviews Microbiology, 2007. **5**(11supp): p. S7.
313. Michels, P.A., F. Bringaud, M. Herman, and V. Hannaert. *Metabolic functions of glycosomes in trypanosomatids.* Biochimica et Biophysica Acta (BBA)-Molecular Cell Research, 2006. **1763**(12): p. 1463-1477.
314. Cruz, A.K., R. Titus, and S.M. Beverley. *Plasticity in chromosome number and testing of essential genes in Leishmania by targeting.* Proceedings of the National Academy of Sciences, 1993. **90**(4): p. 1599-1603.
315. Robinson, K.A. and S.M. Beverley. *Improvements in transfection efficiency and tests of RNA interference (RNAi) approaches in the protozoan parasite Leishmania.* Molecular and Biochemical Parasitology, 2003. **128**(2): p. 217-228.
316. Lye, L.-F., K. Owens, H. Shi, S.M. Murta, A.C. Vieira, S.J. Turco, C. Tschudi, E. Ullu, and S.M. Beverley. *Retention and loss of RNA interference pathways in trypanosomatid protozoans.* PLoS Pathogens, 2010. **6**(10): p. e1001161.
317. Sollelis, L., M. Ghorbal, C.R. MacPherson, R.M. Martins, N. Kuk, L. Crobu, P. Bastien, A. Scherf, J.J. Lopez-Rubio, and Y. Sterkers. *First efficient CRISPR-C as9-mediated genome editing in L eishmania parasites.* Cellular Microbiology, 2015. **17**(10): p. 1405-1412.
318. Sander, J.D. and J.K. Joung. *CRISPR-Cas systems for editing, regulating and targeting genomes.* Nature Biotechnology, 2014. **32**(4): p. 347.
319. Hsu, P.D., E.S. Lander, and F. Zhang. *Development and applications of CRISPR-Cas9 for genome engineering.* Cell, 2014. **157**(6): p. 1262-1278.
320. Zhang, W.-W. and G. Matlashewski. *CRISPR-Cas9-mediated genome editing in Leishmania donovani.* MBio, 2015. **6**(4): p. e00861-15.
321. Zhang, W.-W., P. Lypaczewski, and G. Matlashewski. *Optimized CRISPR-Cas9 genome editing for Leishmania and its use to target a multigene family, induce chromosomal translocation, and study DNA break repair mechanisms.* MSphere, 2017. **2**(1): p. e00340-16.
322. Banaszynski, L.A., L.-c. Chen, L.A. Maynard-Smith, A.L. Ooi, and T.J. Wandless. *A rapid, reversible, and tunable method to regulate protein function in living cells using synthetic small molecules.* Cell, 2006. **126**(5): p. 995-1004.
323. Bayle, J.H., J.S. Grimley, K. Stankunas, J.E. Gestwicki, T.J. Wandless, and G.R. Crabtree. *Rapamycin analogs with differential binding specificity permit orthogonal control of protein activity.* Chemistry & Biology, 2006. **13**(1): p. 99-107.
324. Senturk, S., N.H. Shirole, D.G. Nowak, V. Corbo, D. Pal, A. Vaughan, D.A. Tuveson, L.C. Trotman, J.B. Kinney, and R. Sordella. *Rapid and tunable method to temporally control gene editing based on conditional Cas9 stabilization.* Nature Communications, 2017. **8**: p. 14370.
325. Soysa, R., K.D. Tran, B. Ullman, and P.A. Yates. *Integrating ribosomal promoter vectors that offer a choice of constitutive expression profiles in Leishmania donovani.* Molecular and Biochemical Parasitology, 2015. **204**(2): p. 89-92.
326. Wu, X., A.J. Kriz, and P.A. Sharp. *Target specificity of the CRISPR-Cas9 system.* Quantitative Biology, 2014. **2**(2): p. 59-70.
327. Nishimasu, H., F.A. Ran, P.D. Hsu, S. Konermann, S.I. Shehata, N. Dohmae, R. Ishitani, F. Zhang, and O. Nureki. *Crystal structure of Cas9 in complex with guide RNA and target DNA.* Cell, 2014. **156**(5): p. 935-949.
328. Jiang, W., D. Bikard, D. Cox, F. Zhang, and L.A. Marraffini. *RNA-guided editing of bacterial genomes using CRISPR-Cas systems.* Nature Biotechnology, 2013. **31**(3): p. 233.
329. Horn, D. *Codon usage suggests that translational selection has a major impact on protein expression in trypanosomatids.* BMC Genomics, 2008. **9**(1): p. 2.
330. Alvarez, F., C. Robello, and M. Vignali. *Evolution of codon usage and base contents in kinetoplastid protozoans.* Molecular Biology and Evolution, 1994. **11**(5): p. 790-802.

331. Dow, L.E., J. Fisher, K.P. O'rourke, A. Muley, E.R. Kastenhuber, G. Livshits, D.F. Tschaharganeh, N.D. Socci, and S.W. Lowe. *Inducible in vivo genome editing with CRISPR-Cas9.* Nature Biotechnology, 2015. **33**(4): p. 390.
332. Zetsche, B., S.E. Volz, and F. Zhang. *A split-Cas9 architecture for inducible genome editing and transcription modulation.* Nature Biotechnology, 2015. **33**(2): p. 139.
333. Fu, Y., J.A. Foden, C. Khayter, M.L. Maeder, D. Reyon, J.K. Joung, and J.D. Sander. *High-frequency off-target mutagenesis induced by CRISPR-Cas nucleases in human cells.* Nature Biotechnology, 2013. **31**(9): p. 822.
334. Hsu, P.D., D.A. Scott, J.A. Weinstein, F.A. Ran, S. Konermann, V. Agarwala, Y. Li, E.J. Fine, X. Wu, and O. Shalem. *DNA targeting specificity of RNA-guided Cas9 nucleases.* Nature Biotechnology, 2013. **31**(9): p. 827.
335. Cho, S.W., S. Kim, Y. Kim, J. Kweon, H.S. Kim, S. Bae, and J.-S. Kim. *Analysis of off-target effects of CRISPR/Cas-derived RNA-guided endonucleases and nickases.* Genome Research, 2013.
336. Moyersoen, J., J. Choe, A. Kumar, F.G. Voncken, W.G. Hol, and P.A. Michels. *Characterization of Trypanosoma brucei PEX14 and its role in the import of glycosomal matrix proteins.* European journal of biochemistry, 2003. **270**(9): p. 2059-2067.
337. Pattanayak, V., S. Lin, J.P. Guilinger, E. Ma, J.A. Doudna, and D.R. Liu. *High-throughput profiling of off-target DNA cleavage reveals RNA-programmed Cas9 nuclease specificity.* Nature Biotechnology, 2013. **31**(9): p. 839.
338. Okwor, I. and J. Uzonna. *Social and economic burden of human leishmaniasis.* The American Journal of Tropical Medicine and Hygiene, 2016. **94**(3): p. 489-493.
339. Singh, O.P. and S. Sundar. *Developments in diagnosis of visceral leishmaniasis in the elimination era.* Journal of Parasitology Research, 2015. **2015**.
340. Rigaud, J.-L., B. Pitard, and D. Levy. *Reconstitution of membrane proteins into liposomes: application to energy-transducing membrane proteins.* Biochimica et Biophysica Acta (BBA)-Bioenergetics, 1995. **1231**(3): p. 223-246.
341. LEvy, D., A. Bluzat, M. Seigneuret, and J.-L. Rigaud. *A systematic study of liposome and proteoliposome reconstitution involving Bio-Bead-mediated Triton X-100 removal.* Biochimica et Biophysica Acta (BBA)-Biomembranes, 1990. **1025**(2): p. 179-190.
342. Kim, M. and E. Song. *Iron transport by proteoliposomes containing mitochondrial F1Fo ATP synthase isolated from rat heart.* Biochimie, 2010. **92**(4): p. 333-342.

- END -